Title
Cyanobacterial Production of Isoprene

Author
Chaves, Julie

Publication Date
2017

Peer reviewed|Thesis/dissertation

Cyanobacterial Production of Isoprene

By

Julie Elizabeth Chaves

A dissertation submitted in partial satisfaction of the

Requirements for the degree of

Doctor of Philosophy
in
Comparative Biochemistry
in the
Graduate Division
of the
University of California Berkeley

Committee in charge:
Professor Anastasios Melis, Chair
Professor Fenyong Liu
Professor Krishna Niyogi

Summer 2017

Cyanobacterial Production of Isoprene

by Julie Elizabeth Chaves

Abstract

Cyanobacterial Production of Isoprene

By

Julie Elizabeth Chaves

Doctor of Philosophy in Comparative Biochemistry

University of California Berkeley

Professor Anastasios Melis, Chair

Photosynthesis for the generation of isoprene in cyanobacteria was demonstrated with *Synechocystis*, entailing a process where a single host microorganism acts both as photocatalyst and processor, photosynthesizing and emitting isoprene hydrocarbons. A practical aspect of the commercial exploitation of this process in mass culture is the need to prevent invading microorganisms that might cause a culture to crash, and to provide an alternative to fresh water in scale-up applications. Growth media poised at alkaline pH are desirable in this respect, as high pH might favor the growth of the cyanobacteria, while at the same time discouraging the growth of invading predatory microbes and grazers. In addition, demonstration of salinity tolerance would enable the use of seawater for cyanobacteria cultivations. However, it is not known if *Synechocystis* growth and the isoprene-producing metabolism can be retained under such theoretically non-physiological conditions. We applied the gaseous/aqueous two-phase photobioreactor system with *Synechocystis* transformed with the codon-optimized isoprene synthase gene (*SkIspS*) of *Pueraria montana* (kudzu). Rates of growth and isoprene production are reported under control, and a combination of alkalinity and salinity conditions. The results showed that alkalinity and salinity do not exert a negative effect on either cell growth or isoprene rate and yield in *Synechocystis*. The work points to a practical approach in the design of cyanobacterial growth media for applications in commercial scale up and isoprene production.

The concept applied in this work entails application of an isoprene synthase transgene from terrestrial plants, heterologously expressed in cyanobacteria, thereby reprogramming carbon flux in the terpenoid biosynthetic pathway toward formation and spontaneous release of this volatile chemical from the cell and liquid culture. However, flux manipulations and carbon-partitioning reactions between isoprene (the product) and native terpenoid biosynthesis for cellular needs are not yet optimized for isoprene yield. The primary reactant for isoprene biosynthesis is dimethylallyl diphosphate (DMAPP), whereas both DMAPP and its isopentenyl diphosphate (IPP) isomer are needed for cellular terpenoid biosynthesis. This aspect of the work addressed the function of an isopentenyl diphosphate (IPP) isomerase in cyanobacteria and its role in carbon partitioning between IPP and DMAPP, both of which serve, in variable ratios, as reactants for the synthesis of different cellular terpenoids. The project was approached upon the

heterologous expression in *Synechocystis* of the isopentenyl diphosphate isomerase gene (*FNI*) from *Streptococcus pneumoniae,* a non-photosynthetic bacterium, using isoprene production as a "reporter process" for substrate partitioning between DMAPP and IPP. It is shown that transgenic expression of the *FNI* gene in *Synechocystis* resulted in a 250% increase in the isoprene production rate and yield, suggesting that the FNI isomerase shifted the composition of the endogenous DMAPP-IPP steady-state pool toward DMAPP, thereby enhancing rates and yield of isoprene production.

Efforts to heterologously produce quantities of isoprene hydrocarbons (C_5H_8) renewably from CO_2 and H_2O through the photosynthesis of cyanobacteria face barriers, including low levels of recombinant enzyme accumulation compounded by their slow innate catalytic activity. This aspect of the work sought to alleviate the "expression level" barrier upon placing the isoprene synthase (IspS) enzyme in different fusion configurations with the cpcB protein, the highly expressed β-subunit of phycocyanin. Different *cpcB*IspS* fusion constructs were made, distinguished by the absence or presence of linker amino acids between the two proteins. Length and composition of linker amino acids was variable with lengths of 7, 10, 16 and 65 amino acids designed to confer optimal activity to the IspS through spatial positioning between the cpcB and IspS. Results showed that fusion constructs with the highly expressed cpcB gene, as the leader sequence, improved transgene expression in the range of 61- to 275-fold over what was measured with the unfused IspS control. However, the specific activity of the IspS enzyme was attenuated in all fusion transformants, possibly because of allosteric effects exerted by the leader cpcB fusion protein. This inhibition varied depending on the nature of the linker amino acids between the cpcB and IspS proteins. In terms of isoprene production, the results further showed a tradeoff between specific activity and transgenic enzyme accumulation. For example, the *cpcB*L7*IspS* strain showed only about 10% the isoprene synthase specific activity of the unfused *cpcB-IspS* control but it accumulated 254-fold more IspS enzyme. The latter more than countered the slower specific activity and made the *cpcB*L7*IspS* transformant the best isoprene-producing strain in this work. Isoprene to biomass yield ratios improved from 0.2 mg g^{-1} (isoprene to biomass, w:w) in the unfused *cpcB-IspS* control to 5.4 mg g^{-1} in the *cpcB*L7*IspS* strain, a 27-fold improvement.

Our final approach unified the lessons previously learned. The combination of an optimized *cpcB*IspS* fusion construct with the overexpression of the FNI protein resulted in up to a 60-fold increase in isoprene yield, relative to that obtained upon the expression of the *IspS* gene alone in *Synechocystis*, reaching a yield of 12.3 mg g^{-1} (isoprene to biomass, w:w). The latter is the highest verifiable constitutive photosynthetic isoprene production measured with homoplasmic lines, in which the heterologous isoprene synthase gene is encoded by the *Synechocystis* genomic DNA. Thus, the work constitutes a major step forward in the development of a cyanobacterial engineering platform for isoprene production.

For

Elaine Barrios

Thank you for teaching me the true meaning of triumph.

Table of Contents

Table of Contents ii
Acknowledgements iv
Curriculum Vitae v

Chapter 1: Introduction 1

Chapter 2: Isoprene production in Synechocystis under alkaline and saline growth conditions

2.1 Introduction 9
2.2 Materials and Methods 9
2.3 Results 14
2.4 Discussion 26
2.5 References 27

Chapter 3: Role of isopentenyl-diphosphate isomerase in heterologous cyanobacterial (Synechocystis) isoprene production

3.1 Introduction 30
3.2 Materials and Methods 30
3.3 Results 32
3.4 Discussion 47
3.5 References 48
3.6 Supplemental materials 52

Chapter 4: Engineering isoprene synthase expression and activity in cyanobacteria

4.1 Introduction 55

4.2 Materials and Methods 55
4.3 Results 58
4.4 Discussion 95
4.5 References 96
4.6 Supplemental materials 99

Chapter 5: Remodeling terpenoid metabolism in cyanobacteria for isoprene production

5.1 Introduction 105
5.2 Materials and Methods 105
5.3 Results 107
5.4 Discussion 118
5.5 References 120
5.6 Supplemental materials 121

Acknowledgments

First, I would like to thank Dr. Fiona Davies. Your lectures in PMB 180 on cyanobacterial production of isoprene are what motivated me to pursue my undergraduate senior honors thesis in the Melis lab. Your guidance in the beginning days of my career set the stage for my entire thesis.

Dr. Paloma Rueda, thank you for your kind, generous, and patient guidance. It was so easy to learn from you because of your ability to make even the most difficult experiments and concepts accessible. Your influence has been instrumental to my success.

Dr. Henning Kirst, you have been with me through my entire journey as a PhD student. Thank you for being incredibly smart and helpful, working with me through some of my most challenging moments. I have learned a tremendous amount from you. Thank for 5 years of professional and personal mentorship over morning coffee at Yalis, surfing in Pacifica, and beers at Triple Rock.

To my NSF SAGE IGERT fellowship group, thank you for inviting me to participate in expanding our knowledge base around green energy. Our projects, conversations, and meetings have opened my mind to the many forces and possibilities involved in our field.

Finally, I would like to thank my PI, Anastasios Melis. Five years ago you approached me with a question that changed my life, "Would you like to get a PhD?" Thank you for your rigorous auspices and careful attention to my training. I am truly proud, and honored to have developed as a scientist in your lab.

Curriculum Vitae

Julie E. Chaves

Current Position
Ph.D. Graduate Student
Comparative Biochemistry Program
Office: 324 Barker Hall
University of California Berkeley, CA 94720-3102

Graduate Student Researcher
Melis Lab, Department of Plant and Microbial Biology
471 Koshland Hall
University of California Berkeley, CA 94720-3102
Tel: (510) 642- 6209
E-mail: jechaves@berkeley.edu

Citizenship: USA

Education:
Ph.D Candidate: **University of California, Berkeley**
Comparative Biochemistry, August 2017
UC GPA: 3.91

Bachelor of Arts: **University of California, Berkeley**
Integrative Biology, May 2012
UC GPA: 3.613

Associate of Science: **American River College, Sacramento, CA**
May, 2010
ARC GPA: 3.47

Honors:
NSF SAGE IGERT fellowship recipient, University of California, Berkeley (2013-2015)

Honors upon graduation in Integrative Biology, University of California, Berkeley (2012)

Undergraduate Honors Research student, Melis Lab, Department of Plant and Microbial Biology, University of California, Berkeley (2011-2012)

Honors graduate of Science, American River College, Sacramento, California (2010)

Current Research Interest:

Developing molecular solutions to pressing environmental problems, relating particularly to renewable fuels and chemicals. Current research project entails the direct photosynthetic production of hydrocarbon fuels and chemicals (isoprene), optimizing organism growth conditions and enhancing product yield through metabolic engineering. Methods of cultivation to reduce contamination have been developed through growth conditions and media selection. The research also aims to increase photosynthetic carbon partitioning toward the isoprenoid fuel-producing pathway, improving the commercial viability of the process.

Research Experience:

Undergraduate Honors Research Student (2011-2012), Melis Lab, Department of Plant and Microbial Biology, University of California, Berkeley. I received training under the auspices of Professor Melis and postdoctoral scholar Dr. Fiona Bentley. Investigated metabolic engineering aspects of isoprene hydrocarbons production in the cyanobacterium *Synechocystis* PCC 6803, heterologously transformed with the isoprene synthase gene from the vine kudzu (*Pueraria montana*). Developed optimal growth media for cyanobacterial productivity under mass culture conditions, and overexpressed glycogen catabolic genes of the isoprene producing *Synechocystis* cell line to increase product (isoprene) yields.

Undergraduate Research Student (2008), California State University, Sacramento. Science Transfer Project. I received training under Professor Mary McCarthy, Ph.D. This project investigated the toxicity of tobacco cigarette smoke and the accumulation capacity of cigarette smoke on cotton fiber.

Student Researcher (2008), California State University, Sacramento. "Introduction to Summer Research" Program. I received training under Professor Mary McCarthy, PhD. This was an independent ethno-botanical research project studying the effect of traditional medicines of Pacific Islander and Native American indigenous cultures on a breast cancer cell line.

Professional Affiliations:

Graduate Student Instructor (Jan 2014- May 2014), University of California Berkeley**.** Instructor of Molecular and Cell Biology c31 discussion section, a general biology course for non-majors. Responsible for preparation and design of weekly discussion sections, weekly quizzes, all major course projects, and grading of all course assignments. Provided weekly office hours for students, and general teaching assistance for all concepts taught in the course.

Graduate Student Instructor (Aug 2013- Dec 2013), University of California, Berkeley**.** Instructor of Biology 1A-Lab course. Responsible for the preparation and grading of weekly assignments and exams, providing in-laboratory lectures, providing instruction and troubleshooting for experiments, and providing general teaching assistance for all biological concepts taught in the course.

Science Transfer Project (2008-2010), California State University, Sacramento. Organization aimed to increase diversity in the sciences through recruitment of minorities and women into research.

Future Pharmacists of America (2009), American River College, Sacramento. Cofounder/publicity chair of a pre-pharmacy organization for community college students.

Responsibilities included communication with the general student population about membership, career related events, volunteer opportunities, career options and requirements in the field of pharmacy.

Additional Activities:

Community Resources for Science BASIS (Bay Area Students in Science) Program (Jan 2014- Present), University of California Berkeley. Volunteer science instructor for third grade elementary students in multiple schools around the east bay area. Provided 1-hour basic chemistry lessons once a month with four other volunteers.

Think College Now Elementary (2011) Oakland, CA. Teacher's aid assisting in grading, computer data input, and classroom activities.

Publications:

Chaves JE and Melis A (2017) Remodeling terpenoid metabolism in cyanbacteria for isoprene production. Manuscript in progress for submission in August 2017.

Chaves JE, Romero PR, Kirst H, Melis A (2017) Engineering isoprene synthase expression and activity in cyanobacteria. Manuscript submitted for publication June 20, 2017

Chaves JE, Romero PR, Kirst H, Melis A (2016) Role of isopentenyl-diphosphate isomerase in heterologous cyanobacterial (Synechocystis) isoprene production. Photosynth Res 130(13):517-527

Chaves JE, Kirst H, Melis A. (2014) Isoprene production in *Synechocystis* under alkaline and saline growth conditions. J Appl Phycol DOI: 10.1007/s10811-014-0395-2

Invited Oral Presentations:

Chaves JE, Romero PR, Kirst H, Melis A. "Engineering isoprene synthase expression and activity in cyanobacteria" at the 2nd International Solar Fuels Conference, UC San Diego, July 10, 2017.

Chaves JE, Romero PR, Kirst H, Melis A. "Engineering isoprene synthase expression and activity in cyanobacteria" at 7th International Conference on Algal Biomass, Biofuels and Bioproducts Conference, Miami FL, June 20, 2017.

Chaves JE, Romero PR, Kirst H, Melis A. "Engineering isoprene synthase expression and activity in cyanobacteria" at Photosynthesis, Carbon fixation, and the Environment Symposium, UC Berkeley, June 14, 2017.

Chaves JE, Bentley FK, Melis A. "Growth Media for Isoprene Production in Cyanobacterium *Synechocystis."* Science Transfer Project Meeting. California State University of Sacramento. Sacramento, CA. 13 September 2013. Part of a series of talks to inspire and encourage community college students from underserved populations in the Science Transfer Project program to pursue a higher education in the sciences.

Chaves JE, Bentley FK, Melis A. "Growth Media for Isoprene Production in Cyanobacterium *Synechocystis*." 22nd Western Photosynthesis Conference. Asilomar Conference Grounds, Pacific Grove, CA. 4 January 2013. Oral presentation.

Chaves JE, Williams T, McCarthy M. "Accumulation Capacity of Cigarette Tobacco Smoke on Cotton Fiber." Science Transfer Project Research Seminar. California State University of Sacramento, CA. 21 May 2008. Oral Presentation.

Chaves JE, McCarthy M. "The Potential use of Durian as an anti-cancer agent." Science Transfer Project Research Seminar. California State University of Sacramento, CA. 8

August 2008. Oral Presentation.

Posters at Meetings

Chaves JE, Bentley FK, Melis A**.** "Application of Alkalinity and Salinity for Cyanobacteria Production of Isoprene." International Solar Fuels Conference. Uppsala Concert and Congress. Uppsala, Sweden. 25 April 2015. Poster Presentation.

Chaves JE, Bentley FK, Melis A**.** "Application of Alkalinity and Salinity for Cyanobacteria Production of Isoprene." Berkeley Center for Green Chemistry: Challenges and Opportunities at the Intersection of Health, Materials, and the Built Environment. The David Brower Center. Berkeley, CA. 20 February 2014. Poster Presentation.

Chaves JE, Bentley FK, Melis A. "Growth Media for Isoprene Production in Cyanobacterium *Synechocystis."* Science Transfer Project Meeting. California State University of Sacramento. Sacramento, CA. 13 September 2013. Part of a series of talks to inspire and encourage community college students from underserved populations in the Science Transfer Project program to pursue a higher education in the sciences.

Chaves JE, Bentley FK, Melis A. "Optimizing Growth Media in Cyanobacterium *Synechocystis*." Comparative Biochemistry Graduate Program Reception. University of California Berkeley, Berkeley, CA. 19 November 2013. Poster presentation.

Chaves JE, Bentley FK, Melis A. "Optimizing Growth Media and Fuels Production in the Cyanobacterium *Synechocystis*." UC Berkeley "Cal Day". University of California Berkeley, CA. 21 April 2012. Poster presentation of Honors Research.

Chaves JE, Williams T, McCarthy M. "Accumulation Capacity of Cigarette Tobacco Smoke on Cotton Fiber." 20th Annual ACS Undergraduate Research Symposium. Santa Clara University, CA. 3 May 2008. Poster presentation.

Chapter 1: *Introduction*

1. Introduction

Cyanobacteria are photoautotrophic prokaryotes that use solar energy, CO_2, and H_2O to produce chemical energy and store it as biomass via oxygenic photosynthesis. The ability of cyanobacteria, like other photosynthetic systems, to carry out oxygenic photosynthesis at a high quantum yield (Ley and Mauzerall 1982; Bjorkman and Demmig 1987) makes them an excellent candidate for sunlight-driven production of renewable fuel and chemicals. Cyanobacteria can be cultivated in open racetrack ponds (Herrera et al. 1989) or closed photobioreactors (Melis 2012) on marginal land that is not suitable for agriculture, which would alleviate the issue of encroachment on land used for food crops.

Terpenoid products are a particularly attractive group of chemicals, as they are incredibly diverse, ranging in the tens of thousands of different molecules across all living organisms. This diversity lends itself to the ability to use the terpenoid biosynthetic pathway for the generation of a multitude of products including: pharmaceuticals, plastics, cosmetics, nutrition supplements, personal health care compounds, fuels, and general feedstock for the industrial chemical sector. Cyanobacteria produce terpenoids naturally through the methylerythritol 4-phosphate (MEP) pathway, mostly for the generation of pigments and prenyl molecules for photosynthesis. In this work, we reprogrammed carbon flux through the MEP pathway so as to enhance the photosynthetic production of the hemiterpene, isoprene (C_5H_8), heterologously conferred to the cyanobacterium *Synechocystis* sp PCC 6803.

In the context of product generation, the cyanobacterium *Synechocystis* sp. PCC6803 has been genetically engineered with a codon-optimized *Pueraria montana* (kudzu) isoprene synthase gene (Lindberg et al. 2010; Bentley and Melis 2012), conferring upon *Synechocystis* the property of photosynthetic isoprene hydrocarbon production (**Fig. 1.1**). Isoprene (2-methyl-1,3-butadiene; C_5H_8) is naturally produced by photosynthesis in the leaves of many species of trees, as well as other herbaceous and deciduous land plants and shrubs. Isoprene is synthesized in the chloroplast of the mesophyll cells, diffuses through the chloroplast envelope and the cell membrane and cell wall, and is emitted through the stomata of the leaves into the atmosphere. The yearly production of isoprene emissions by vegetation was estimated to be about 600 million metric tonnes (Guenther et al. 2006), with about half of that produced by tropical broadleaf trees, and the remainder originating from the photosynthesis of shrubs. Aquatic photosynthetic systems, however, including microalgae and cyanobacteria, are not endowed with the isoprene synthase gene and lack the isoprene production process (Lichtenthaler 2007; 2010). Isoprene hydrocarbons are a useful terpenoid product, currently serving as feedstock in the synthetic chemistry industry for the production of multiple commercial commodities such as rubber, adhesives, plastics and perfumes. It also has great potential to be used as a renewable fuel similarly to other short-chain hydrocarbons.

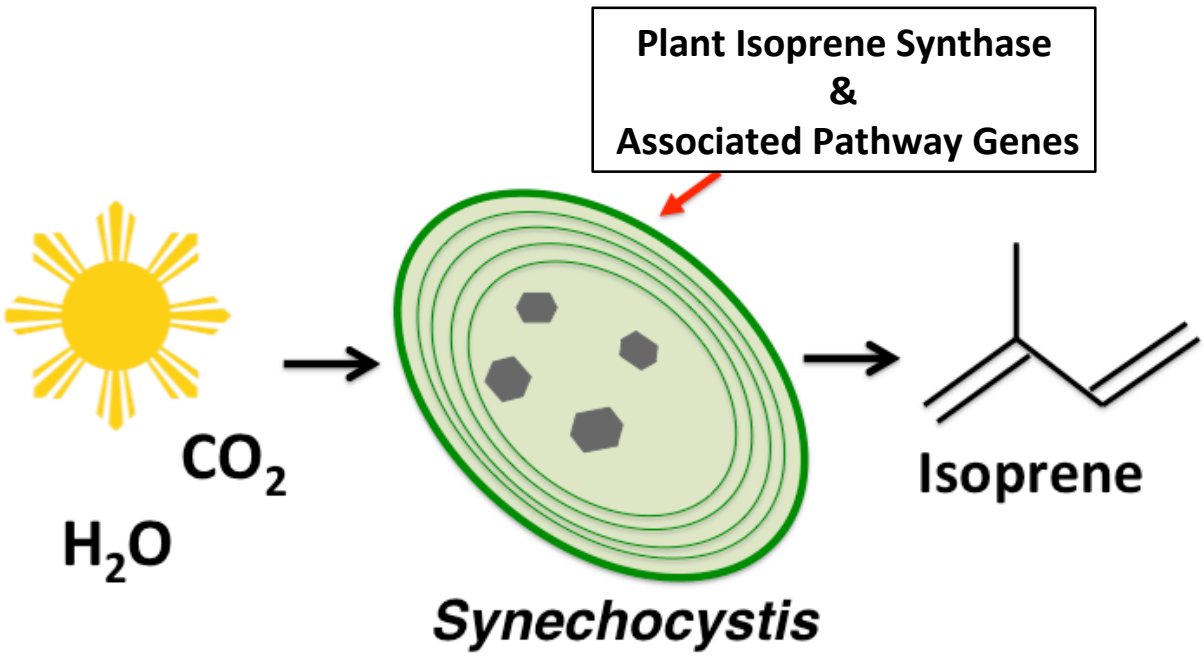

Fig. 1.1 Schematic depicting the endowment of photosynthetic production of isoprene in the cyanobacteria *Synechocystis*.

The process for cyanobacterial growth, and the sequestration and harvesting of the volatile isoprene molecules has been established in gaseous/aqueous two-phase photobioreactors (Bentley and Melis 2012). In the lab, this approach utilized custom made 1 L fed-batch bioreactors, which are fitted with a long aerator tube to enable delivery of gases (CO_2 or air), and a short tube with a septum for sampling the chemical composition of the gaseous headspace and the biomass content of the liquid phase (**Fig. 1.2**). Typically, cultures are flushed with CO_2, sufficient to fill the headspace, and then sealed to contain the isoprene produced by photosynthesis. **Chapter 2** of this work has further optimized this process for commercial scale up through the utilization of a saline/alkaline growth media for contamination avoidance and resource mitigation.

Terpenoids are the largest class of naturally occurring chemicals. They are functionally important as the basis of photosynthetic pigments comprising the phytol tail of chlorophylls, all carotenoids, quinone prenyl side-chains, growth regulators and plant hormones such as abscisic acid (ABA) and gibberellic acid, and structural components of cell walls and membranes such as bactoprenol and steroids. In addition, they are the source of plant defensive compounds against herbivores, and the molecules that confer scents and fragrance to leaves and flowers.

The universal precursors for terpenoid synthesis in plants, animals, insects, and microorganisms are the 5-carbon metabolites isopentenyl diphosphate (IPP) and its isomeric form dimethylallyl diphosphate (DMAPP) (Lichtenthaler 2007; 2010). In cyanobacteria, microalgae, and plant chloroplasts, IPP and DMAPP are generated through the MEP pathway from glyceraldehyde-3-phosphate (G3P) and pyruvate (Pyr) by the action of a set of seven consecutive enzymatic reactions (Bentley et al. 2014), with the final enzyme, 4-hydroxy-3-methyl-2-(E)-butenyl-diphosphate reductase (*IspH*) generating an IPP/DMAPP ratio of 3:1 (McGarvey and Croteau 1995; Lichtenthaler 2010; Formighieri and Melis 2014), but measured to be 5.6:1 in tobacco (Tritsch et al. 2010) and 6:1 in *E. coli* (Adam et al. 2002). Most isoprenoid synthesis occurs upon head-to-tail additions of one or several IPPs to DMAPP (Lichthenthaler 2010), yielding molecules with 10, 15, 20, or greater than 40 5-carbon structures (**Fig. 1.3**). Therefore, a high IPP-to-DMAPP steady-state ratio makes sense, as there is a greater requirement for IPP than for DMAPP for the synthesis of the vast majority of isoprenoid products. However, the isoprene synthase utilizes only DMAPP as a substrate for isoprene production. **Chapter 3** describes a method to drive carbon flux away from IPP into DMAPP by overexpression of a heterologous isopentenyl diphosphate isomerase (FNI) from *Streptococcus pneumoniae.*

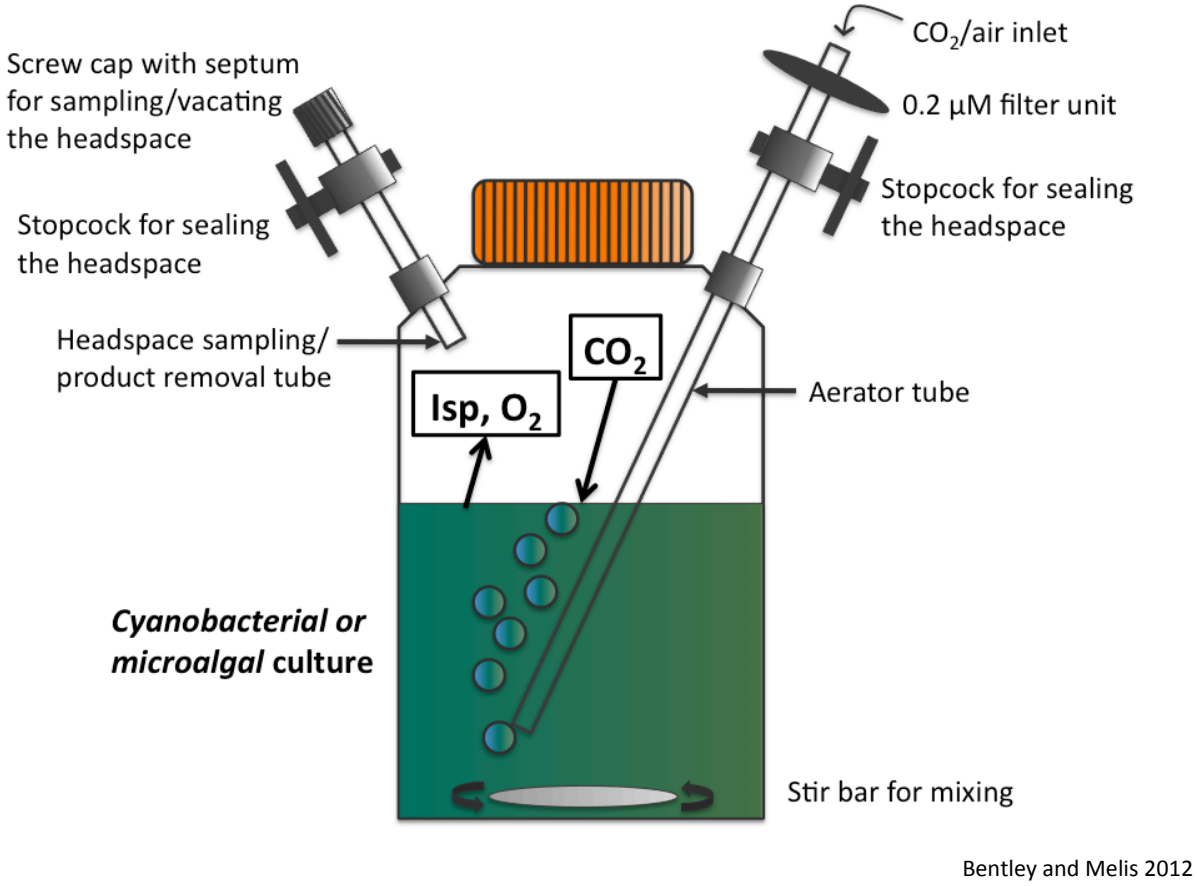

Fig. 1.2 Gaseous/aqueous two-phase photobioreactor.

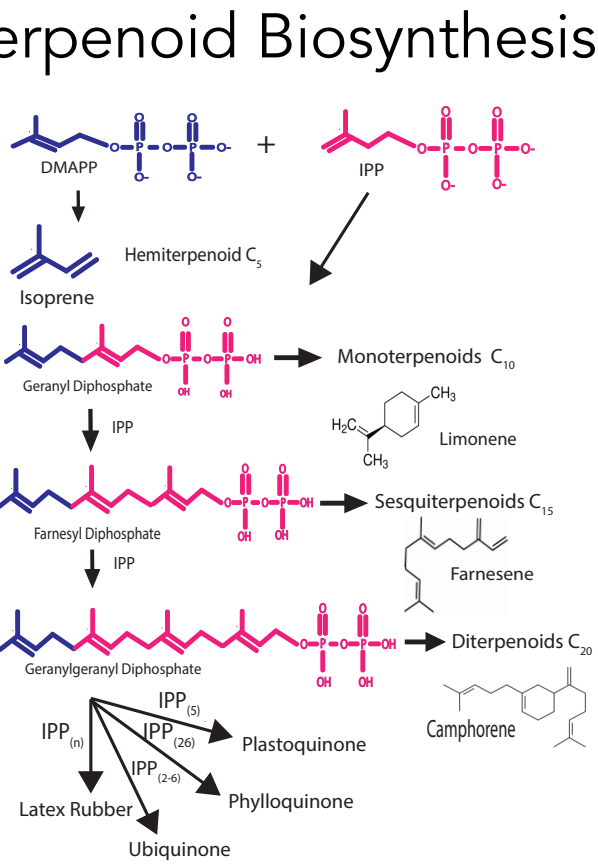

Fig. 1.3 Biosynthesis of terpenoid molecules from dimethylallyl diphosphate (DMAPP) and isotentenyl diphosphate (IPP).

Engineering of microbes for isoprene (C_5H_8) production has shown a requirement for improvements and modifications to address a number of different rate and yield limitations in the targeted biosynthetic pathway. In general, transgene expression for heterologous product synthesis requires finding and optimizing novel transcriptional regulators such as strong and/or inducible promoters, and ribosome binding sites (Oliver et al. 2014; Zhou et al. 2014; Kim et al. 2016; Wang et al. 2017). Overexpression of terpene synthase enzymes, all of which appear to have a slow k_{cat}, poses an additional unique set of problems. Previous studies, including papers from this lab (Lindberg et al. 2010, Bentley and Melis 2012; 2014; Aremu et al., 2014, Chaves et al. 2016; Gao et al. 2016, Pade et al. 2016), focused on isoprene synthase transgene codon-use optimization, mode of cyanobacterial transformation, as well as enhancements in the flux of endogenous cellular carbon to the universal terpenoid precursors isopentenyl-diphosphate (IPP) and dimethylallyl-diphosphate (DMAPP). However, the critical question of the level of expression of the terpenoid biosynthetic pathway transgenes has not been investigated. This question is central to the quest for high yields of isoprene production, measured as the isoprene to biomass carbon partitioning ratio of the process (Melis 2013) because the terpenoid biosynthetic pathway enzymes, and especially that of the isoprene synthase, have a very slow k_{cat}, in the range of 4-5 s^{-1} (Sasaki et al. 2005; Zurbriggen et al. 2012). A successful strategy by which to overcome the slow k_{cat} of transgenic or native enzymes is to overexpress the enzyme in question so that greater amounts of the desired enzyme could compensate for their slow k_{cat}. Example of this successful strategy is offered by the ribulose-1,5-bisphosphate carboxylase/oxygenase (Rubisco), which has a slow k_{cat}, in the range of 3-4 s^{-1} (McNevin et al. 2006). Nature's solution to the slow Rubisco k_{cat} was to substantially enhance the amount of the Rubisco protein in the stroma of the photosynthetic apparatus, making Rubisco one the most abundant proteins on Earth (Formighieri and Melis 2014). In **Chapter 4**, we fused the isoprene synthase to the most abundant protein in the cyanobacterial cell, the β-subunit of phycocyanin, to greatly overexpress the isoprene synthase protein.

In **Chapter 5**, we combined the methods developed in **Chapter 3** and **Chapter 4**, overexpressing both the FNI and the IspS fusion proteins in the same recipient cell. This combination resulted in up to 62-fold increase in isoprene production, reaching a yield of 12.3 mg g^{-1} (isoprene to biomass, w:w).

Chapter 2: *Isoprene production in Synechocystis under alkaline and saline growth conditions*

This work was published in the following scientific journal:

Chaves JE, Kirst H, Melis A (2015) Isoprene production in Synechocystis under alkaline and saline growth conditions. J Appl Phycol 27(3):1089-1097

This work was performed with the following persons:

JEC performed the experimental work. HK and AM assisted with experimental design. JEC and AM wrote the manuscript.

2.1 Introduction

In addition to the above-mentioned properties of cyanobacteria that make them attractive for bio-based chemicals production, many cyanobacteria strains have the capacity to tolerate extreme environmental conditions such as alkaline pH and salinity (Pikuta et al. 2007). Growth media poised at alkaline pH is desirable, as it would permit growth of the cyanobacteria, while at the same time discouraging the growth of other invading alkaline intolerant contaminants and predatory microbes and grazers (McGinn et al. 2011). Example of this premise is offered by the carbonate-requiring alkalophilic cyanobacteria *Arthrospira platensis* and *Arthrospira maxima* (*Spirulina* commercially), which thrive at high concentrations of Na-carbonate at pH values 9–11, conditions that prevent most predatory microbes and grazers from establishing themselves in the cultures (Dismukes et al. 2008). The ability of *Synechocystis* to be grown in a saline environment presents the opportunity to use seawater for cultivation instead of fresh water, a limited resource. In a commercial scale up setting in which cultures are grown continuously in vast quantities of non-sterile water, these properties are potentially valuable. In this work, we further developed the gaseous/aqueous two-phase photobioreactor system with *Synechocystis* to operate under alkaline pH and salinity conditions. Rates of growth and isoprene production in *Synechocystis* transformed with the *SkIspS* gene are reported under these extremophile conditions. The results suggest a practical method by which to prevent contamination and reduce resource demand of the *Synechocystis* growth media suitable for application in commercial scale up.

2.2 Materials and Methods

Strains employed. The wild type strain of *Synechocystis* sp. PCC 6803 and its *SkIspS* transformant (Lindberg et al. 2010; Bentley and Melis 2012) containing the codon-optimized kudzu isoprene synthase gene were used in this study. Both strains were maintained on 1% agar BG-11 plates supplemented with 10 mM TES-NaOH (pH 8.2), 0.3% sodium thiosulfate, and 5 mM glucose. The transformant strain was maintained on plates containing 25 µg/mL kanamycin. For acclimation purposes, the *SkIspS* transformant strain was also maintained on plates containing 25 mM $NaHCO_3$ (pH 10.5), and 100 mM, 200 mM, or 600 mM NaCl in addition to the 25 µg/mL kanamycin. Liquid cultures were grown in BG-11 media containing 25 mM of 4-(2-Hydroxyethyl)piperazine-1-ethanesulfonic acid (HEPES; pK=7.5)**,** Tricine (pK=8.1), 3-(Cyclohexylamino)-1-propanesulfonic acid (CAPS; pK=10.5), Na_2CO_3 (pK_b=10.2) or Na_2HPO_4, (pK_b=7.0) depending on the target pH of each culture.

Growth conditions. Growth of *Synechocystis* wild type and *SkIspS* cultures at different pH values were conducted in 300 mL starter cultures, which were grown for 2-3 days in BG-11 media supplemented with 25 mM HEPES (pH 7.5) or 25 mM CAPS (pH 10) for each strain. Starter cultures for *SkIspS* transformants were grown in the presence of 25 µg/mL kanamycin.

Experimental cultures were then inoculated from starter cultures into pH 7, 8, 9, 10, and 11 media at an $OD_{730}\approx0.05$. The pH of these cultures was under the control of a buffer (HEPES, TRICINE, or CAPS) selected according to the pKa of the compound, at a concentration of 25

mM. All cultures were grown at 25°C under constant aeration and illumination at 75 μmol photons m^{-2} s^{-1} for 6-10 days.

Comparative growth analysis of *Synechocystis* wild type and *SkIspS* strains at pH 10 was conducted under defined salinity conditions in 300 mL starter cultures, which were grown for 2-3 days in BG-11 media supplemented with 25 mM Na_2CO_3 (pH 10.5). Starter cultures in media with salinity at 100, 200, or 600 mM NaCl were grown only at pH 10.5.

Batch culture growth for isoprene production. Gaseous/Aqueous two-phase bioreactors (Bentley and Melis 2012) were inoculated with 700 mL cultures of *Synechocystis* cells at an OD_{730}=0.05 in BG-11 media containing 25 mM of Na_2HPO_4 at pH 7 or 25 mM of Na_2CO_3 and at pH 10.5. Cultures with 100, 200 or 600 mM NaCl were grown only at pH 10.5. Cultures were grown at 25°C under continuous illumination at 75 μmol photons m^{-2} s^{-1}, and continuous aeration until an OD_{730} of 0.4-0.5 was reached. Inorganic carbon in the form of 100% CO_2 was slowly bubbled through the bottom of the liquid culture in the reactor for a total of 5 s, delivering about 100 mL of 100% CO_2. By varying the volume of 100% CO_2 bubbled through the culture, we determined that 100 mL of 100% CO_2 was necessary and sufficient to support growth without causing pH changes to the growth medium. The presence of 25 mM $NaHCO_3$/Na_2CO_3 in the growth media contributed to the inorganic carbon supply and also supported cell growth.

After flushing with 100% CO_2, the reactor was then sealed to prevent exchange of gases with the surrounding atmosphere and also to prevent escape of the isoprene vapor accumulating in the culture headspace. The sealed reactor was incubated under continuous slow stirring and illumination of 150 μmol photons m^{-2} s^{-1} at 35°C. Isoprene accumulation was measured every 24 h by GC analysis upon sampling the headspace of the reactor. Small aliquots from the liquid phase were also removed every 24 h for biomass accumulation measurements. Following this sampling, the reactor was flushed with 100 mL of 100% CO_2, and sealed again for another 24 h cycle. This cycle was repeated every 24 h for up to 96 h.

Growth analysis, pigment determination, and isoprene quantification. Growth curves of *Synechocystis* wild type and *SkIspS* transformants were plotted from measurements of culture aliquots taken every 24 h, analyzing optical density of the culture at 730 nm with a Shimadzu UV-1800 UV-Vis spectrophotometer. Growth was independently assessed gravimetrically from the dry cell biomass by filtering 5-10 mL culture aliquots through 0.22 μm Millipore filters, thoroughly washing the samples with 10-20 mL of distilled water in order to remove extraneous salts, then drying each sample at 90°C for 6 h and measuring the dry cell weight (dcw). Chlorophyll *a* was quantified from 1 mL culture aliquots upon pigment extraction with 100% methanol and spectrophotometric quantification of the pigments at 665 nm according to Lichthenthaler (1987). The pH of each culture bubbled with air was measured at time zero, before aeration began, and at the end of each growth experiment (6-10 days), with a Fisher Scientific Dual Channel pH/Ion meter. The pH of each culture bubbled with 100% CO_2 was measured every 24 h, before the repeat flushing of the culture with CO_2.

Isoprene was quantified from its GC signal amplitude upon injection of 1 mL gaseous aliquot from the reactor headspace (**Fig. 2.1**), based on a calibration curve constructed from serial dilutions of vaporized isoprene standard, measured with a Shimadzu 8A GC apparatus

(Shimadzu, Columbia, MD) (**Fig. 2.2**). For the calibration curve, 1 mL sample from each vaporized standard was injected in the GC and the peak amplitude of the sample was recorded (**Fig. 2.1**). Resultant peak areas (in cm^2) were plotted against the known amount of isoprene injected (in μg, **Fig. 2.2**)) and the slope of the standard curve was used to determine the amount of isoprene produced by *SkIspS* transformants in experimental cultures.

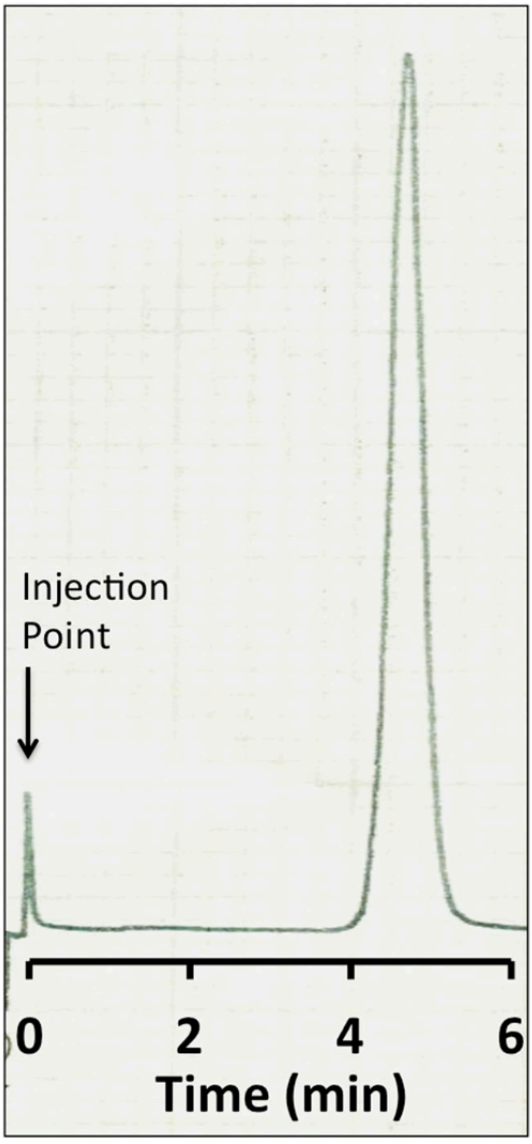

Fig. 2.1 Gas chromatography analysis of isoprene (2-methyl-1,3-butadiene; C_5H_8) standard. One mL of a vaporized isoprene sample comprising 0.087 µg pure isoprene was injected into the column inlet of the GC. The retention time for isoprene under these GC conditions was 4.3 min. Samples collected from the headspace of experimental cultures were similarly analyzed from their single peak amplitudes at 4.3 min.

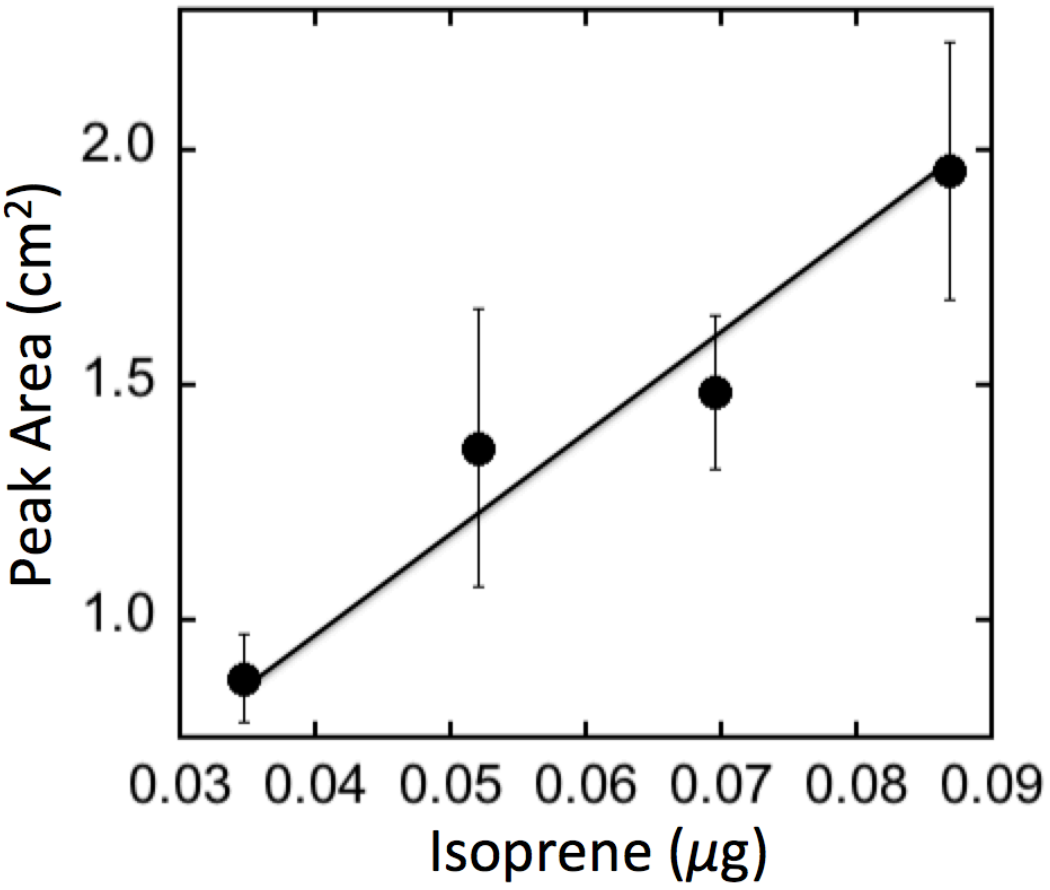

Fig. 2.2 Isoprene calibration curve. Serial dilutions of pure vaporized isoprene standard were prepared, and a 1 mL aliquot of each dilution was injected into the column inlet of the GC. The peak area produced by the chromatogram is plotted as a function of the amount of isoprene (μg) injected in each 1 mL sample. The slope of the straight line was used to determine the amount of isoprene produced in experimental cultures.

2.3 Results

Cell growth and isoprene production as a function of pH upon bubbling with air. The photoautotrophic rate of growth of the *Synechocystis* wild type and the *SkIspS* transformant was about the same at each pH tested: 7, 8, 9, and 10, under a light intensity of 75 μmol photons m^{-2} s^{-1} at 25°C and continuous bubbling with air in 300 mL liquid cultures (**Fig. 2.3**). The doubling time was calculated at each condition by measuring the duplication rate during the exponential growth phase. Under these light-limiting conditions, the wild type registered an average doubling time of 33 h (**Fig. 2.3A**), and the *SkIspS* transformants had an average doubling time of 32 h at pH 7 and 8, and an average doubling time of 26 h at pH 10 and 11 (**Fig. 2.3B**). A systematic analysis of the average doubling times of wild type and SkIspS transformant as a function of the pH of the culture medium is shown in **Fig. 2.4**. The results showed that alkaline conditions were more favorable to growth, as they accelerated cell duplication time in both the wild type and the *SkIspS* transformants; further showing that alkalinity has no adverse effect on the fitness and growth of *Synechocystis*. It is also of interest to note that the *SkIspS* transformants appeared to grow faster, by about 15%, relative to the wild type, regardless of the pH of the medium, an observation consistent with earlier results by Bentley and Melis (2012).

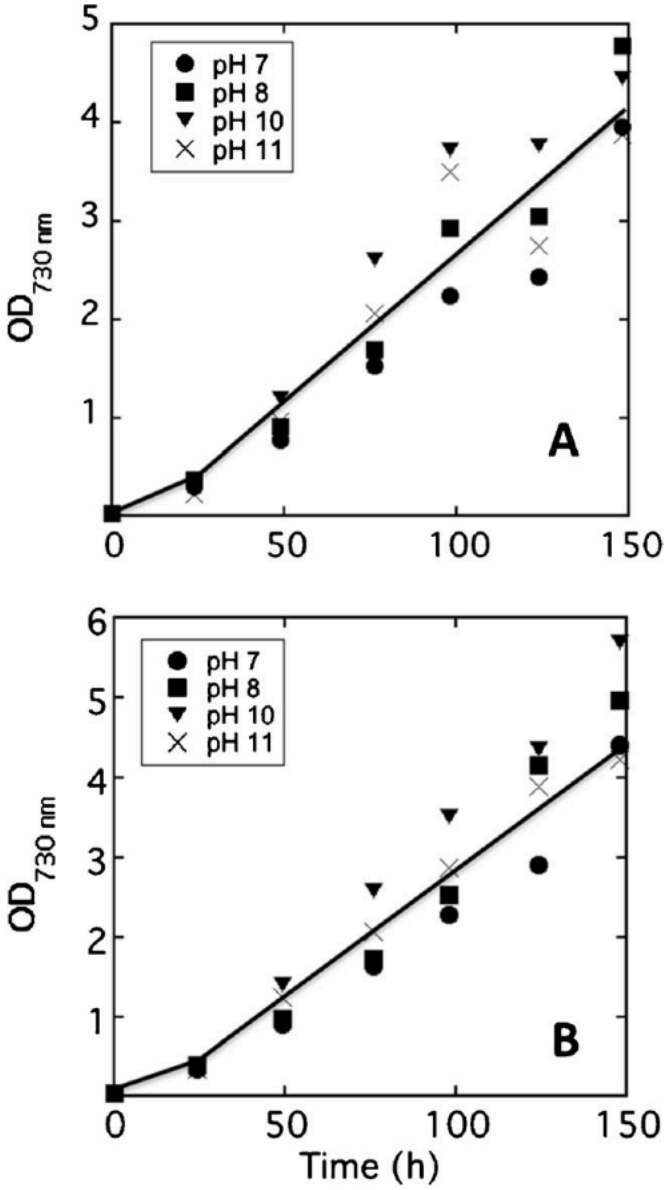

Fig. 2.3 Photoautotrophic growth of *Synechocystis* wild type (A) and *SkIspS* cell lines (B). Cells were grown in 300 mL liquid cultures of BG-11 supplemented with 25 mM of Hepes (pH 7 and 8), Tricine (pH 9), or CAPS (pH 10 and 11), under conditions of continuous slow aeration and illumination of 75 µmol photons m^{-2} s^{-1} for 150 h. Growth of the set of four cultures was measured in three independent experiments. Standard error of the points shown for the cultures grown at pH 7 was ±0.06, at pH 8 was ±0.08, at pH 10 was ±0.03, and at pH 11 was ±0.08.

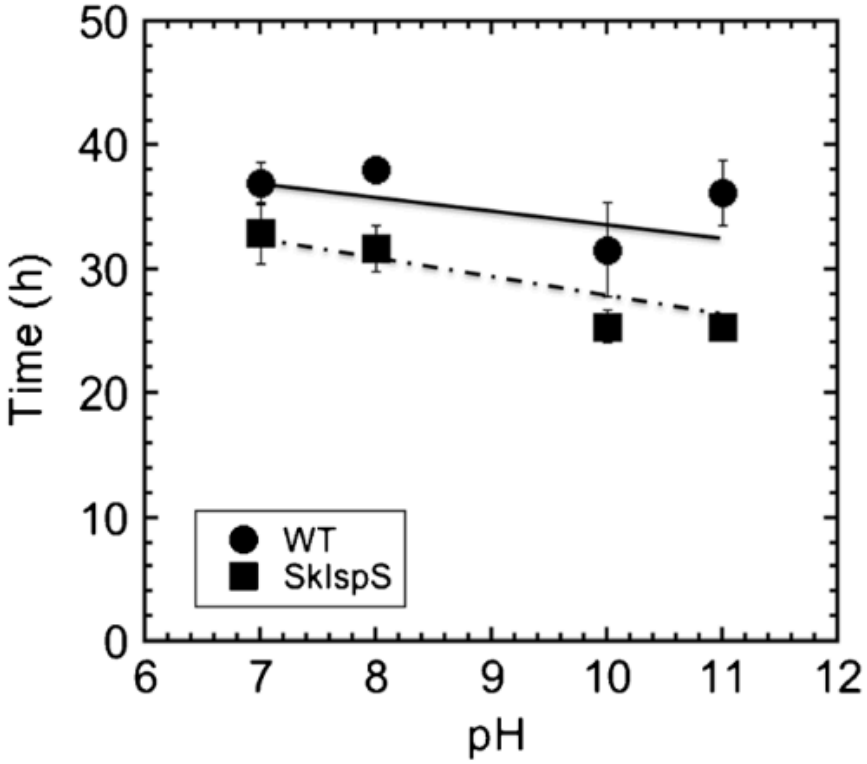

Fig. 2.4 Cell duplication time of *Synechocystis* as a function of pH under conditions of continuous slow aeration and illumination. Wild type cells (circles) and *SkIspS* transformants (squares). For other conditions, please see legend of Fig. 2.3.

Cell growth and isoprene production as a function of pH upon filling the reactor with 100% CO_2. Rates of wild type and *SkIspS* transformant growth was also determined in the sealed gaseous-aqueous two-phase 1 L reactor developed by Bentley and Melis (2012). In this case, inoculated cultures were first bubbled with air for 2 days to bring up the biomass prior to placement in the Bentley-Melis reactor. The aqueous phase of the reactor (700 mL) contained the culture, whereas the gaseous phase (500 mL) was supplemented with 100% CO_2, slowly bubbled into the bottom of the liquid culture, so as to fill the gaseous phase (Bentley and Melis 2012). Cells were grown in such sealed reactors under a light intensity of 150 μmol photons m^{-2} s^{-1} at 35°C. At both pH 7 and pH 10, cell mass accumulation increased linearly and by approximately 7 fold over 96 h, as measured by optical density at 730 nm (**Fig. 2.5A**). The dry cell biomass of these cultures accumulated at a rate of 6.3 mg L^{-1} h^{-1} under both pH 7 and pH 10 growth conditions (**Fig. 2.5B**), indicating that the *SkIspS* transformants were able to grow equally well under alkaline pH, when cultivated in the gaseous-aqueous two-phase reactor with 100% CO_2. The pH of the culture in the liquid phase was measured every 24 h to determine whether there were changes due to cell nutrient uptake or CO_2 bubbling. We found that the pH of the cultures inoculated at pH 10 was maintained between 9.6 and 10.4 (**Fig. 2.5C, squares**). Cultures inoculated at pH 7 showed an increase in pH to 7.8 at time point zero after 2 days of bubbling with air. Thereafter, they showed a pH fluctuation between 7.5 and 8.2 for the majority of the experiments. Occasionally, the pH of these cultures increased to 9.2 during the last 24 h of the 96 h growth period (**Fig. 2.5C, circles**). This increase in pH is understood to originate from OH^- efflux from the cells in a process designed to balance the HCO_3^- and nutrient uptake by the cells, and is manifested when the buffering capacity of the system is not adequate (Naus and Melis 1991; Sonoda et al. 1998). Isoprene production by the *Synechocystis* cells and accumulation of these volatile hydrocarbons in the gaseous phase of the reactor occurred with a rate of about 0.63 μg L^{-1} h^{-1}, statistically indistinguishable among the samples grown at pH 7 (**Fig. 2.5D, circles**) or pH 10 (**Fig. 2.5D, squares**).

At the end of the 96 h growth period, cultures were routinely examined, both visually and microscopically to assess health and robustness of the cells (**Fig. 2.6**). Results routinely revealed that wild type and the *SkIspS* transformant strains both were able to grow equally well under neutral (**Fig. 2.6A,B**) or alkaline pH (**Fig. 2.6C,D**), when cultivated in the gaseous-aqueous two-phase reactor with supplemental 100% CO_2 bubbled through the culture.

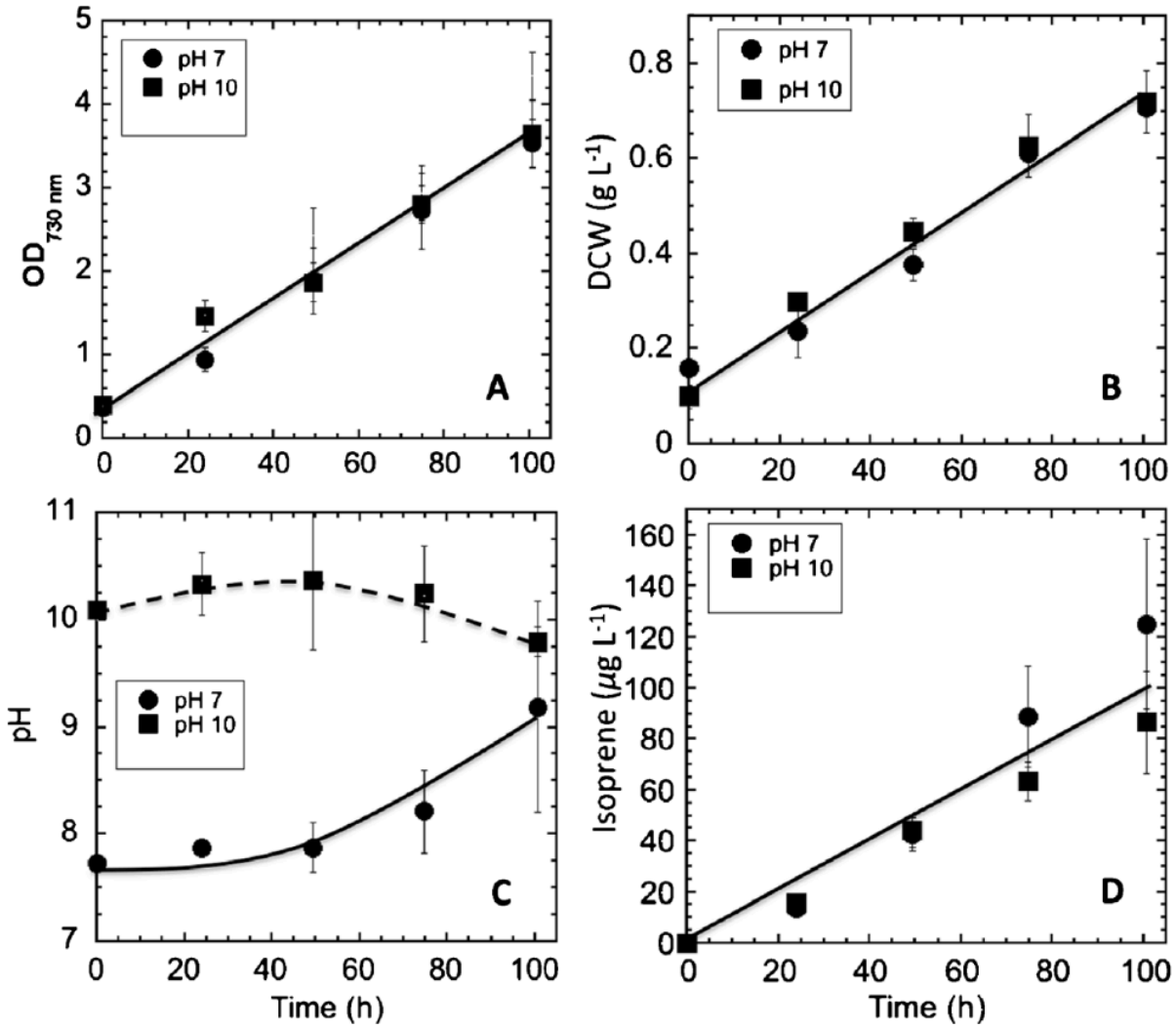

Fig. 2.5 Photoautotrophic growth of *Synechocystis SkIspS* transformants suspended at pH 7 (circles) and pH 10 (squares). A sealed gaseous-aqueous two-phase 1 L reactor (Bentley and Melis (2012) was used for these measurements. The liquid culture comprised 700 mL of pH 7 or pH 10 growth medium, which was bubbled with 100 mL of 100% CO_2, sealed, and incubated for 24 h under continuous illumination of 150 μmol photons m^{-2} s^{-1}, prior to measurement. The liquid phase $OD_{730\ nm}$, (**A**) DCW (**B**), and pH (**C**), and the gaseous phase isoprene content (**D**) were measured every 24 h. Following this 24 h sampling, the reactor was flushed with 100 mL of 100% CO_2 to purge the accumulated products of photosynthesis and to replenish the inorganic carbon supply so as to enable a resumption of photosynthesis and growth.

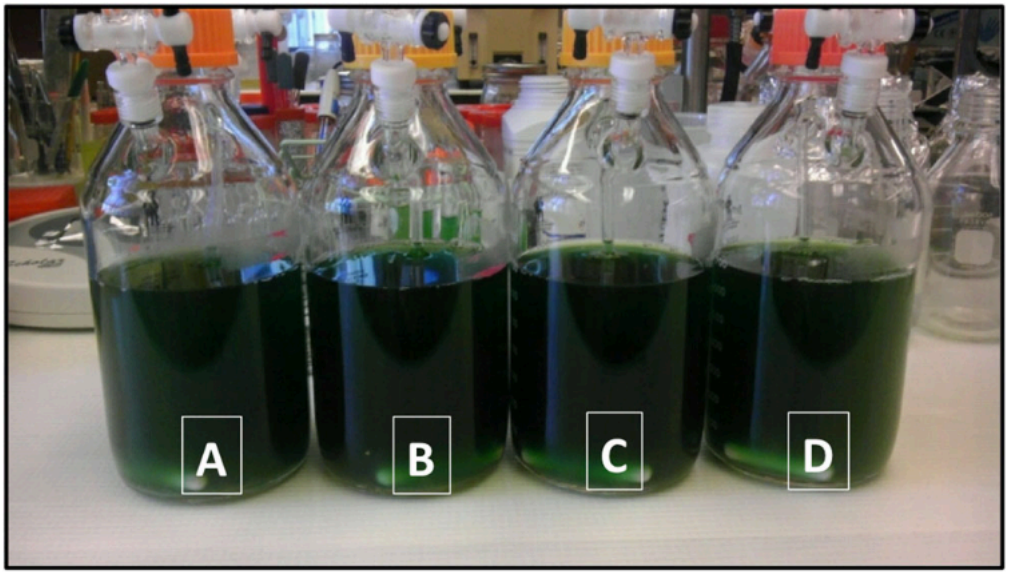

Fig. 2.6 Gaseous-aqueous two-phase reactors for the growth of Synechocystis *SkIspS* transformants under sealed conditions (Bentley and Melis 2012). The 500 mL headspace of the reactors was bubbled with 100 mL of 100% CO_2 every 24 h. Isoprene accumulating in the headspace during photosynthesis of the cyanobacteria was quantified every 24 h prior to refilling the reactor with CO_2. The cultures shown were grown for 96 h at pH 7 (**A, B**), and pH 10 (**C, D**).

Cell growth and isoprene production under alkaline and saline conditions. Photoautotrophic growth and isoprene production were measured at pH 10 with an additional salinity load to the growth medium. Cell growth and biomass accumulation at pH 10 in the presence of 100 or 200 mM NaCl were the same as the control, with an average increase in $OD_{730\ nm}$ of approximately 6.6 fold over 96 hours (**Fig. 2.7A,** solid symbols). The optical density $OD_{730\ nm}$ increase in the presence of 600 mM NaCl was also linear during growth (**Fig. 2.7A,** x symbols), although the slope of the growth curve at 600 mM NaCl was about half of that measured with the lower NaCl concentrations. This signifies changes in the optical properties of and scattering of light by the cells at the 600 mM NaCl concentration.

Cell biomass accumulated at a rate of 6.8 mg L^{-1} h^{-1} under most salinity conditions examined, i.e., pH 10 without salinity, and pH 10 with 100 and 200 mM added NaCl (**Fig. 2.7B**). For cells grown in the presence of 600 mM NaCl, there was a ~24 h lag, after which the rate of biomass accumulation reached 7.4 mg L^{-1} h^{-1}, i.e., similar to that measured in the other cultures **(Fig. 2.7B)**. These results showed that *Synechocystis* wild type and transformants have the capacity to grow normally under the combination of two extreme media conditions, i.e., higher than normal pH and salinity, up to that encountered in seawater (600 mM). Absorbance spectra of these cells were measured at the exponential growth phase of the cultures (**Fig. 2.7C**). The spectra were normalized to the absorbance maximum of phycocyanin at 625 nm. It was then revealed that the Chl *a* absorbance maximum at 678 nm was greater for the cells grown in the presence of NaCl than that in the control. These results suggested a greater Chl *a*/phycobilisome ratio under salinity compared to the control (**Fig. 2.7C**). As Chl *a* is the dominant light-harvesting pigment of PSI, and phycocyanin is the dominant light-harvesting pigment of PSII (Glazer and Melis 1987), the results suggest a higher PSI relative to PSII content in cells grown under salinity conditions. This hypothesis was tested upon application of direct light-*minus*-dark absorbance difference spectrophotometric measurements for the quantification of PSI and PSII in *Synechocystis SkIspS* transformant thylakoids (Melis 1989). Results from this analysis are shown in **Table 2.1**. A PSI/PSII ratio of 4.5:1 was measured in BG11 pH 10 grown cells. The ratio was elevated to 5.6:1 when cells were grown in BG11 pH 10 plus salinity. These results are consistent with previous studies, showing that salt loading in *Synechocystis* can result in an increase in PSI content to enhance cyclic electron flow, thus increasing the production of ATP (Manodori and Melis 1984) for salt extrusion (Schubert and Hagemann 1990).

Isoprene production measurements from these samples showed that, within the error of the measurement, rate and yield were not significantly changed by an increase in salinity (**Fig. 2.7D**). An average rate of isoprene accumulation of 0.48 μg L^{-1} h^{-1} was measured under most conditions, i.e., pH 10 without salinity, and pH 10 with 100 or 200 mM added NaCl. As with the respective growth curves, cells grown in the presence of 600 mM NaCl showed a ~24 h lag in isoprene production, however, at later times between 24 and 96 h, isoprene accumulation for the 600 mM NaCl cells approached that of the other cultures at 0.41 μg L^{-1} h^{-1} (Fig. 7D). The average amount of carbon partitioning to isoprene versus carbon to biomass was calculated based on the amount of isoprene produced compared to the amount of biomass (dcw) generated. The carbon-partitioning ratio was estimated to be in the range of 0.01-0.02% at pH 10, regardless of the salinity conditions employed (**Fig. 2.8**).

At the end of the 96 h growth period, alkaline and saline *SkIspS* transformant cultures were examined visually and microscopically to assess health and robustness of the cells (**Fig. 2.9**). Results showed that the *SkIspS* transformant strains were equally healthy in the absence (**Fig. 2.9A**) or presence of 100, 200 or 600 mM salinity in the growth medium (**Fig. 2.9B-D**).

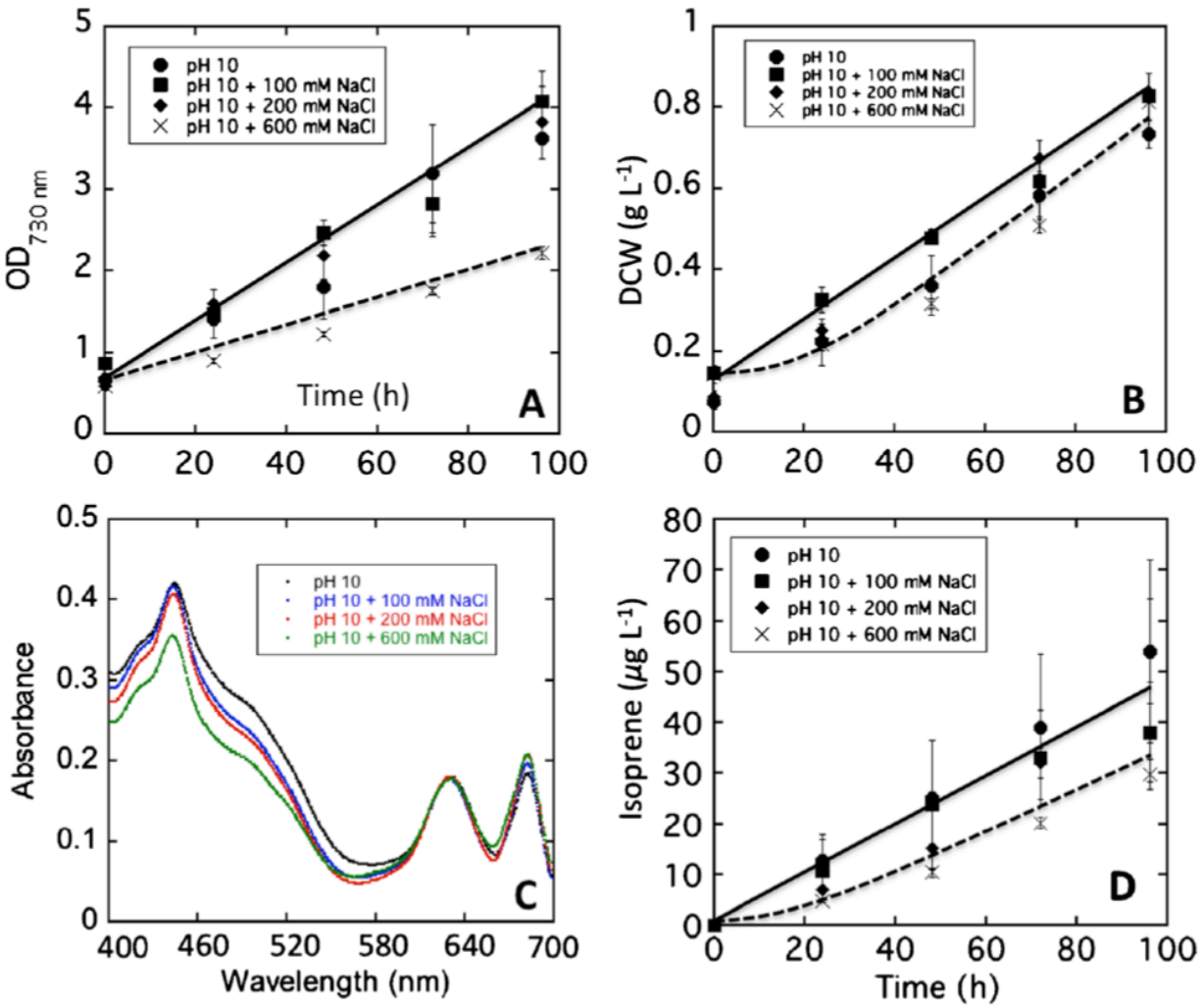

Fig. 2.7 Photoautotrophic growth of the *SkIspS* transformant strains at pH 10 without added salinity (circles), with 100 mM NaCl (squares), 200 mM NaCl (diamonds), or 600 mM NaCl (crosses). A sealed gaseous-aqueous two-phase 1 L reactor was used for these measurements. The 700 mL cultures were bubbled with 100 mL of 100% CO_2 every 24 h under continuous illumination, for a growth period of 96 h. Growth was measured as $OD_{730\ nm}$ (**A**) and dry cell weight (**B**). Pigment content (**C**) was evaluated from the absorbance spectra of intact *SkIspS* transformant strains grown at pH 10 without added salinity (black line), with 100 mM NaCl (red line), 200 mM NaCl (blue line), or 600 mM NaCl (green line). The absorbance spectra were normalized to the 625 nm phycocyanin maximum. Isoprene accumulation was also measured as a function of time every 24 h during culture incubation and cell growth (**D**).

Table 2.1. Chlorophyll and photosystem reaction center ratios in *Synechocystis SkIspS* transformant cells grown photoautotrophically in BG11 medium (control), or in the presence of 100, 200, and 600 mM salinity. The PSI/PSII photosystem stoichiometry was derived from the spectrophotometrically determined Chl/P700 (for PSI) and Chl/Q_A (for PSII) ratio of the respective samples, from which the PSI/PSII ratio was derived (Melis 1989).

Parameter measured	**BG11**	**BG11 + 100 mM NaCl**	**BG11 + 200 mM NaCl**	**BG11 + 600 mM NaCl**
Chl/P700	150±5	157±5	155±7	169±17
Chl/Q_A	672±95	908±27	863±37	924±88
PSI/PSII	4.5±0.7	5.8±0.2	5.6±0.4	5.5±0.8

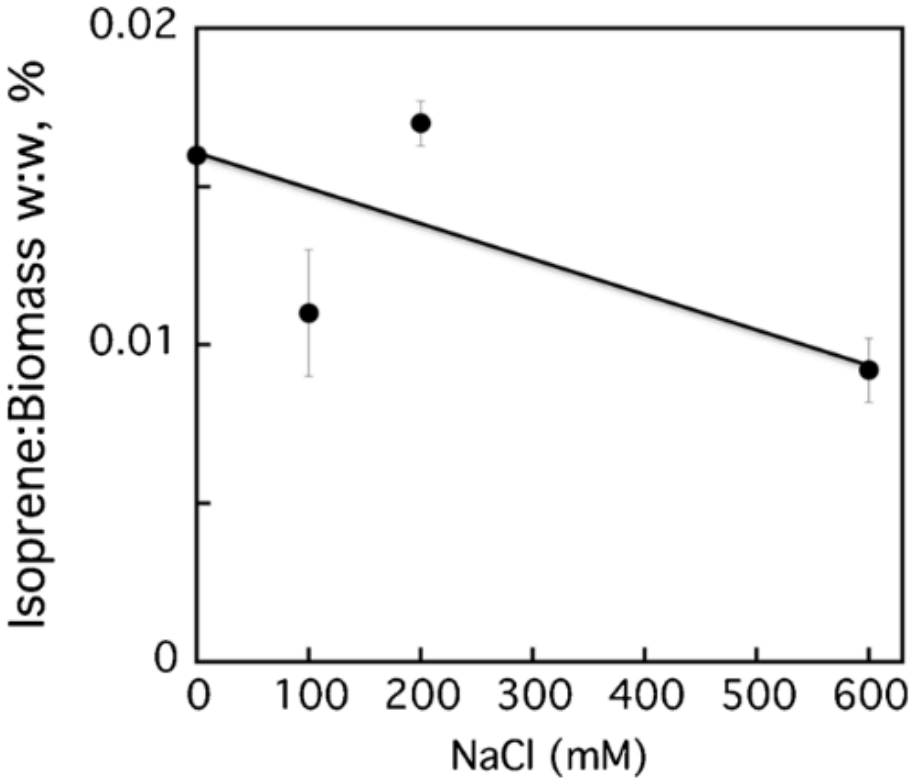

Fig. 2.8 Isoprene to biomass carbon partitioning ratios. *SkIspS* transformant strains were grown at pH 10 without added salinity, with 100, 200 or 600 mM NaCl for 96 hours. The biomass and respective isoprene accumulation were measured and calculated for each growth condition. The amount of carbon partitioned to isoprene was calculated based on the weight of isoprene produced compared to the weight of biomass produced, assuming that approximately one half of the *Synechocystis* biomass is contributed by carbon.

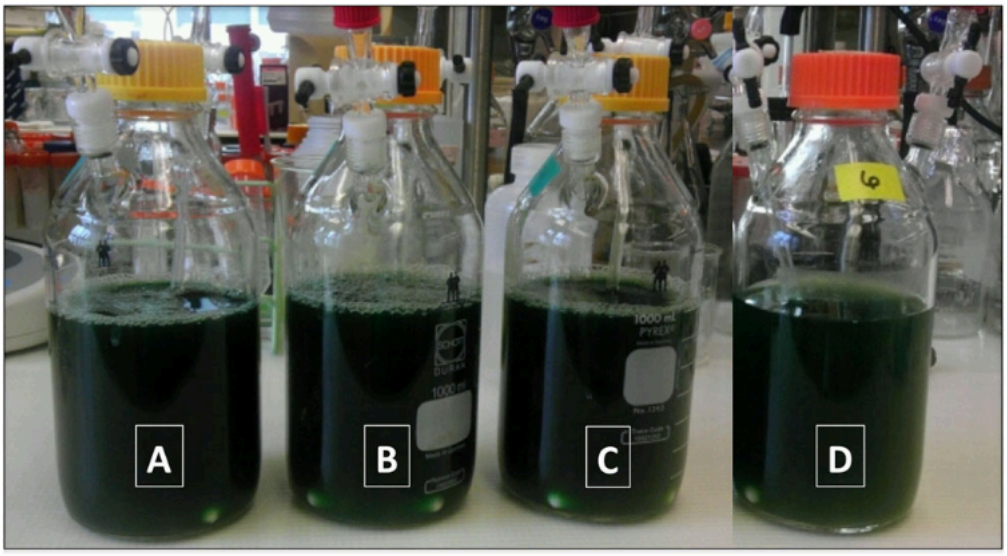

Fig. 2.9 Gaseous-aqueous two-phase reactors for the growth of *SkIspS* transformants under sealed conditions. The 500 mL headspace of the reactors were filled with 100 mL of 100% CO_2 every 24 h. Isoprene accumulating in the headspace during photosynthesis of the cyanobacteria was quantified every 24 h, prior to refilling of the reactor with CO_2. The cultures shown were grown for 96 h at pH 10 without added salinity (**A**), with 100 mM NaCl (**B**), 200 mM NaCl (**C**), or with 600 mM NaCl (**D**).

2.4 Discussion

The transformant *SkIspS* strain of *Synechocystis* has helped validate the notion of "Photosynthetic Biofuels", entailing heterologous transformation of a photosynthetic microorganism to endow the property of synthesis and release of isoprene in the aquatic environment (Lindberg et al. 2010; Bentley et al. 2012). The present work contributed a practically important approach for *SkIspS* transformant growth and isoprene production under a combination of alkaline pH and salinity. A previous study has shown that *Synechocystis* is able to survive under higher than normal pH through the up-regulation of many genes that help maintain the intracellular pH, including those encoding monovalent cation/anion antiporters that import protons (Summerfield and Sherman 2008). The ability to grow under alkaline pH is particularly important because high pH can substantially lower the number of contaminants, opportunistic microorganisms, and cyanobacterial grazers from invading and crashing a mass culture (McGinn et al. 2011). For example, many bacteria found in wastewater (e.g. *E. coli*) have an upper pH tolerance limit of 9.2 (Parhad and Rao 1974), and thus would be unable to grow in the BG-11 pH 10 media. Wastewater is important in this respect, as it is rich in nutrients necessary and sufficient to support photosynthetic microorganism growth, and could be used as fertilizer supplement to seawater for commercial scale up applications (Pittman et al. 2011), while at the same time providing a means of environmental remediation.

Further, the ability of the cyanobacteria to grow and produce in brackish water and saline environments, at or above seawater concentrations, provides an alternative to limited fresh water supplies for cultivation. It has been estimated that current microalgal scale up processes could require between 34 and 3,400 gallons of water per gallon of biofuel produced, depending on the amount of evaporation, and the water recycling methods applied (Cooney et. al. 2011, Yang et. al. 2011). Depending on the geographical region, cultivation of 10 billion gallons of microalgal cultures per year could potentially consume between 70% and 170% of the total water supply destined for agricultural irrigation (Pate et. al. 2011), indirectly raising the food *versus* fuel issue. Thus, the cultivation of cyanobacteria/microalgae for fuel and chemicals production will greatly benefit from the ability to grow these microorganisms in vastly abundant seawater.

Salinity tolerance has been shown in several strains of cyanobacteria to be due to the presence of Na^+/H^+ anti-porters that work through the passive diffusion of protons under normal conditions, and active extrusion of Na^+ under high pH. The exposure to high salinity environments has also been shown to up-regulate expression of the putative gene (*sll*1864) coding for a Cl^- channel in *Synechocystis*. The synthesis under salinity stress and accumulation in the cell of compatible solutes, such as sucrose, glucosylglycerol, and glycine betaine, would help to compensate for the change in osmotic potential, and to maintain cell turgor pressure (Hagemann 2011). Tolerance of *Synechocystis* to salinity would make the strain an even better candidate for commercial scale up. The use of saline growth media, especially at NaCl concentrations equivalent to seawater (600 mM), would further minimize the need of fresh water for industrial scale cultures, as seawater could be used in supplement with or instead of fresh, brackish, or wastewater.

The work also showed that a combination of alkalinity and salinity during growth did not impede the *SkIspS* strain of *Synechocystis* from their ability to generate isoprene. However, with the present state-of-the-art, carbon partitioning to isoprene (Melis 2013) is modest and more work is

needed to enhance the efficiency and yield of the isoprene production process. Bentley and Melis (2012) showed that the amount of photosynthetic carbon partitioned to isoprene production was 0.08%, including the amount of isoprene that dissolves into the culture media (Henry's law). In this work, we estimated the isoprene-to-biomass carbon-partitioning ratio to be consistent with the earlier results from this lab. In this respect, it should be mentioned that recent studies have successfully employed metabolic engineering approaches to increase isoprene production, such as the overexpression of the rate limiting enzymes in the methylerythritol (MEP) biosynthetic pathway in *E. coli* (Xiaomei et al. 2012; Zurbriggen et al. 2012), and the heterologous expression of the mevalonic acid biosynthetic pathway for isoprene production in cyanobacteria (Bentley et al. 2014). Further metabolic engineering approaches, in combination with growth in media optimized for contamination avoidance and materials sustainability, will provide a valuable approach for the photosynthetic production of isoprene.

2.5 References

Bentley FK, Melis A (2012) Diffusion-based process for carbon dioxide uptake and isoprene emission in gaseous/aqueous two-phase photobioreactors by photosynthetic microorganisms. Biotechnol Bioeng. 109(1):100-109

Bentley FK, Zubriggen A, Melis A (2014) Heterologous expression of the mevalonic acid pathway in cyanobacteria enhances endogenous carbon partitioning to isoprene. Mol. Plant 7(1): 71-86

Bjorkman O, Demmig B (1987) Photon yield of O_2 evolution and chlorophyll fluorescence characteristics at 77-K among vascular plants of diverse origins. Planta 170:489–504

Cooney MJ, Young G, Pate R (2011) Bio-oil from photosynthetic microalgae: case study. Bioresource Tech 102(1):166-177

Dismukes GC, Carrieri D, Bennette N, Ananyev GM, Posewitz MC (2008) Aquatic phototrophs: efficient alternatives to land-based crops for biofuels. Curr Opin Biotech 19:235–240

Glazer AN, Melis A (1987) Photochemical reaction centers: structure, organization, and function. Annu. Rev. Plant Physiol. 38: 11-45

Guenther A, Karl T, Harley P, Wiedinmyer C, Palmer PI, Geron C (2006) Estimates of global terrestrial isoprene emissions using MEGAN (Model of Emissions of Gases and Aerosols from Nature. Atmos. Chem. Phys. 6 (11): 3181-3210

Hagemann M (2011) Molecular biology of cyanobacterial salt acclimation. FEMS Microbiol Rev 35(1):87-123

Herrera A, Boussiba S, Napoleone V, Hohlberg A (1989) Recovery of C-phycocyanin from the cyanobacterium *Spirulina maxima*. J Appl Phycol 1:325-331

Ley AC, Mauzerall D (1982) Absolute absorption cross-section of photosystem-II and the minimum quantum requirement for photosynthesis in Chlorella vulgaris. Biochim Biophys Acta 680 (1982) 95–106

Lichtenthaler HK (1987) Chlorophylls and carotenoids: pigments of photosynthetic biomembranes. Methods Enzymol 148: 350–382

Lichtenthaler HK (2007) Biosynthesis, accumulation and emission of carotenoids, α-tocopherol, plastoquinone, and isoprene in leaves under high photosynthetic irradiance. Photosynth Res 92:163-179

Lichtenthaler HK (2010) Biosynthesis and emission of isoprene, methylbutenol and other

volatile plant isoprenoids. In, The Chemistry and Biology of Volatiles. Edited by Andreas Herrmann. John Wiley & Sons, West Sussex, UK, pp. 11-47

Lindberg P, Park S, Melis A (2010) Engineering a platform for photosynthetic isoprene production in cyanobacteria, using *Synechocystis* as the model organism. Metabol Engin 12:70-79

Manodori M, Melis A (1984) Photochemical apparatus organization in *Anacystis nidulans* (Cyanophyceae). Plant Physiol 74(1):67-71

McGinn PJ, Dickinson KE, Bhatti S, Frigon J-C, Guiot SR, O'Leary SJB (2011) Integration of microalgae cultivation with industrial waste remediation for biofuel and bioenergy production: opportunities and limitations. Photosynth. Res. 109: 231-247

Melis A (1989) Spectroscopic methods in photosynthesis: photosystem stoichiometry and chlorophyll antenna size. Phil Trans R Soc Lond B 323: 397-409

Melis A (2012) Photosynthesis-to-Fuels: From sunlight to hydrogen, isoprene, and botryococcene production. Energy Environ Sci 5(2): 5531-5539

Melis A (2013) Carbon partitioning in photosynthesis. Curr Opin Chem Biol. 17:453–456

Naus J, Melis A (1991) Changes of photosystem stoichiometry during cell growth in *Dunaliella salina* cultures. Plant Cell Physiol 32: 569-575

Pate R, Klise G, Wu B (2011) Resource demand implications for US algae biofuels production scale-up. Appl Energy 88(10):3377-3388.

Parhad NM, Rao NU (1974) Effect of pH on survival of *Escherichia coli*. Journal (Water Pollution Control Federation) 46(5):980-986

Pikuta EV, Hoover RB, Tang J (2007) Microbial extremophiles at the limits of life. Crit Rev Microbiol 33**:**183-209

Pittman JK, Dean AP, Osundeko O (2011) The potential of sustainable algal biofuel production using wastewater resources. Biores Technol 102:17-25

Schubert H, Hagemann M (1990) Salt effects on 77K fluorescence and photosynthesis in the cyanobacterium *Synechocystis* sp. PCC 6803. FEMS Microbiol Lett 72(1-2):169-172

Sonoda M, Katoh H, Vermaas W, Schmetterer G, Ogawa T (1998) Photosynthetic electron transport involved in PxcA-dependent proton extrusion in *Synechocystis* sp strain PCC6803: Effect of pxcA inactivation on CO_2, HCO_3^-, and NO_3^- uptake. J Bacteriol 180:3799-3803

Summerfield TC, Sherman LA (2008) Global transcriptional response of the alkali-tolerant cyanobacterium *Synechocystsis* sp. PCC 6803 to a pH 10 environment. Appl Environ Microbiol 74(17): 5275-5284

Xiaomei LV, Haoming Xu, Hongwei Yu (2012) Significantly enhanced production of isoprene by ordered coexpression of dxs, dxr, and idi in *Escherichia coli*. App Microbiol Technol 97(6): 2357-2365

Yang J, Xu M, Zhang X, Hu Q, Sommerfeld M, Chen Y (2011) Life-cycle analysis on biodiesel production from microalgae: water footprint and nutrients balance. Biores Tech 102(1):159-165

Zurbriggen A, Kirst H, Melis A (2012) Isoprene production via the mevalonic acid pathway in *Escherichia coli* (Bacteria). BioEnergy Res 5(4): 814-828

Chapter 3: *Role of isopentenyl-diphosphate isomerase in heterologous cyanobacterial (Synechocystis) isoprene production*

This work was published in the following scientific journal:

Chaves JE, Romero PR, Kirst H, Melis A. (2016) Role of isopentenyl-diphosphate isomerase in heterologous cyanobacterial (Synechocystis) isoprene production. Photosyn Res 130(1-3):517-527.

This work was performed with the following persons:

JEC performed the experiments. PPR, KH, and AM assisted with experimental design. JEC and AM wrote the manuscript.

3.1 Introduction

It is evident that synthesis of natural terpenoids would consume greater stoichiometric amounts of IPP than DMAPP, the IPP/DMAPP ratio required depending on the target molecule. For example, phytol and carotenoids (Lagarde et al 2000) are synthesized from C-20 diterpenes and would require an IPP/DMAPP ratio of 3:1, whereas the C-45 prenyl tail of the abundant in thylakoids plastoquinone-9 (McCauley and Melis 1986) would require an IPP/DMAPP ratio of 8:1. Other, less abundant terpenoids, e.g. C-10 myrcene and β-phellandrene (Formighieri and Melis 2016), would require an IPP/DMAPP ratio of 2:1. On the contrary, synthesis of C-5 isoprene (C_5H_8) would require only DMAPP, as this is the only substrate serving as its reactant (Zhou et al. 2013).

The IPP/DMAPP ratio may be modulated *in vivo* depending on the chloroplast or cellular needs by action of the enzyme isopentenyl diphosphate isomerase (*Ipi*), which interconverts IPP and DMAPP (der Heijden 1997; Barkely et al. 2004; Okada et al. 2008; Weise et al. 2013). *In vitro*, the IPP isomerase reportedly shifts the balance toward DMAPP, resulting in an DMAPP/IPP ratio of 2.1:1 of *E. coli* (Zhou et al. 2013) or DMAPP/IPP=2.2:1 in *Saccharomyces cerevisiae* extracts (Street et al. 1990). *In vivo*, ratios of DMAPP/IPP have been measured to be slightly higher at 2.8:1 in *E. coli* (Zhou et al. 2013). The regulation of this interconversion in cyanobacteria is not well understood, and the in-vitro and in-vivo DMAPP/IPP ratios produced by the native *Synechocystis* IPP isomerase have not yet been determined. Evidence was presented suggesting a lack of IPP isomerase activity in the cyanobacterium *Synechocystis* sp. PCC 6803 (Ershov 2000), suggesting either inability of *Synechocystis* to modulate the DMAPP/IPP ratio in the cell, or that this enzyme does not play a role in the isoprenoid biosynthesis in this microorganism.

Heterologous isoprene production in cyanobacteria (Lindberg et al. 2010; Bentley and Melis 2012; Pade et al. 2016) can be used as a "reporter process" for the function of the IPP isomerase by monitoring the rate and yield of isoprene production, which depends on the pool of DMAPP in the cell. We hypothesized that shifting the balance of the IPP/DMAPP toward DMAPP in *Synechocystis* should improve rates and yield of the "reporter process" and result in greater amounts of its product. Accordingly, this work applied heterologous expression of the FNI gene from *Streptococcus pneumoniae*, encoding an IPP isomerase that normally functions in conjunction with the mevalonic acid pathway in these bacteria (Zurbriggen et al. 2012; Bentley et al. 2014) as a tool by which to alter the cellular endogenous DMAPP-to-IPP ratio. Outcome of the transgenic expression of the *FNI* gene in *Synechocystis* was a 250% increase in the "reporter isoprene" rate and yield, showing the function and significance of the IPP isomerase in these photosynthetic microorganisms.

3.2 Materials and Methods

Strains and culturing conditions. *Synechocystis* sp. from the Pasteur Culture Collection strain number 6803 was employed as the experimental strain and is referred to as wild type (WT). The isoprene producing *Synechocystis* strain (*SkIspS*) was previously developed in this lab (Lindberg and Melis 2010), expressing a codon-optimized isoprene synthase from *Pueraria montana*

(kudzu) in the *psbA2* gene locus. *Synechocystis* strain *SkIspS* was used as the recipient strain in this work.

All strains employed in this work were maintained on 1% agar-BG11 media supplemented with 10 mM TES-NaOH pH 8.2, and 0.3% Na-thiosulfate. Kanamycin (25 μg/mL) and chloramphenicol (30 μg/mL) were added into agar plates and used to maintain transformants. Starter cultures were inoculated in 300 mL growth media with cell from an agar plate and allowed to grow initially under illumination at 30 μmol photons m^{-2} s^{-2} until an OD_{730}=0.3 was reached. Illumination was then increased to 50 μmol photons m^{-2} s^{-2} until an OD_{730}=0.65-0.75 was reached. Illumination was further increased to 100 μmol photons m^{-2} s^{-2} until the culture reached a density enough to support dilution in 700 mL growth medium to an OD_{730}=0.65. Liquid cultures were grown in BG11 media buffered with 25 mM NaH_2PO_4 (pH 7.5) at 28°C, under continuous aeration and illumination at 150 μmol photons m^{-2} s^{-1}.

***Synechocystis* transformation.** Transformations were performed as previously established (Kirst et al. 2014). A DNA construct comprising the chloramphenicol resistance cassette was designed to replace the *cpc* operon in the *SkIspS* strain, generating the control strain *SkIspS, Δcpc+CmR*. A DNA construct comprising the "isopentenyl diphosphate isomerase" gene (*FNI*) from *Streptococcus pneumoniae* (Zubbrigen et al. 2012), followed by the chloramphenicol resistance cassette was designed to replace the *cpc* operon in the *SkIspS* strain, generating the *SkIpsS*, *Δcpc+SSpFNI+CmR* transformant strain. Transgene constructs were flanked by 500 base pairs of the upstream and downstream sequences of the *cpc* operon for homologous recombination. Complete segregation of the transgenes into all copies of the genome was confirmed by genomic DNA PCR analysis.

Protein analysis. Cells were grown in 300 mL volume cultures to an OD_{730} of 2.5, pelleted by centrifugation, and re-suspended in 5-10 mL of 50 mM Tris-HCl (pH 8). The cell suspension was then incubated with lysozyme at room temperature for 30 min, and then washed in fresh 50 mM Tris-HCl (pH 8) three times. Protease inhibitor (1 mM PMSF) was added to samples before lysing of the cells by French press (3x1200 psi). Disrupted cell suspensions were centrifuged at 2,250 g for 3 min to pellet cell debris and glycogen grains. The supernatant was supplemented with an equal volume of solubilization solution, comprising 250 mM Tris-HCl, pH 6.8, 7% w/v SDS, 20% w/v glycerol, 2 M urea, and a few grains of bromophenol blue. Samples were solubilized upon incubation at room temperature for 1-2 h. At the end of the solubilization incubation, samples were supplement with 10% β-mercaptoethanol. The solubilized total cellular proteins were subjected to SDS-PAGE and Western blot analysis. SDS-PAGE resolved proteins were either stained with Coomassie brilliant blue or transferred to PVDF membrane for immunodetection using rabbit immune serum containing specific polyclonal antibodies against the ISPS (Lindberg et al. 2010) or FNI proteins (Zubriggen et al. 2012).

Isoprene, photosynthetic pigment, and biomass accumulation. Liquid cultures grown for biomass accumulation and isoprene production were grown photoautotrophically in the absence of antibiotics. Glass bottle bioreactors (1 L volume) were designed in this lab specifically for quantitative biomass and isoprene production measurements, (Bentley and Melis 2012). The 1 L bioreactors were loaded with ~700 mL liquid BG11 growth medium containing 25 mM NaH_2PO_4 (pH 7.5), and then inoculated with *Synechocystis* starter cultures at an OD_{730} = 0.65.

Unless otherwise indicated, the bioreactors were further loaded with inorganic carbon, delivered to the liquid culture by slowly bubbling 500 mL of 100% CO_2 gas through the bottom of the liquid culture to fill the reactor headspace. Bioreactors were then sealed and cultures were stirred slowly and continuously at 28°C under constant illumination at 100 μmol photons m^{-2} s^{-2}.

Isoprene accumulation in the headspace of the reactor was determined by gas chromatography (Shimadzu 8A GC-FID) analysis of 1 mL gaseous samples from the bioreactor headspace. Isoprene quantification was determined based on a calibration of isoprene standard (Acros Organics, Fair Lawn, NJ, USA), as described (Chaves et al. 2015). Chlorophyll *a* and total carotenoids were extracted in 100% methanol and measured spectrophotometrically according to Lichtenhaler (1987). Biomass accumulation in the liquid phase of the reactor was determined upon collection of 50 mL aliquots, followed by centrifugation, rinsing with deionized water, and cell re-suspension in 2 mL of deionized water. Re-suspended samples were rinsed through 0.2 μm filter paper, dried on aluminum trays for 6 h at 90°C, and weighed to determine the dry cell weight. Cell growth was also determined spectrophotometrically by measuring the optical density of live cell cultures at 730 nm with a Shimadzu UV-1800 UV-visible spectrophotometer.

3.3 Results

Construction of a chloramphenicol resistant *FNI* overexpressing strain. The *Synechocystis* recipient strain used in this work carried the codon-optimized kudzu isoprene synthase *SkIspS* gene, the latter being in the *psbA2* locus (**Fig. 3.1a**). The nucleotide sequence of the *SkIspS* transgene is shown in the supplementary materials. The recipient strain also included an unmodified *cpc* operon (**Fig. 3.1b**), which encodes for the phycocyanin β-subunit (cpcB), the α-subunit (cpcA), and the associated linker polypeptides (cpcC1, cpcC2, and cpcD). The *Synechocystis* codon-optimized chloramphenicol resistance *CmR* cassette was introduced via double homologous recombination into the *cpc* operon locus (**Fig. 3.1c**) of the recipient strain already carrying the codon-optimized kudzu isoprene synthase *SkIspS* gene. This transformation replaced the cpc operon with the chloramphenicol resistance *CmR* cassette, generating the "SkIspS, ΔCPC+CmR" strain. Alternatively, the *Synechocystis*-codon optimized *Streptococcus pneumoniae* "isopentenyl diphosphate isomerase" gene (*FNI*), followed by the chloramphenicol resistance *CmR* cassette was introduced via double homologous recombination into the *cpc* operon locus (**Fig. 3.1d**) of the recipient strain already carrying the codon-optimized kudzu isoprene synthase *SkIspS* gene. This transformation replaced the *cpc* operon with the chloramphenicol resistance *CmR* cassette, generating the "SkIspS, Δcpc+SSpFNI+CmR" strain. Replacement of the native *cpc* operon with either the *CmR* (Fig. 1c) or the *FNI-CmR* construct (Fig. 1d) resulted in two different phycocyanin-less mutants. These were analyzed molecularly and biochemically for their genetic and protein expression properties.

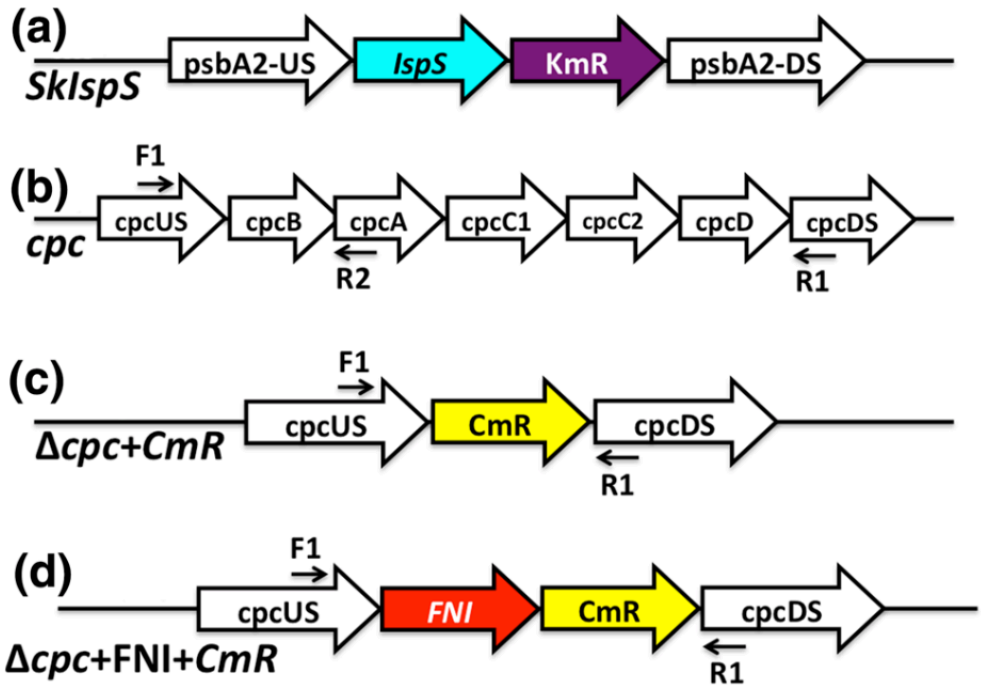

Fig 3.1 Schematic overview of the constructs designed to transform the genomic DNA of *Synechocystis*, as used in this work. **a** organization of the DNA in the *psbA2* locus of the *Synechocystis* recipient strain, in which the native *psbA2* gene was replaced by the *IspS-KanR* construct. **b** Organization of the DNA in the *cpc* operon locus of the recipient strain. The CPC-operon, includes the *cpcB* gene, encoding the phycocyanin β-subunit; *cpcA*, encoding the phycocyanin α-subunit; *cpcC1* and *cpcC2* encoding the phycocyanin rod linker polypeptides; and the *cpcD* encoding an additional small linker polypeptide. **c** DNA construct for the replacement of the *cpc* operon with a chloramphenicol resistance cassette (*CmR*) designed for double homologous recombination in the *cpc* operon locus of the *Synechocystis* recipient strain. **d** DNA construct for the expression of the "isopentenyl diphosphate isomerase" gene (*FNI*) from *Streptococcus pneumoniae* along with a chloramphenicol resistance cassette (*CmR*) designed for double homologous recombination in the *cpc* operon locus of the *Synechocystis* recipient strain. F1 and R1: forward (F1) and reverse (R1) primers designed to amplify the *cpc* operon DNA region between the *cpc* promoter and terminator. F1 and R2: forward (F1) and reverse (R2) primers designed to amplify the *cpc* operon DNA region between the *cpc* promoter and *cpcB* gene.

Transformation and protein expression profile of the Δcpc+CmR strain. Genomic DNA analysis, the state of homoplasmy, and protein expression profiles were investigated. State of homoplasmy of the *SkIpsS* and *ΔcpcCmR* strains was tested by PCR amplification of genomic DNA using primers flanking the insertion site, as well as primers specific to the recipient strain. In the recipient strain (*SkIpsS*), primers F1 and R1 (Fig. 1b) flanking the *cpc* operon amplified a 3.6 kb product, corresponding to the DNA of the full cpc operon (**Fig. 3.2**, SkIpsS in left panel). In the *SkIpsS*, *Δcpc+CmR* transformant, primers F1-R1 amplified a 1.0 kb product, corresponding to the CmR insert (**Fig. 3.2**, SkIpsS, Δcpc+CmR in left panel). Primers F1-R2 targeting upstream and inside the *cpcB* coding region (Fig. 1b) generated a 1.3 kb product in the *SkIpsS* recipient strain (**Fig. 3.2**, SkIpsS in right panel), but failed to generate any product in the *SkIpsS*, *Δcpc+CmR* control strain (**Fig. 3.2**, SkIpsS, Δcpc+CmR in right panel). The latter is evidence that the *Δcpc+CmR* transformant has reached a state of homoplasmy.

SDS-PAGE and Western blot analysis of total cellular protein extracts was employed to assess expression of the *IspS* and the overall protein expression profile of the recipient strain (SkIspS) and the chloramphenicol expressing transformant (SkIpsS, Δcpc+CmR). The *Synechocystis* recipient strain showed expression of the phycocyanin cpcB (β-subunit) and cpcA (α-subunit) as dominant proteins in the 15-20 kD region (**Fig. 3.3**, upper panel). However, the chloramphenicol expressing transformant (SkIpsS, Δcpc+CmR) lacked these major proteins. Instead, it specifically expressed the chloramphenicol resistance conferring protein, seen in **Fig. 3.3**, upper panel, as a 24 kD protein. Western blot analysis with isoprene synthase-specific polyclonal antibodies showed the presence of the IspS protein in all these lines, migrating to about 65 kD in the gel electrophoresis (**Fig. 3.3**, lower panel). These results suggest successful replacement of the *cpc* operon by the *CmR* cassette, and low levels of expression of the CmR protein. The *SkIpsS*, *Δcpc+CmR* transformant served as a control strain in these measurements.

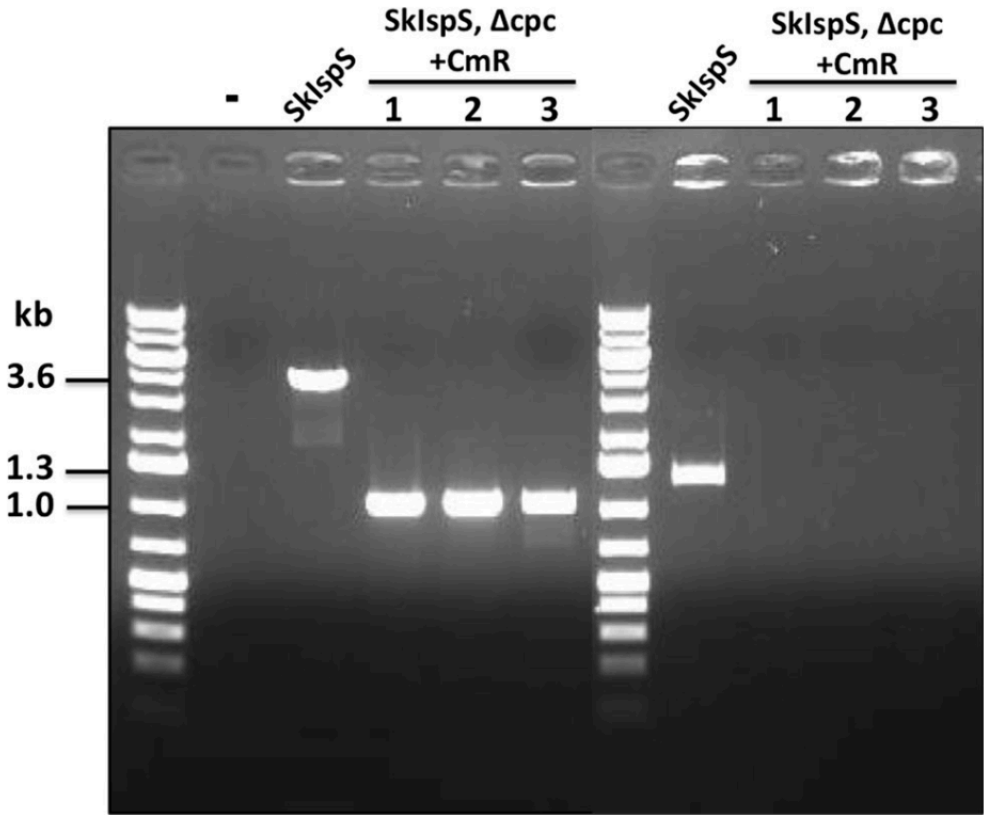

Fig. 3.2 Genomic DNA PCR analysis with selected forward (F) and reverse (R) primers positioned on the genomic DNA of *Synechocystis* recipient (*SkIspS*) and *SkIspS*, *Δcpc+CmR* transformants. **(Left panel)** PCR reactions using primers F1 and R1 (primer positions given in Fig. 1) amplifying the DNA region of the *cpc* operon between the *cpc* promoter and terminator. The recipient strain (*SkIspS*) yielded a single 3.6 kb product, corresponding to the full *cpc* operon genes. Three different *SkIspS*, *Δcpc+CmR* lines yielded a single 1 kb product, corresponding to the *Δcpc+CmR* DNA. **(Right panel)** PCR reactions using primers F1 and R2 amplifying the DNA region between the *cpc* promoter and the *cpcB* gene. The recipient strain (*SkIspS*) yielded a single 1.3 kb product. Three different *SkIspS*, *Δcpc+CmR* lines failed to yield any PCR products.

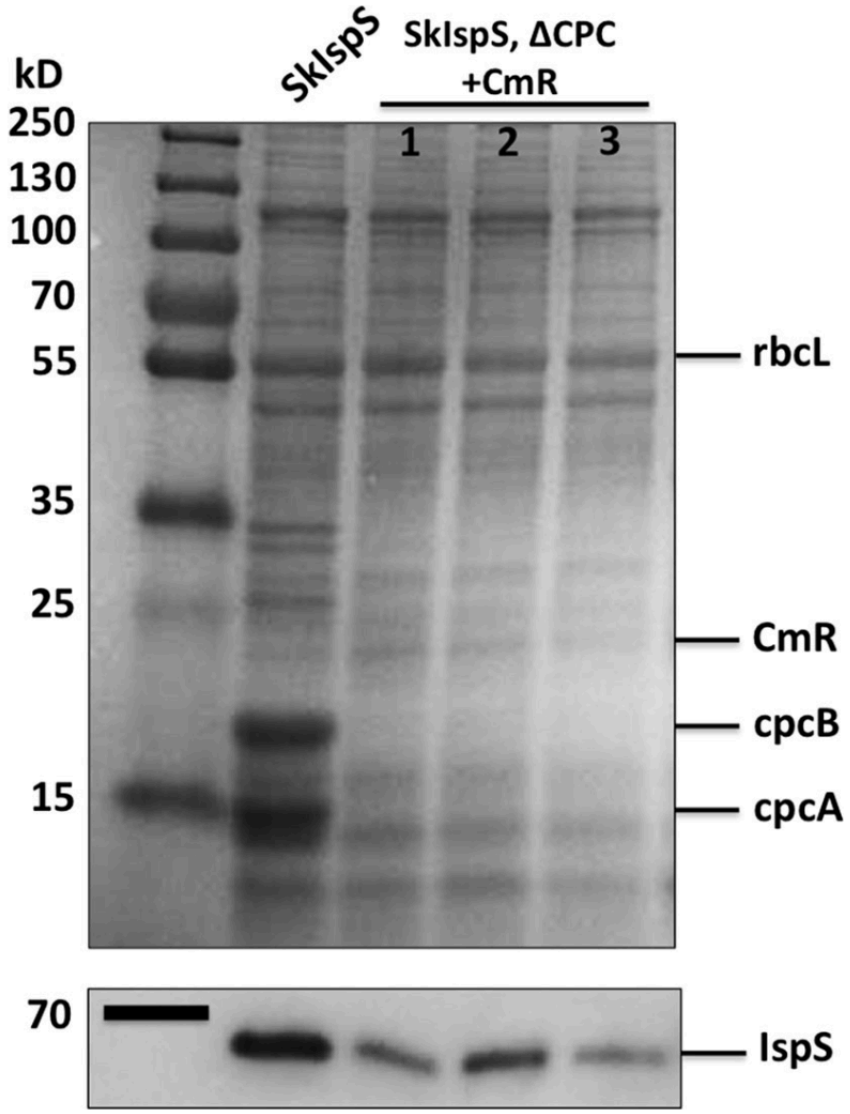

Fig. 3.3 (Upper panel) SDS-PAGE analysis of total protein extracts from *Synechocystis* recipient strain (SkIspS) and three *CmR* transformant lines (*SkIspS*, *Δcpc+CmR*). Molecular weight markers are indicated in kD. Note the presence of the cpcB and cpcA phycocyanin subunits in the recipient SkIspS strain, migrating in the 15-20 kD region, and the absence of these proteins from the *SkIspS*, *Δcpc+CmR* lines. **(Lower panel)** Western blot analysis of protein extracts from *Synechocystis* recipient strain (*SkIspS*) and three *CmR* transformant lines (*SkIspS*, *Δcpc+CmR*), probed with specific polyclonal antibodies raised against the IspS protein.

Transformation and protein expression profile of the SkIpsS, Δcpc+SSpFNI+CmR strain. The *Synechocystis*-codon optimized *Streptococcus pneumoniae* isopentenyl diphosphate isomerase gene (*FNI*), followed by the chloramphenicol resistance *CmR* cassette (Fig. 1d), was introduced via double homologous recombination into the *cpc* operon locus (Fig. 1b) of a strain already carrying the codon-optimized kudzu isoprene synthase *SkIspS* gene, the latter being in the *psbA2* locus (Fig. 1a). Replacement of the native *cpc* operon with the *FNI-CmR* construct generated an isoprene producing, *FNI* overexpressing strain termed SkIpsS, Δcpc+SSpFNI+CmR. State of homoplasmy of three independent lines of the SkIpsS, Δcpc+SSpFNI+CmR strains was tested by PCR amplification of genomic DNA using primers flanking the insertion site, as well as primers specific to the recipient strain. In the recipient strain (RS), primers F1 and R1 (Fig. 1b) flanking the *cpc* operon amplified a 3.6 kb product, corresponding to the DNA of the full cpc operon (**Fig. 3.4a**). In the Δcpc+SSpFNI+CmR transformants, the same F1-R1 primers (Fig. 1d) amplified only a 2 kb product, corresponding to the FNI-CmR insert, and failed to amplify a product corresponding to the genes of the full cpc operon. Conversely, primers F1 and R2 (Fig. 1b) flanking the cpc upstream region (F1) and the *cpcB* gene (R2), amplified a 1.3 kb product in the recipient strain only (**Fig. 3.4b**) but failed to amplify any products in the Δcpc+SSpFNI+CmR strains. This genomic DNA PCR analysis provided evidence that the FNI-CmR transgene properly integrated into the recipient *Synechocystis* genomic DNA and segregation of transgenic DNA copies (homoplasmy) has occurred under our selection conditions.

Synechocystis wild type and the recipient strains both showed expression of the phycocyanin cpcB (β-subunit) and cpcA (α-subunit) as dominant proteins in the 15-20 kD region (**Fig. 3.5a**, Wild type and SkIspS). Importantly, the Δcpc+SSpFNI+CmR transgenic lines lacked the phycocyanin proteins but showed the presence of distinct FNI and CmR proteins migrating to about 37 and 24 kD, respectively (Fig. 5a, SkIpsS, Δcpc+SSpFNI+CmR lanes). Smaller amounts of the IspS can also be seen in SDS-PAGE Coomassie stain of the recipient strain (SkIpsS) and Δcpc+SSpFNI+CmR lines, migrating to about 65 kD (Fig. 5a, IspS). Expression of the FNI and IspS proteins was confirmed by Western blot analysis (**Fig. 3.5b**), showing specific cross-reactions with 65 and ~37 kD proteins. This Western blot analysis with the IspS immune serum also showed a minor cross-reaction with a protein migrating to about 45 kD, possibly a partial proteolysis product of the IspS protein. It is evident from both the Coomassie stain in the SDS-PAGE (**Fig. 3.5a**) and the Western blot analysis (**Fig. 3.5b**) that FNI is expressed at higher levels than the IspS.

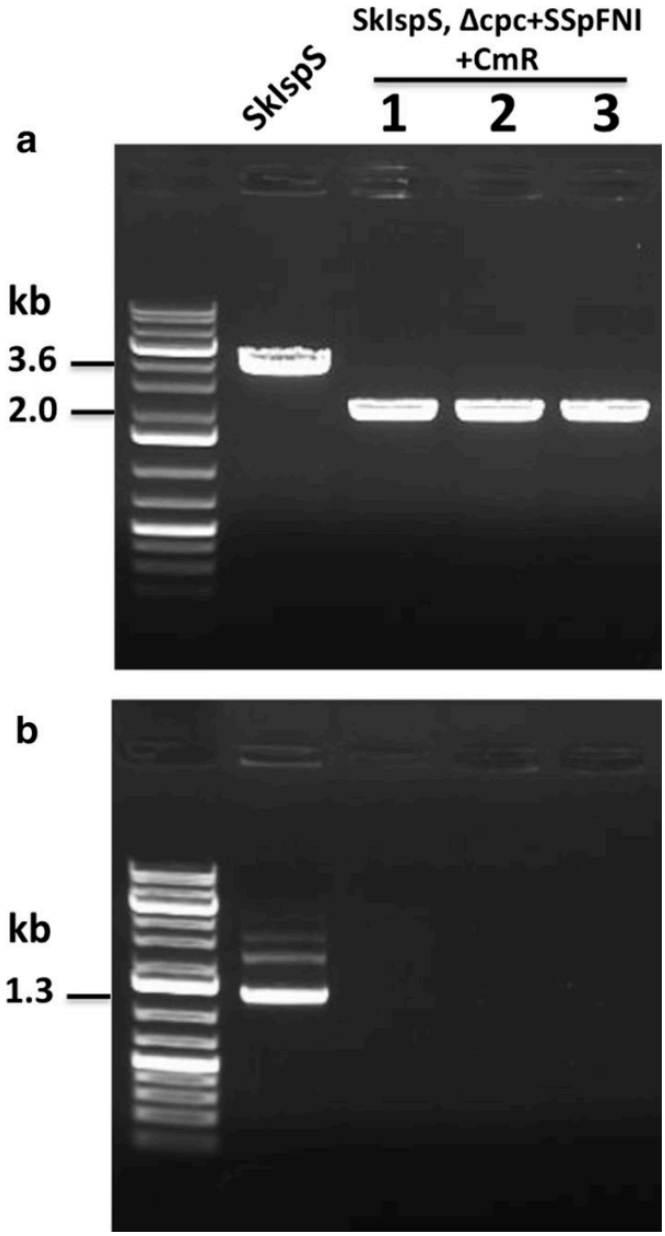

Fig. 3.4 Genomic DNA PCR analysis with selected forward (F) and reverse (R) primers positioned on the genomic DNA of *Synechocystis* recipient (*SkIspS*) strain and three *FNI-CmR* transformant lines (*SkIspS*, *Δcpc+SSpFNI+CmR*). **a** PCR reactions using primers F1 and R1 (primer positions given in Fig. 1) amplifying the DNA region of the *cpc* operon between the *cpc* promoter and terminator. The recipient strain (*SkIspS*) yielded a single 3.6 kb product, corresponding to the full *cpc* operon genes. Three different *FNI-CmR* lines yielded a single 2 kb product, corresponding to the *FNI-CmR* DNA. **b** PCR reactions using primers F1 and R2 amplifying the DNA region between the *cpc* promoter and the *cpcB* gene. The recipient strain (*FNI-CmR*) yielded a single 1.3 kb product. Three different *FNI-CmR* lines failed to yield any PCR products.

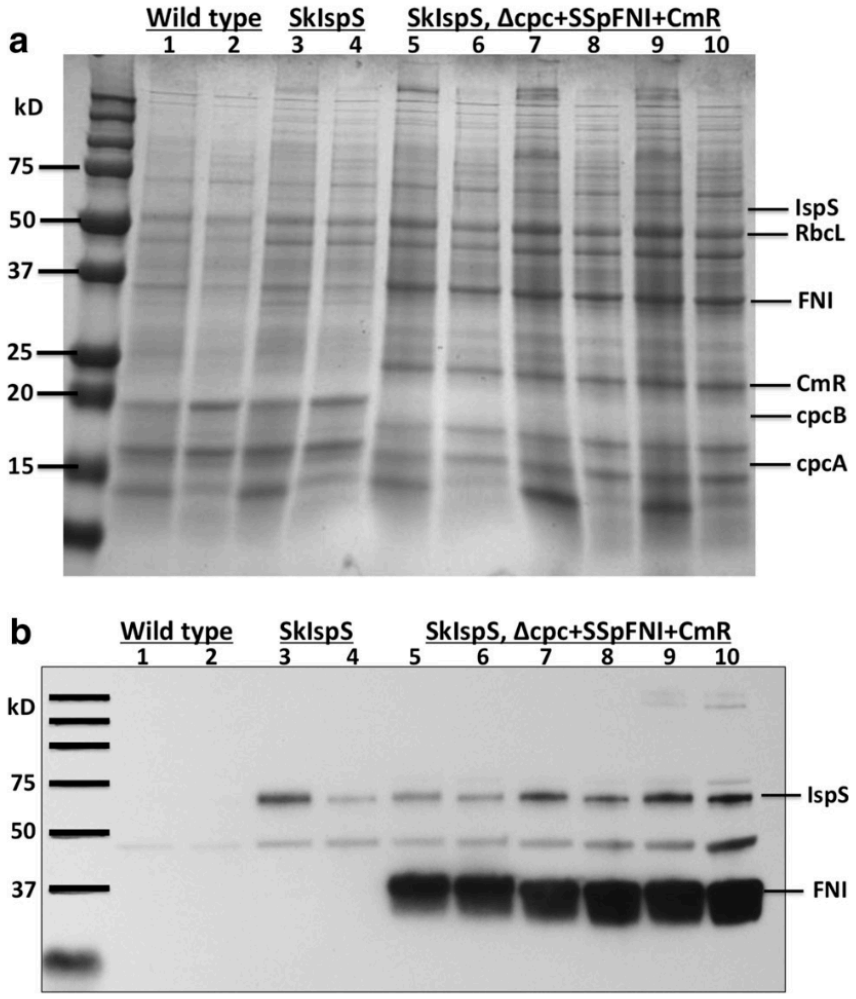

Fig. 3.5 a SDS-PAGE analysis of total protein extracts from *Synechocystis* wild type, the recipient strain (*SkIspS*) and three *FNI-CmR* transformant lines (*SkIspS*, *Δcpc+SSpFNI+CmR*). Molecular weight markers are indicated in kD. Note the presence of the cpcB and cpcA phycocyanin subunits in the wild type and recipient strain (*SkIspS*), migrating to about 18 and 17 kD, respectively, and the absence of these proteins from the *FNI-CmR* transformant lines. Also note the pronounced expression of the FNI and CmR proteins in the *FNI-CmR* lines, and the low expression level of the IspS protein in both the recipient strain (*SkIspS*) and three *FNI-CmR* transformant lines. **b** Western blot analysis of total protein extracts from *Synechocystis* wild type, the recipient strain (*SkIspS*) and three *FNI-CmR* transformant lines (*SkIspS*, *Δcpc+SSpFNI+CmR*) probed with specific polyclonal antibodies raised against the IspS and FNI proteins.

Physiology of wild type, recipient, and *Δcpc+SSpFNI+CmR Synechocystis* transformants. A number of physiological parameters were measured to assess functional properties of the transformants used in this work. Chl/OD_{730} and Chl/DCW was lowered to between 59-68% in the *Δcpc+CmR* relative to the recipient *SkIpsS* strain (**Table 3.1**). Similarly, Chl/OD_{730} and Chl/DCW was lowered to between 57-64% in the *Δcpc+SSpFNI+CmR Synechocystis* transformant relative to the recipient *SkIpsS* strain. These results are consistent with previous pigment measurements in *Δcpc* (*cpc* operon deletion) strains (Kirst et al. 2014), attributed to a decrease in the PSI/PSII stoichiometry as a result of cell acclimation to the removal of the phycocyanin rods (Kirst et al. 2014, Collins et al. 2012, Ajlani et al. 1998). Removal of phycocyanin from the phycobilisomes substantially attenuates the light-harvesting capacity of PSII resulting in a potential over-excitation of PSI. PSI accumulation is then down regulated to rebalance the excitation energy distribution between the two photosystems (Table 1). As PSI contains more chlorophyll *a* molecules than PSII, this PSI/PSII ration adjustment results in lowed chlorophyll *a* per cell.

Total carotenoid accumulation in the above transformants appeared to be slightly elevated to 108-124%, relative to the recipient *SkIpsS* strain. This was not further investigated in this work.

Table 3.1. Pigment content, PSI/PSII photosystem reaction center ratio, and light-saturated rates of *Synechocystis* photosynthesis *SkIspS* recipient strains and **Δ**cpc transformants grown photoautotrophically in the laboratory.

Parameter measured	**SkIspS**	**SkIspS, Δcpc+CmR**	**SkIspS, Δcpc +SSpFNI+CmR**
Chl/OD_{730} (μg)	4.78 ± 0.24 (100%)	3.24 ± 0.22 (68%)	3.05 ± 0.25 (64%)
Chl/DCW (μg mg^{-1})	17.29 ± 1.27 (100%)	10.21 ± 0.82 (59%)	9.94 ± 0.72 (57%)
Car/OD_{730} (μg)	1.64 ± 0.18 (100%)	2.03 ± 0.06 (124%)	1.96 ± 0.13 (120%)
Car/DCW (μg mg^{-1})	5.89 ± 0.47 (100%)	6.29 ± 0.48 (108%)	6.29 ± 0.14 (108%)
PSI/PSII (mol:mol)	2.5±0.08*	1.8±0.13*	1.5±0.15
P_{max} , mmol O_2 (mol Chl)$^{-1}$ s^{-1}	150*	165*	155

Photosystem reaction center ratios were measured spectrophotometrically (Melis 1989). n ≥ 3; means ± SD.
*Kirst et al. 2014

Isoprene and biomass accumulation in control and *FNI* expressing transformants. Rates of *Synechocystis* growth were determined in sealed gaseous-aqueous two-phase photobioreactors developed by Bentley and Melis (2012). Strains overexpressing the *FNI* protein (*SkIpsS*, *Δcpc+SSpFNI+CmR*; **Fig. 3.6, squares**) grew with the same rate as the recipient (*SkIspS*; **Fig. 3.6, circles**) and control (*SkIpsS*, *Δcpc+CmR*; **Fig. 3.6, triangles***)* under a light intensity of 100 μmol photons m^{-2} s^{-1}. This was evidenced both from the increase in the OD_{730} readings (**Fig. 3.6a**) and from the actual dry cell weight (DCW) biomass accumulation (**Fig. 3.6b**) in the cultures. It is important to note that all strains grew at about the same rate upon inoculation of the cultures at a high OD_{730}=0.65 (Fig. 6a) or DCW=0.2 g L^{-1} (Fig. 6b). This high inoculum, in combination with the use of photobioreactors with a ~9.5 cm internal optical direction diameter was necessary and sufficient to ensure absorption of all incoming irradiance by the culture, regardless of the antenna configuration of the strains employed. The linear increase of the biomass as a function of incubation time, with an average doubling of the initial biomass every about 24 h (Bentley and Melis 2012), suggested an overall light-limitation in cell growth, defined by the actual quantitative absorption of incident irradiance by the culture.

Rates of isoprene production were also linear as a function of incubation time, but differed substantially between the recipient strain, the control strain and the FNI transformants. The recipient strain (*SkIspS*) generated about 1.1 μg isoprene L^{-1} h^{-1}, whereas the control strain (*SkIpsS*, *Δcpc+CmR)* generated about 5.1 μg isoprene L^{-1} h^{-1} a 5-fold improvement. This substantial increase in the yield of isoprene can be attributed to the deletion of the *cpc* operon in the *SkIpsS*, *Δcpc+CmR* transformant, resulting in the conservation of substantial amounts of cellular metabolits, as these transformants no longer consume endogenous carbon for the synthesis of phycocyanin. The extra metabolic resources are then available to alternative sinks, e.g. isoprene synthesis.

The FNI transformants (*SkIpsS*, *Δcpc+SSpFNI+CmR*) produced 12.8 μg isoprene L^{-1} h^{-1}, an additional 2.5-fold improvement (**Fig. 3.7**). This differential rate of isoprene production translated into an altered isoprene-to-biomass carbon-partitioning ratio from 0.13 mg g^{-1} in the recipient (*SkIspS*) strain, to 0.73 mg g^{-1} in the control (*SkIpsS*, *Δcpc+CmR)* strain, and 1.8 mg g^{-1} in the FNI over expressing (*SkIpsS*, *Δcpc+SSpFNI+CmR*) strain (**Fig. 3.8**).

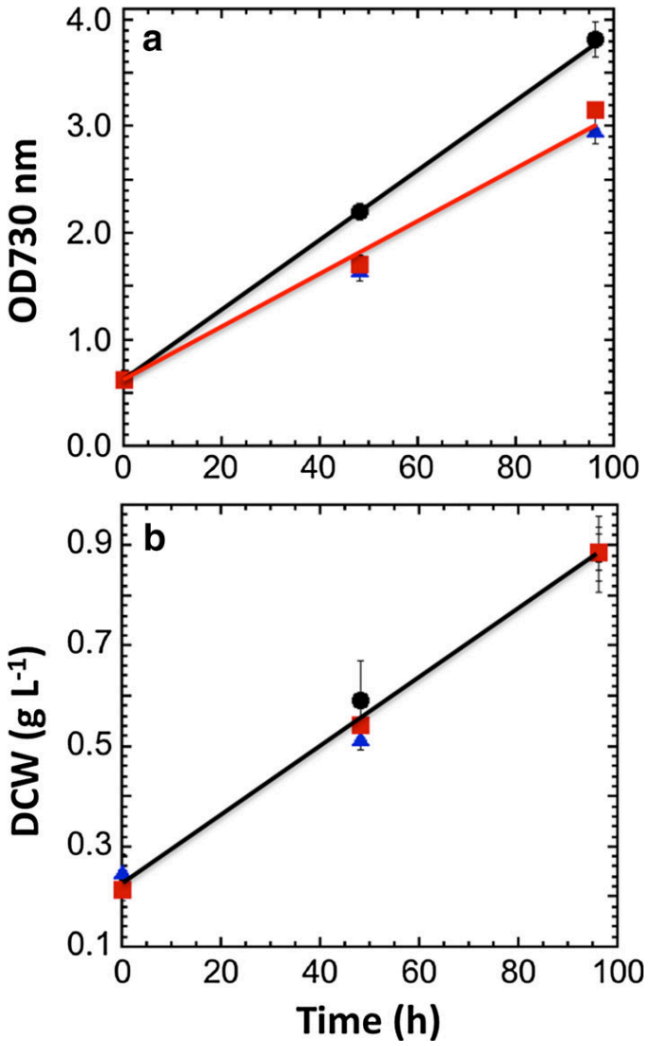

Fig. 3.6 Photoautotrophic growth of the recipient *SkIspS* strain (black circles), the *CmR* transformant (*SkIspS, Δcpc+CmR*) (blue triangles) and FNI-CmR expressing strain *SkIspS*, *Δcpc+SSpFNI+CmR* strain (red squares) measured from the increment in the optical density of the cultures at 730 nm (**a**) or from the accumulating dry cell weight (DCW) of the respective biomass (**b**). Cells were cultivated in a sealed gaseous-aqueous two-phase photobioreactor system (Bentley and Melis 2012) in which the liquid phase comprised 700 mL of BG11 growth medium and the gaseous phase comprised 500 mL of 100% CO_2.

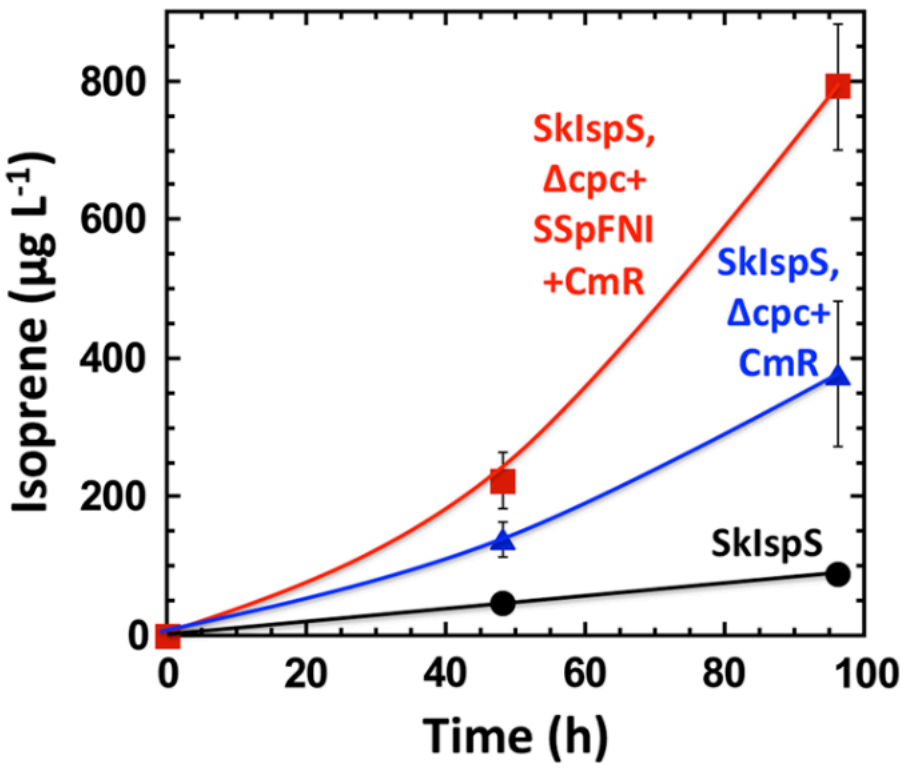

Fig. 3.7 A sealed gaseous-aqueous two-phase 1.2 L reactor (Bentley and Melis (2012) was used for *Synechocystis* isoprene production measurements. The liquid culture comprised 700 mL of BG11 growth medium, whereas the gaseous phase was filled with 100% CO_2. Upon assembly and culture inoculation, the reactor was sealed and incubated under continuous illumination of 100 μmol photons m^{-2} s^{-1}. Every 48 h, sampling of the reactor for biomass and isoprene content was followed by flushing the gaseous products and by refilling the gaseous phase with 100% CO_2 to sustain growth and productivity. Note the much steeper rate of isoprene production by the control strain *SkIspS*, *Δcpc+CmR* (blue triangles) compared to the recipient *SkIspS* strain (black circles), and the even greater rate of isoprene production by the FNI-CmR strain *SkIspS*, *Δcpc+SSpFNI+CmR* (red squares).

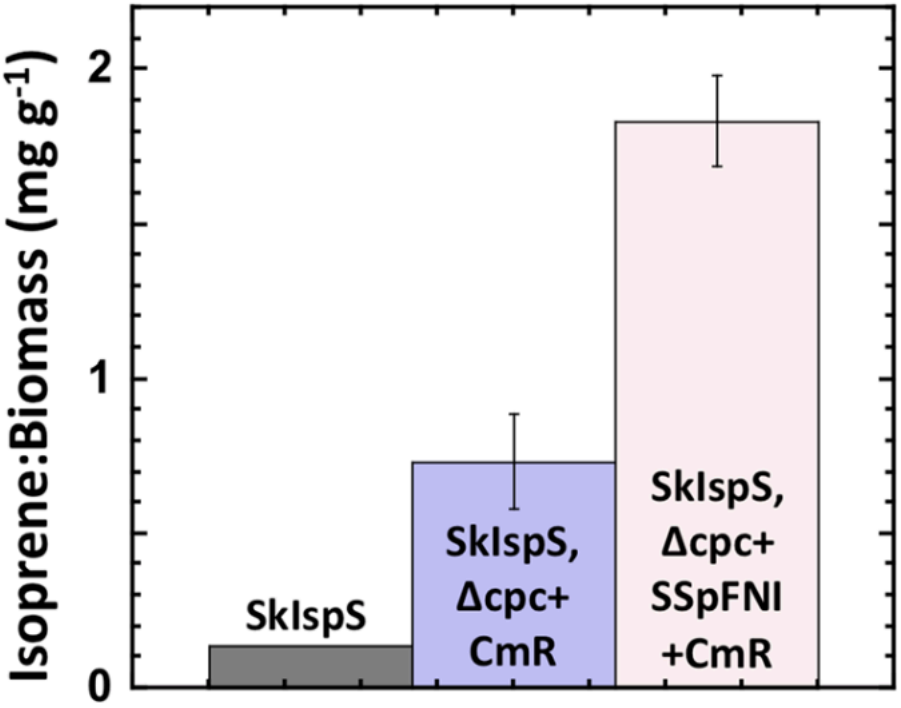

Fig. 3.8 Calculated isoprene-to-biomass (w:w) ratios for the recipient (*SkIspS*), CmR control (*SkIspS*, *Δcpc+CmR)*, and FNI-CmR overexpression strain (*SkIspS*, *Δcpc+SSpFNI+CmR)*. A 5-fold increase (from 0.13 to 0.73 mg g^{-1}) was observed in the isoprene-to-biomass ratio upon the deletion of the *cpc* operon in the (*SkIspS*, *Δcpc+CmR)* compared to the recipient strain (*SkIspS*). An additional 2.5-fold increase (from 0.73 to 1.8 mg g^{-1}) in the isoprene-to-biomass carbon-partitioning ratio was noted upon expression of the isopentenyl diphosphate isomerase (*FNI*) gene in the *SkIspS*, *Δcpc+SSpFNI+CmR* strain.

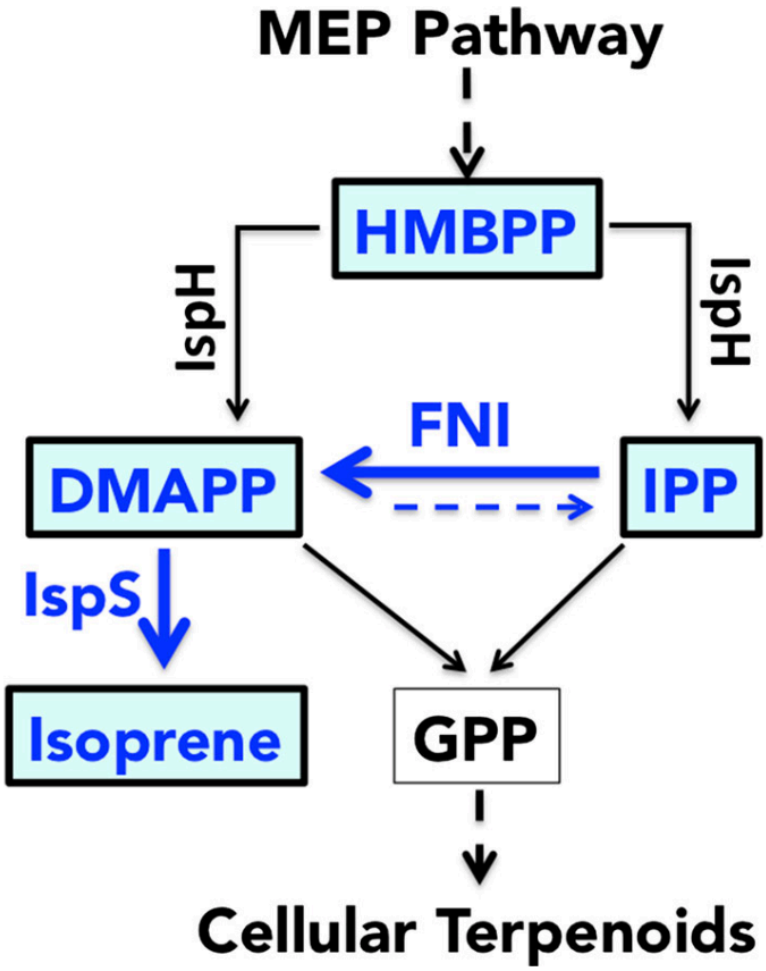

Fig. 3.9 Schematic depicting the regulation of carbon flow through the native MEP pathway for the generation of the universal terpenoid precursors dimethylallyl diphosphate (DMAPP) and isopentenyl diphosphate (IPP). DMAPP and IPP are isomers derived from the same precursor metabolite, the hydroxy-2-methyl-2-butenyl-4-diphosphate (HMBPP) upon the action of the IspH enzyme. The native equilibrium between DMAPP and IPP in the cell is shifted toward DMAPP by a heterologous isopentenyl diphosphate isomerase (FNI). As DMAPP is the only substrate for the isoprene synthase (IspS), which produces the hemiterpene isoprene, the FNI supported shift int eh IPP-DMAPP equilibrium favors isoprene production. Native terpenoid biosynthesis requires DMAPP and IPP condensation to produce geranyl diphosphate (GPP), the precursor for all other cellular terpenoids.

3.4 Discussion

The work provided evidence that a heterologous IPP isomerase in cyanobacteria can play a role in modulating the DMAPP/IPP ratio of the cells, as evidenced by the effect they have on the isoprene "reporter process", i.e., rate and yield of photosynthetic isoprene production. The effect is schematically depicted in reaction pathway of **Fig. 3.9**. The majority of the intermediate metabolite HMBPP is preferentially partitioned toward IPP, with a IPP:DMAPP ratio in a 3:1 (McGarvey and Croteau 1995; Lichtenthaler 2010; Formighieri and Melis 2014), but measured to be 5.6:1 in tobacco (Tritsch et al. 2010). Higher amounts of IPP are needed for the synthesis of longer chain terpenoids. However, the heterologous expression of FNI in this case pushes the equilibrium between IPP and DMAPP toward the DMAPP, effectively enhancing the concentration of the metabolite serving as the substrate of the IspS enzyme and reactant for isoprene synthesis (Fig. 9). This metabolic alteration is manifested as greater yield of isoprene in the SkIspS, Δcpc+SSpFNI+CmR strain.

Expression of the *FNI* gene, a *Streptococcus pneumoniae* IPP isomerase, in a *Synechocystis* recipient strain that harbored the isoprene synthase (*IspS*) gene, resulted in a 250% increase in the yield of isoprene production by these cyanobacteria (Fig. 8). This finding is qualitatively similar to that recently reached in work by Gao et al (2016). They employed a different cyanobacterial strain (*Synechococcus elongatus* PCC 7942), and a different isopentenyl diphosphate isomerase cloned from yeast, to show enhancements in phototrophic isoprene production. Interestingly, Gao et al. (2016) reported that during a relatively long 21 d cultivation period, their best performing SE52 and SE54 strains initially partitioned about 15% of the captured carbon for the synthesis of isoprene and 85% of photosynthetic carbon for the synthesis of biomass. During the subsequent stationary phase (after day 3), SE52 directed approximately 65% of carbon flux to isoprene synthesis. Altogether, during their 21 d cultivation, strains SE52 and SE54 directed about 40% and 22%, respectively, of photosynthetic carbon toward isoprene production. This became possible upon improvement in carbon flux through the MEP pathway by relieving an MEP pathway bottleneck upon overexpression of the *dxs* and *IspG* genes. However, these findings cannot be independently tested, as Gao et al. (2016) did not provider the DNA sequences of the constructs used for any of their transformants. The latter is of import, as work by other investigators (Leonard et al. 2010; Xiao et al. 2012; Zurbriggen et al. 2012) has indicated that manipulation of the endogenous MEP pathway genes may not substantially alter the highly regulated endogenous 5% supply of precursor metabolites through the MEP pathway.

Expression of the *FNI* and *IspS* genes in *Synechocystis* in this work was assessed by SDS-PAGE Coomassie stain (Fig. 5a) and Western blot analysis (Fig. 5b) of total cyanobacterial protein extracts. Both of these protein chemistry analytical methods showed sufficient expression of the 37 kD protein FNI protein, with excellent visibility of this transgenic protein in the Coomassie stain of the SkIspS, Δcpc+SSpFNI+CmR SDS-PAGE gels and Western blot analysis. Expression levels of the 65-kD IspS protein, however, were less pronounced in the Coomassie stained SDS-PAGE gels and Western blot analysis, showing a faint band at 65 kD, present in the recipient SkIspS and SkIspS, Δcpc+SSpFNI+CmR strains but not in the wild type (Fig. 5a and 5b). Under these conditions, it is likely that limiting amounts of the IspS protein caused a limitation in the yield of product synthesis.

In *Synechocystis* PCC 6803, a stable knock out line of the sll1556 gene encoding the IPP isomerase was previously made by Poliquin et al. (2004), and examined by scanning electron microscopy. It was reported that thylakoid membrane development was significantly altered by the absence of the IPP isomerase, although these developmental changes did not alter growth rates under a variety of low light intensity conditions. The outer wall of the mutant cells lacking the sll1556 gene contained more fibrous extensions, and there were fewer thylakoids per central cell section in the mutant than in the wild type, indicating deficient isoprenoid biosynthesis in the absence of the IPP isomerase. However, the specific isoprenoids affected by this mutation were not identified in this study.

The IPP isomerase was also reported to be a rate-limiting enzyme in the terpenoid biosynthesis of green algae (Sun 1998), plants (Albrecht and Sandmann 1994) and multiple other organisms (Chen et al. 2012; Kajiwara et al. 1997). Three different IPP isomerase enzymes from *Haematococcus pluvialis*, *Phaffia rhodozyma*, and *Saccaromyces cerevisiae* were overexpressed independently in *E. coli,* along with the carotenoid biosynthesis gene cluster from *Erwinia* (Kajiwara et al. 1997). Presence of an overexpressed IPP isomerase contributed to 1.7-4.5 fold increase in carotenoid production, indicating that the IPP isomerase plays a role in substrate partitioning for heterologous carotenoid biosynthesis in these organisms. Several other groups have also overexpresed the IPP isomerase to enhance heterologous carotenoid synthesis in *E. coli* (Lemuth et al. 2011; Wang et al. 2009; Gallagher et al. 2003; Albrecht et al. 1994). Overexpression of the native IPP isomerase in *Eucommia ulmoides* resulted in a 3- to 4-fold increase in the production of the most widely used isoprenoid polymer, trans-polyisoprene rubber (Chen et al. 2012).

Isomerase enzymes of other biosynthetic pathways were also reported to enhance product formation. Overexpression of the chalcone isomerase from the flavonol biosynthetic pathway up-regulated end product synthesis by up to a 66-fold in tomato (Muir et al. 2001), and 12-fold increase in *Salvia Involucrata* (Li et al. 2006). Integration of multiple copies of the *Piromyces* xylose isomerase (*XYLA*) gene, resulting in xylose isomerase overexpression, was employed to enhance by about 9-fold xylose assimilation for ethanol production in *Saccharomyces cerevisiae* (Zhou et al. 2012). Thus, isomerase enzymes have proven to play critical roles in multiple biosynthetic pathways.

3.5 References

Adam P, Hecht S, Eisenreich W, Kaiser J, Gräwert T, Arigoni D, Rohdich F (2002) Biosynthesis of terpenes: studies on 1-hydroxy-2-methyl-2-(E)-butenyl 4-diphosphate reductase. Proc Natl Acad Sci USA 99(19):12108-12113.

Ajlani G, Vernotte C (1998) Construction and characterization of a phycobiliprotein-less mutant of *Synechocystis* sp. PCC 6803. Plant Mol Biol 37(3):577-580.

Albrecht M, Sandmann G (1994) Light-stimulated carotenoid biosynthesis during transformation of maize etioplasts is regulated by increased activity of isopentenyl pyrophosphate isomerase. Plant Physiol 105(2):529-534.

Arganoff BW, Eggerer H, Henning U, Lynen F (1959) Biosynthesis of terpenes. J Biol Chem 235(2):326-332.

Barkley SJ, Shrivallabh BD, Poulter CD (2004) Type II isopentenyl diphosphate isomerase from *Synechocystis* sp. strain PCC 6803. J Bacteriol 186.23:8156-8158.

Bentley FK, Melis A (2012) Diffusion-based process for carbon dioxide uptake and isoprene emission in gaseous/aqueous two-phase photobioreactors by photosynthetic microorganisms. Biotech Bioeng 109:100-109

Bentley FK, Zurbriggen A, Melis A (2013) Heterologous expression of the mevalonic acid pathway in cyanobacteria enhances endogenous carbon partitioning to isoprene. Mol Plant 7(1):71-86.

Chaves JE, Kirst H, Melis A (2015) Isoprene production in Synechocystis under alkaline and saline growth conditions. J Appl Phycol *27*(3):1089-1097.

Chen R, Harada Y, Bamba T, Nakazawa Y, Gyokusen K (2012) Overexpression of an Isopentenyl diphosphate isomerase gene to enhance trans-polyisoprene production in *Eucommia ulmoides* Oliver. BMC Biotechnol 12:8.

Collins AM, Liberton M, Jones HD, Garcia OF, Pakrasi HB, Timlin JA (2012) Photosynthetic pigment localization and thylakoid membrane morphology are altered in *Synechocystis* 6803 phycobilisome mutants. Plant Physiol 158(4):1600-1609.

der Heijden, R (1997) Isopentenyl diphosphate isomerase: a core enzyme in isoprenoid biosynthesis. A review of its biochemistry and function. Nat Prod Rep 14(6):591-603

Ershov Y, Gantt RR, Cunningham FX, Gantt E (200) Isopentenyl diphosphate isomerase deficiency in *Synechocystis* sp. strain PCC6803. FEBS Lett 473:337–340.

Formighieri C, Melis A (2014) Regulation of β-phellandrene synthase gene expression, recombinant protein accumulation, and monoterpene hydrocarbons production in *Synechocystis* transformants. Planta 240(2):309-324.

Formighieri C, Melis A (2016) Sustainable heterologous production of terpene hydrocarbons in cyanobacteria. Photosynth Res. In press DOI 10.1007/s11120-016-0233-2

Gallagher C, Cervantes-Cervantes M, Wurtzel E (2003) Surrogate biochemistry: use of *Escherichia coli* to identify plant cDNAs that impact metabolic engineering of carotenoid accumulation. Appl Microbiol Biotechnol 60(6):713-719.

Gao X, Gao G, Liu D, Zhang H, Nie X, Yang C (2016) Engineering the methylerythritol phosphate pathway in cyanobacteria for photosynthetic isoprene production from CO_2. Energy Environ Sci 9:1400-1411.

Halfmann C, Gu L, Zhou R (2014) Engineering cyanobacteria for the production of a cyclic hydrocarbon fuel from CO_2 and H_2O. Green Chem 16:3175–3185.

Kajiwara S, Fraser P, Kondo K, Misawa N (1997) Expression of an exogenous isopentenyl diphosphate isomerase gene enhances isoprenoid biosynthesis in *Escherichia coli*. Biochem J 324:421-426.

Kirst H, Formighieri C, Melis A (2014) Maximizing photosynthetic efficiency and culture productivity in cyanobacteria upon minimizing the phycobilisome light-harvesting antenna size. Biochim Biophys Acta (Bioenergetics) 1837(10):1653-1664.

Khosla C, Keasling JD (2003) Metabolic engineering for drug discovery and development. Nat Rev Drug Discov 2(12):1019-1025.

Lagarde D, Beuf L, Vermaas W (2000) Increased production of zeaxanthin and other pigments by application of genetic engineering techniques to *Synechocystis* sp. strain PCC 6803. Appl Environ Microbiol 66(1):64-72.

Lee GSJ, McCain JH, Bhasin MM (2007) Synthetic organic chemicals. Kent and Riegel's Handbook of Industrial Chemistry and Biotechnology. pp 345-403.

Lemuth K, Steuer K, Albermann C (2011) Engineering of a plasmid-free *Escherichia coli* strain for improved in vivo biosynthesis of astaxanthin. Microb Cell Fact 10(1):29.

Leonard E, Ajikumar PK, Thayer K, Xiao WH, Mo JD, Tidor B, Stephanopoulos G, Prather KL (2010) Combining metabolic and protein engineering of a terpenoid biosynthetic pathway for overproduction and selectivity control. Proc Natl Acad Sci USA. 107(31):13654-13659

Li FX, Jin ZP, Zhao DX, Cheng LQ, Fu CX, Ma F (2006) Overexpression of the *Saussurea medusa* chalcone isomerase gene in *S. involucrata* hairy root cultures enhances their biosynthesis of apigenin. Phytochemistry 67(6):553-560.

Li Z, Sharkey TD (2013) Metabolic profiling of the methylerythritol phosphate pathway reveals the source of post-illumination isoprene burst from leaves. Plant Cell Environ 36(2):429-437.

Lichtenthaler HK (2007) Biosynthesis, accumulation and emission of carotenoids, α-tocopherol, plastoquinone, and isoprene in leaves under high photosynthetic irradiance. Photosynth Res (2007) 92:163–179

Lichtenthaler HK (2010) Biosynthesis and emission of isoprene, methylbutanol and other volatile plant isoprenoids. The Chemistry and Biology of Volatiles, edited by Andreas Herrmann. John Wiley & Sons, Ltd (New York), pp 11-47.

Lindberg P, Park S, Melis A (2010) Engineering a platform for photosynthetic isoprene production in cyanobacteria, using *Synechocystis* as the model organism. Metab Eng 12(1):70-79.

McCauley SW, Melis A (1986) Quantitation of plastoquinone photoreduction in spinach chloroplasts. Photosynth Res 8(1):3-16.

McGarvey DJ, Croteau R (1995) Terpenoid metabolism. Plant Cell 7(7):1015.

Muir SR, Collins GJ, Robinson S, Hughes S, Bovy A, De Vos CR, Verhoeyen ME (2001) Overexpression of petunia chalcone isomerase in tomato results in fruit containing increased levels of flavonols. Nat Biotechnol 19(5):470-474.

Nagarajan A, Winter R, Eaton-Rye J, and Burnap R (2011) A synthetic DNA and fusion PCR approach to the ectopic expression of high levels of the D1 protein of photosystem II in *Synechocystis* sp PCC 6803. J Photochem Photobiol B 104:212–219.

Okada K, Kasahara H, Yamaguchi S, Kawaide H, Kamiya Y, Nojiri H, Yamane H (2008) Genetic evidence for the role of isopentenyl diphosphate isomerases in the mevalonate pathway and plant development in Arabidopsis. Plant Cell Physiol 49(4):604-616.

Pade N, Erdmann S, Enke H, Dethloff F, Dühring U, Georg J, Wambutt J, Kopka J, Hess WR, Zimmermann R, Kramer D, Hagemann M (2016) Insights into isoprene production using the cyanobacterium *Synechocystis* sp. PCC 6803. Biotechnol Biofuels. In press doi: 10.1186/s13068-016-0503-4

Poliquin K, Ershov YV, Cunningham FX, Woreta TT, Gantt RR, Gantt E (2004) Inactivation of sll1556 in *Synechocystis* strain PCC 6803 impairs isoprenoid biosynthesis from pentose phosphate cycle substrates in vitro. J Bacteriol 186(14):4685-4693.

Puan KJ, Wang H, Dairi T, Kuzuyama T, Morita CT (2005) *fldA* is an essential gene required in the 2-*C*-methyl-D-erythritol 4-phosphate pathway for isoprenoid biosynthesis. FEBS Lett 579(17):3802-3806.

Schuurmans RM, Schuurmans JM, Bekker M, Kromkamp JC, Matthijs HC, Hellingwerf KJ (2014) The redox potential of the plastoquinone pool of the cyanobacterium *Synechocystis* species strain PCC 6803 is under strict homeostatic control. Plant Physiol 165(1):463-475.

Street IP, Poulter CD (1990) Isopentenyldiphosphate: dimethylallyldiphosphate isomerase: construction of a high-level heterologous expression system for the gene from

Saccharomyces cerevisiae and identification of an active-site nucleophile. Biochemistry 29(32):7531-7538.

Sun Z, Cunningham FX, Gantt E (1998) Differential expression of two isopentenyl pyrophosphate isomerases and enhanced carotenoid accumulation in a unicellular chlorophyte. Proc Natl Acad Sci USA 95(19):11482-11488.

Tritsch D, Hemmerlin A, Bach TJ, Rohmer M (2010) Plant isoprenoid biosynthesis via the MEP pathway: in vivo IPP/DMAPP ratio produced by (E)-4-hydroxy-3-methylbut-2-enyl diphosphate reductase in tobacco BY-2 cell cultures. FEBS Lett 584(1):129-134.

Wang Y, Qiu C, Zhang F, Guo B, Miao Z, Sun X, Tang K (2009) Molecular cloning, expression profiling and functional analyses of a cDNA encoding isopentenyl diphosphate isomerase from *Gossypium barbadense*. Biosci Rep *29*:111-119.

Weise SE, Li Z, Sutter AE, Corrion A, Banerjee A, Sharkey TD (2013) Measuring dimethylallyl diphosphate available for isoprene synthesis. Anal Biochem 435(1):27-34.

Xiao Y, Savchenko T, Baidoo EE, Chehab WE, Hayden DM, Tolstikov V, Corwin JA, Kliebenstein DJ, Keasling JD, Dehesh K (2012) Retrograde signaling by the plastidial metabolite MEcPP regulates expression of nuclear stress-response genes. Cell 149(7):1525-1535.

Zhou H, Cheng JS, Wang BL, Fink GR, Stephanopoulos G (2012) Xylose isomerase overexpression along with engineering of the pentose phosphate pathway and evolutionary engineering enable rapid xylose utilization and ethanol production by *Saccharomyces cerevisiae*. Metab Eng 14(6):611-622.

Zhou CF, Li ZR, Wiberley-Bradford AE, Weise SE, Sharkey TD (2013) Isopentenyl diphosphate and dimethylallyl diphosphate/isopentenyl diphosphate ratio measured with recombinant isopentenyl diphosphate isomerase and isoprene synthase. Analyt Biochem 440:130-136

Zurbriggen A, Kirst H, Melis A (2012) Isoprene production via the mevalonic acid pathway in *Escherichia coli* (bacteria). Bioenergy Res 5(4):814-828.

3.6 Supplementary Materials

Oligonucleotides:

F1- GAGATCAGTAACAATAACTCTAGGGTC
R1- GAGATTAGTCATTGTTATGGTTAGTTAATGC
R2- GGTGGAAACGGCTTCAGTTAAAG

DNA Constructs:

***Synechocystis* codon optimized kudzu (*Pueraria montana*) transgenic isoprene synthase *SkIspS* DNA nucleotide sequence used in this work.**

atgCCCTGGCGTGTAATCTGTGCAACTTCTTCCCAATTTACTCAAATTACCGAGCACAA
TTCCCGGCGTAGTGCCAACTATCAACCCAATCTGTGGAACTTTGAGTTCTTACAGAG
CCTGGAAAATGATTTAAAGGTCGAGAAATTGGAGGAGAAGGCCACTAAATTGGAAG
AGGAAGTGCGGTGTATGATTAATCGTGTAGACACCCAACCATTGAGTCTGTTAGAAT
TGATCGATGATGTGCAACGTCTCGGCCTGACATACAAATTCGAAAAAGATATCATTA
AGGCCCTAGAAAACATTGTCTTATTGGATGAAAACAAGAAAAATAAGTCTGACTTG
CATGCCACCGCTTTAAGTTTCCGCTTGTTGCGGCAGCACGGCTTTGAAGTGTCCCAA
GATGTTTTTGAACGGTTCAAAGACAAGGAGGGCGGCTTTTCCGGCGAACTCAAAGG
GGATGTTCAGGGCCTATTGTCTTTGTATGAAGCTAGTTACTTGGGATTTGAAGGCGA
GAATCTGTTAGAAGAAGCTCGCACTTTTTCCATTACACATTTAAAGAACAACCTAAA
GGAAGGGATTAACACAAAAGTGGCTGAGCAGGTGTCTCATGCTCTGGAGTTGCCGT
ATCATCAACGCTTACACCGGCTCGAAGCCCGCTGGTTTTTGGATAAATATGAACCGA
AAGAACCGCATCATCAATTACTGCTCGAACTGGCGAAGCTGGACTTTAATATGGTCC
AAACACTACATCAGAAAGAACTCCAGGACCTAAGTCGGTGGTGGACTGAAATGGGT
CTGGCATCCAAGCTAGATTTTGTGCGCGACCGTTTGATGGAGGTGTACTTCTGGGCA
CTAGGCATGGCTCCCGACCCGCAGTTTGGTGAGTGTCGTAAGGCAGTGACCAAGAT
GTTTGGTTTAGTAACGATCATCGACGACGTTTACGATGTCTATGGCACCCTAGACGA
ATTACAACTCTTTACAGATGCCGTCGAACGTTGGGATGTTAATGCCATCAATACCTT
ACCTGATTACATGAAATTGTGCTTCCTCGCCTTGTATAATACCGTTAATGACACCAG
CTATTCTATTCTGAAGGAAAAAGGCCACAATAACTTAAGCTACCTAACCAAAAGTTG
GCGGGAATTGTGTAAGGCTTTCTTACAGGAAGCCAAATGGTCCAACAACAAAATTA
TCCCCGCATTTTCTAAATACCTGGAAAATGCCTCCGTGTCCTCTTCCGGGGTGGCTTT
GCTAGCACCCAGCTACTTTTCTGTTTGTCAGCAACAGGAGGACATCAGTGACCATGC
CTTGCGGTCCTTAACGGACTTTCATGGCTTAGTGCGGAGTAGCTGCGTCATTTTTCGT
TTATGTAACGATTTGGCTACAAGTGCTGCGGAATTGGAACGTGGGGAAACAACCAA
CAGCATTATCAGTTATATGCACGAAAACGATGGCACCAGTGAAGAGCAGGCACGGG
AAGAACTGCGCAAATTAATCGACGCTGAATGGAAGAAGATGAATCGCGAACGTGTG
TCTGATAGTACCTTATTACCTAAAGCCTTCATGGAAATTGCGGTGAATATGGCCCGC
GTCAGTCATTGCACTTACCAATACGGCGATGGATTAGGTCGGCCCGATTACGCAACG
GAAAATCGGATCAAATTGCTATTGATTGATCCGTTCCCAATTAATCAATTAATGTAC
GTGtaaTCTAG

Codon optimized *Streptococcus pneumoniae* and chloramphenicol resistance transgenic *Δcpc+SSpFNI+CmR* DNA nucleotide sequence used in this work.

FNI- Uppercase
CmR- Lowercase

ATGACTACCAATCGCAAGGATGAGCACATCTTGTATGCACTAGAGCAAAAATCCAG
TTACAACAGCTTTGACGAAGTGGAATTGATCCACTCCTCCTTACCCCTATACAATTTA
GATGAAATTGACTTGTCTACCGAGTTTGCCGGACGCAAATGGGACTTTCCCTTTTAC
ATTAATGCCATGACTGGGGGCAGCAACAAAGGACGGGAGATCAATCAAAAATTAGC
TCAGGTTGCCGAAACTTGTGGCATCCTATTTGTTACCGGCAGTTATAGTGCAGCCCT
GAAAAATCCGACGGATGATTCCTTTAGTGTGAAAAGTTCCCATCCGAATCTCCTCTT
AGGTACAAACATTGGCCTAGATAAACCCGTTGAACTGGGCTTGCAAACAGTGGAAG
AAATGAACCCCGTATTGTTGCAAGTGCATGTTAACGTAATGCAGGAGCTGTTGATGC
CCGAAGGAGAACGGAAATTTCGTTCCTGGCAGTCTCATTTAGCCGACTATTCCAAAC
AAATTCCCGTGCCGATTGTATTGAAAGAAGTTGGGTTTGGCATGGACGCCAAGACA
ATCGAACGCGCTTATGAATTTGGCGTTCGCACCGTTGATTTGTCTGGCCGTGGCGGA
ACTAGCTTTGCTTATATTGAAAATCGGCGGAGTGGCCAACGTGACTATTTGAATCAA
TGGGGCCAATCCACTATGCAGGCCTTGCTGAATGCCCAAGAATGGAAAGACAAAGT
GGAATTACTAGTGAGTGGCGGGGTGCGTAATCCCTTAGATATGATTAAATGCTTAGT
ATTTGGTGCCAAGGCGGTTGGTCTGAGTCGTACCGTGTTGGAACTGGTAGAAACCTA
TACTGTTGAAGAAGTAATTGGGATCGTCCAGGGGTGGAAGGCCGACCTGCGCCTCA
TCATGTGCTCCTTGAACTGTGCCACCATTGCCGATCTGCAAAAAGTTGATTATCTGCT
GTACGGTAAATTGAAAGAAGCGAACGATCAAATGAAAAAAGCGTAGGCGGCCGCgtt
gatcggcacgtaagaggttccaactttcaccataatgaaataagatcactaccgggcgtatttttgagttatcgagattttcaggagctaagga
agctaaaatggagaaaaaaatcactggatataccaccgttgatatatcccaatggcatcgtaaagaacattttgaggcatttcagtcagttgct
caatgtacctataaccagaccgttcagctggatattacggccttttaaagaccgtaaagaaaaataagcacaagttttatccggcctttattcac
attcttgcccgcctgatgaatgctcatccggaattccgtatggcaatgaaagacggtgagctggtgatatgggatagtgttcacccttgttaca
ccgttttccatgagcaaactgaaacgttttcatcgctctggagtgaataccacgacgatttccggcagtttctacacatatattcgcaagatgtg
gcgtgttacggtgaaaacctggcctatttccctaaagggtttattgagaatatgtttttcgtctcagccaatccctgggtgagtttcaccagttttg
atttaaacgtggccaatatggacaacttcttcgcccccgttttcaccatgggcaaatattatacgcaaggcgacaaggtgctgatgccgctgg
cgattcaggttcatcatgccgtctgtgatggcttccatgtcggcagaatgcttaatgaattacaacagtactgcgatgagtggcagggcgggg
cgtaatttttttaaggcagttattggtgcccttaaacgcctggg

Chapter 4: *Engineering isoprene synthase expression and activity in cyanobacteria*

This work was performed with the following persons:

JEC, PRR, HK, and AM designed the project. JEC and PRR conducted the experimental work. JEC and AM wrote the manuscript.

4.1 Introduction

This work sought to apply the fusion protein approach and to develop an understanding of the role of recombinant isoprene synthase enzyme concentration and specific activity on the rate and yield of heterologous isoprene production in cyanobacteria. The terpene synthase protein fusion approach (Formighieri and Melis 2015; 2016) was adapted and applied to achieve substantial levels of isoprene synthase expression and recombinant protein accumulation in cyanobacteria. The approach relies on fusing the 5'end of the terpene synthase gene to the 3'end of a gene that encodes a highly expressed native protein in the cyanobacterial cell. In this case, the leader gene sequence was the *cpcB* gene encoding the β-subunit of phycocyanin (Kirst et al. 2014). The β-subunit of phycocyanin is a component of the peripheral rods in the cyanobacterial phycobilisome light-harvesting antenna and a very abundant protein in the cyanobacterial cell. This construct resulted in a true overexpression of the cpcB*IspS fusion protein, in amounts up to 300-fold greater than what was measured for the heterologous *IspS* gene expression in the absence of a highly expressed leader fusion protein. However, direct fusion of the *IspS* to the *cpcB* gene resulted in very low isoprene synthase specific activity. To alleviate possible masking or allosteric effects of the cpcB protein on the catalytic site of the IspS, and hopefully alter the folding pattern of the fusion protein, linker constructs were designed (Chen et al. 2013) and applied between the cpcB leader and IspS fusion proteins. The use of linker amino acids between the cpcB and IspS proteins had a significant positive effect on isoprene synthase enzymatic activity, suggesting feasibility of engineering the isoprene synthase activity by regulating distance and folding pattern between the two proteins and thereby improving reactant access to the catalytic site of the terpene synthase.

4.2 MATERIALS AND METHODS

Strains and culturing conditions. *Synechocystis* sp. PCC 6803 was employed as the experimental strain and is referred to as the wild type (WT). All strains employed in this work were maintained on 1% agar-BG11 media supplemented with 10 mM TES-NaOH pH 8.2, and 0.3% Na-thiosulfate. Chloramphenicol (30 μg/mL), was added to the agar plates and used to maintain transformants. Liquid cultures were grown in BG11 media buffered with 25 mM NaH_2PO_4 (pH 7.5) at 28°C, under continuous aeration and gradually increasing illumination. Cultures inoculated from a plate started in the lowest illumination at 30 μmol photons m^{-2} s^{-2} until an $OD_{730\ nm}$=0.3 was reached. Illumination was then increased to 50 μmol photons m^{-2} s^{-2} until an $OD_{730\ nm}$=0.65-0.75 was reached. Illumination was then increased to 100 μmol photons m^{-2} s^{-2} until the culture reached a density great enough to support dilution in 700 mL to an $OD_{730\ nm}$=0.65. The latter was subjected to 100% CO_2-loading in the sealed Bentley and Melis (2012) gaseous-aqueous two-phase bioreactor for biomass and isoprene quantification.

IspS-containing constructs. Transformations were performed as previously established (Kirst et al. 2014). DNA constructs were designed to insert the isoprene synthase (*IspS*) gene in the *cpc* operon locus. In the control strain (*cpcB-IspS*), the isoprene synthase gene along with the chloramphenicol resistance cassette were inserted between the *cpcB* and *cpcA* coding regions with a ribosome-binding site placed in front of each. In alternative configurations engineered for isoprene synthase overexpression, the isoprene synthase was designed as a fusion with the *cpcB* gene (*cpcB*IspS*), either with or different nucleotide spacers between the two genes, which

translated into amino acid spacers in the fusion protein. Four different amino acid spacers were designed as links between the cpcB and IspS proteins consisting of:

(i) L7: A single proline followed by the final 6 amino acids of the putative IspS transit peptide, PMPWRVI (*cpcB*L7*IspS*),

(ii) L10: A total of five alternating proline-alanine pairs PAPAPAPAPA (*cpcB*L10*IspS*),

(iii) L16: A combination of 16 amino acids comprising glutamic acid (E), alanine (A), lysine (K), EAAAKEAAAKEAAAKA (*cpcB*L16*IspS*), and

(iv) L65: Comprising the 60 N-terminus amino acids of the isoprene synthase itself followed by 5 amino acids of the IspS transit peptide, CPWRVICATSSQFTQITEHNSRRSANYQPNLWNFEFLQSLENDLKVEKLEEKATKLE EEVRPWRVI (*cpcB*L65*IspS*).

Pigment analysis. Chlorophyll *a* and carotenoids were extracted from the cells in 100% methanol. The absorbance of the methanol extract was measured at 665 nm and 470 nm, corrected for any non-specific absorbance at 710 nm. For this purpose, absorbance spectra of cell extracts were scanned spectrophotometrically from 400-750 nm with a Shimadzu UV-1800 UV-visible spectrophotometer. Readings of the absorbance at the above wavelengths were taken from the spectra. Pigment concentrations were calculated from the absorbance at these wavelengths according to equations given by Lichtenthaler (1987). Cell lysates were collected by French press disruption as described below. Broken cell suspensions were then centrifuged at 2,250 g for 3 min to pellet cell debris and glycogen grains.

Protein analysis. Cells were grown in 300 mL liquid cultures to an OD_{730} of 2.5, pelleted by centrifugation, and re-suspended in 5-10 mL of 50 mM Tris-HCl (pH 8). Protease inhibitor (1 mM PMSF) was added to samples before lysing of the cells by French press (2x1500 psi). Disrupted cell suspensions were centrifuged at 2,250 g for 3 min to pellet cell debris and glycogen grains. An aliquot of the supernatant was used for pigment concentration determination, as described above. The supernatant was supplemented with an equal volume of solubilization solution, comprising 250 mM Tris-HCl, pH 6.8, 7% w/v SDS, 20% w/v glycerol, 2 M urea, and a few grains of bromophenol blue. Samples were solubilized upon incubation at room temperature for 1-2 h. At the end of the solubilization incubation, samples were supplemented with 5% β-mercaptoethanol. The solubilized total cellular proteins were subjected to SDS-PAGE and Western blot analysis. SDS-PAGE-resolved proteins were either stained with Coomassie brilliant blue or transferred to a nitrocellulose membrane for immunodetection using rabbit immune serum containing specific polyclonal antibodies against the IspS protein (Lindberg et al. 2010).

Isoprene and biomass accumulation. Liquid cultures for biomass accumulation and isoprene production were grown photoautotrophically in the absence of antibiotics. Glass bottle bioreactors (1 L volume) were designed in this lab specifically for quantitative biomass and isoprene production measurements, (Bentley and Melis 2012). The 1-L bioreactors were loaded with ~700 mL liquid BG11 growth medium containing 25 mM NaH_2PO_4 (pH 7.5), and then inoculated with *Synechocystis* starter cultures to an $OD_{730\ nm} = 0.65$. Unless otherwise indicated, the bioreactors were further loaded with inorganic carbon, delivered to the liquid culture by slowly bubbling 500 mL of 100% CO_2 gas through the bottom of the liquid culture to fill the

reactor headspace. Bioreactors were then sealed and cultures were stirred slowly and continuously at 28°C under constant illumination at 100 µmol photons m^{-2} s^{-2}.

Isoprene accumulation in the headspace of the reactor was determined by gas chromatography (Shimadzu 8A GC-FID) analysis of 1 mL gaseous samples from the bioreactor headspace. Isoprene quantification was determined based on a calibration of isoprene standard (Acros Organics, Fair Lawn, NJ, USA), as described (Chaves et al. 2015). Biomass accumulation in the liquid phase of the reactor was determined upon collection of 50 mL aliquots, followed by centrifugation, rinsing of the pellet with deionized water, and cell re-suspension in 2 mL of deionized water. The latter were transferred onto aluminum trays, dried for 6 h at 90°C, and weighed to determine the dry cell weight (dcw). Cell growth was also determined spectrophotometrically by measuring the optical density of live cell cultures at 730 nm with a Shimadzu UV-1800 UV-visible spectrophotometer.

Photosynthetic activity. Oxygen evolution of the cells was measured with an S1 Clark-type oxygen electrode (Oxygraph Plus System, Hansatech Instruments Ltd, United Kingdom) at 23°C illuminated with a high intensity 100 W tungsten-halogen light source. Cell suspensions were loaded into the oxygen electrode chamber at a concentration of 0.6 µM chlorophyll in 2 mL samples. Sodium bicarbonate (20 µL of 0.5 M solution, pH 7.4) was added to the samples just before measuring to prevent carbon limitation during photosynthesis. After determining the rate of dark respiration, the cells were illuminated with gradually increasing light intensities. Oxygen evolution was recorded for 2-5 minutes at each light intensity allowing linear progression of the slope.

In-vitro assay enzymatic activity. Liquid cultures of *Synechocystis* strains containing the fusion isoprene synthase constructs (*cpcB*IspS*, *cpcB*L16*IspS, cpcB*L7*IspS*) were grown in 5 L cultures to an OD = 3.5, pelleted by centrifugation at 4000 g for 15 min, resuspended in buffer (50 mM bicine, pH 8.0, 30 mM NaCl, 50 mM $MgCl_2$, 50 mM KCl, 5% glycerol, 1 mM DTT), and lysed by French press (2x1500 psi). Disrupted cell suspensions were centrifuged at 2,250 g for 3 min to pellet cell debris and glycogen grains. The membranes of crude cell lysates were separated by ultracentrifugation at 143,000 g for 60 min. The soluble fraction of the cell lysate was then filtered and concentrated using Amicon Ultra 15 50 kD filters (Millipore, USA). Aliquots of the concentrated crude cell extracts were then run on an SDS PAGE gel and stained with Coomassie brilliant blue. Protein concentrations were determined based on the intensity of the cpcB*IspS fusion protein appearing as a band at 85 kD relative to a BSA standard. The Bio-Rad ChemiDoc imaging system was used to photograph the Western blot and the Bio-Rad Image Lab software was utilized to quantify the relative IspS protein levels between the different strains based on band intensity.

In vitro reactions were conducted in 100 µL mixtures containing 50 mM Bicine, pH 8.0, 30 mM NaCl, 50 mM $MgCl_2$, 50 mM KCl, 5% glycerol, 1 mM DTT, 12 µg cpcB*LX*IspS, and varying concentrations of DMAPP, as described (Zubriggen et al. 2012). Reactions were incubated for 15 min at 42°C, then 1 mL aliquots of the headspace were sampled for isoprene content by gas chromatography, as described above.

4.3 RESULTS

***Synechocystis* transformations.** The *cpcB-IspS, cpcB*IspS* and *cpcB*L(7,10,16,65)*IspS* constructs (**Fig. 4.1**) were introduced into the *Synechocystis* genomic DNA at the *cpc* locus via double homologous recombination. Each of the *cpcB*IspS* and *cpcB*L(7,10,16,65)*IspS* fusion constructs with the attendant chloramphenicol resistance cassette (CmR) replaced the native *cpcB* gene, while maintaining the rest of the native *cpc* operon (*cpcA*, *cpcC1*, *cpcC2*, *cpcD*) in place (**Fig. 4.1**). In the control strain (Fig. 1, cpcB-IspS), the *IspS* gene and its corresponding CmR cassette were inserted in-between the *cpcB* and *cpcA* genes without a fusion between any of these genes/proteins. A more detailed schematic presentation of the linker amino acids used between the cpcB and IspS fusion constructs is shown in **Fig. 4.2**. Detailed nucleotide sequences of the inserted genes are given in the Supplementary Materials.

The state of homoplasmy of the transformant strains was tested by PCR analysis of the *Synechocystis* genomic DNA using primers (forward, F1 and reverse R1, **Fig. 4.1**) flanking the site of the homologous recombination. In the wild type, the F1 and R1 primers amplified a 1.2 kb product. The *cpcB-IspS* and *cpcB*IspS* strains amplified a 3.8 kb product and failed to amplify the 1.2 kb wild type product (**Fig. 4.3A, left-half**). Exclusion PCR was performed using the same primers (F1 and R1) with a shorter extension time (30 s), sufficient for the wild type to generate product. The premise of exclusion PCR is that a short extension time enables product accumulation from short DNA sequences, while excluding those from long DNA sequences under the same conditions and primers. In this case, the wild type amplified the 1.2 kb product (**Fig. 4.3A, right-half**), while the *cpcB-IspS* and *cpcB*IspS* strains failed to amplify a product. Taken together, these results show absence of wild type copies of the *Synechocystis* DNA in the *cpcB-IspS* and *cpcB*IspS* transformants, evidence of having achieved transgenic DNA homoplasmy.

A similar comparative *Synechocystis* genomic DNA PCR analysis was conducted for the *cpcB*L7*IspS* and *cpcB*L10*IspS* (**Fig. 4.3B**), *cpcB*L16*IspS* (**Fig. 4.3C**), and *cpcB*L65*IspS* transformants (**Fig. 4.3D**). In all cases, the evidence showed that *Synechocystis* transformants have reached a state of transgenic genomic DNA homoplasmy.

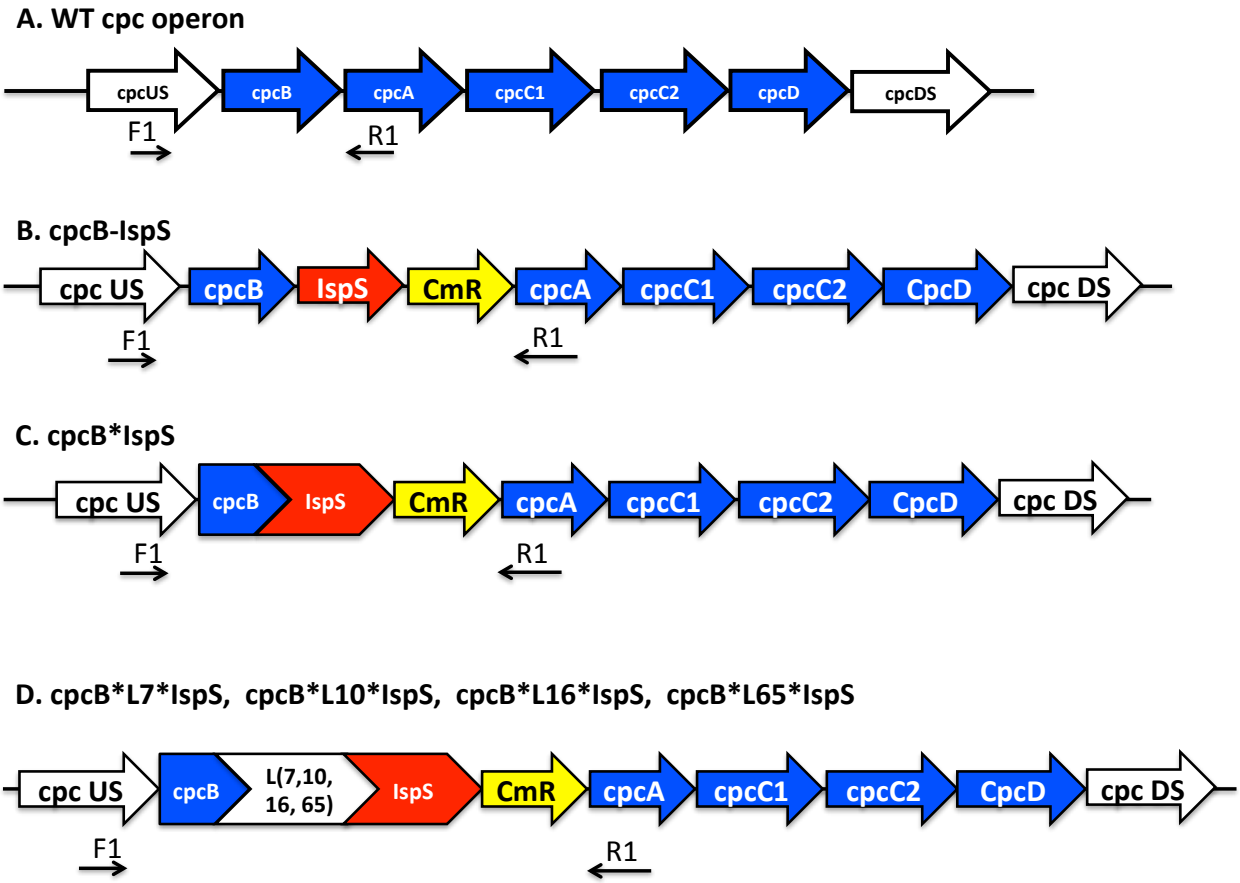

Figure 4.1. DNA constructs for *Synechocystis* transformant strains were designed to replace the native *cpcB* gene with different versions of the *cpcB* fused to the *IspS* followed by a chloramphenicol resistance (*CmR*) cassette. (**A**) Schematic of the *cpc* operon in the wild type. (**B**) In the control *cpcB-IspS* strain, the *IspS* and *CmR* genes were inserted between the *cpcB* and the *cpcA* in a non-fusion configuration. (**C**) A direct *cpcB*IspS* fusion without a linker, and (**D**) four different linker-separated versions *cpcB*L7*IspS*, *cpcB*L10*IspS*, *cpcB*L16*IspS*, and *cpcB*L65*IspS* consisting of variable number (7, 10, 16, 65) and composition of amino acid.

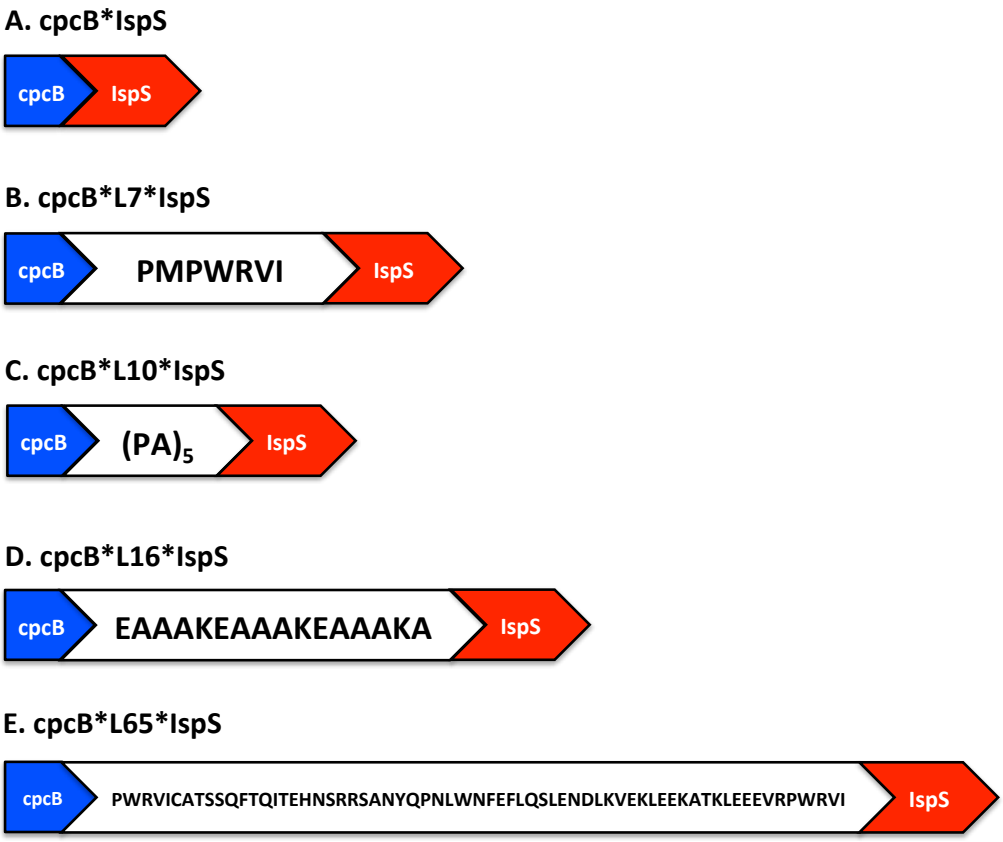

Figure 4.2. The amino acid sequences of the linkers for each of the fusion strains employed in this work: **(A)** *cpcB*IspS,* **(B)** *cpcB*L7*IspS* **(C)** *cpcB*L10*IspS* **(D)** *cpcB*L16*IspS* and **(E)** *cpcB*L65*IspS.*

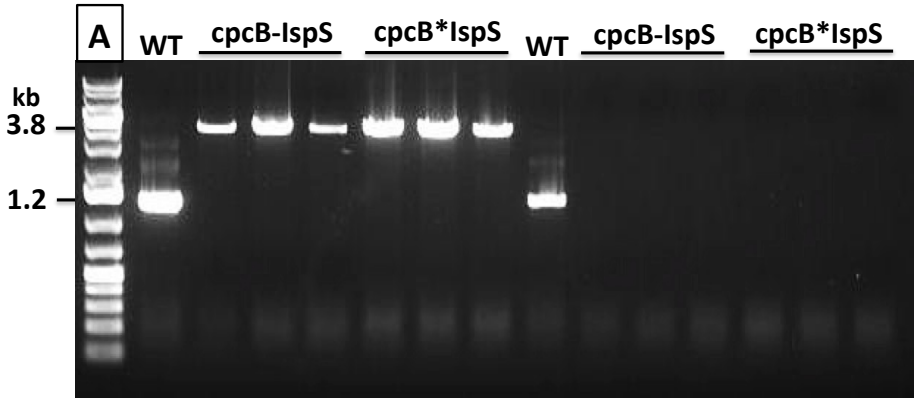
A
WT
cpcB-IspS
cpcB*IspS
WT
cpcB-IspS
cpcB*IspS
kb
3.8
1.2

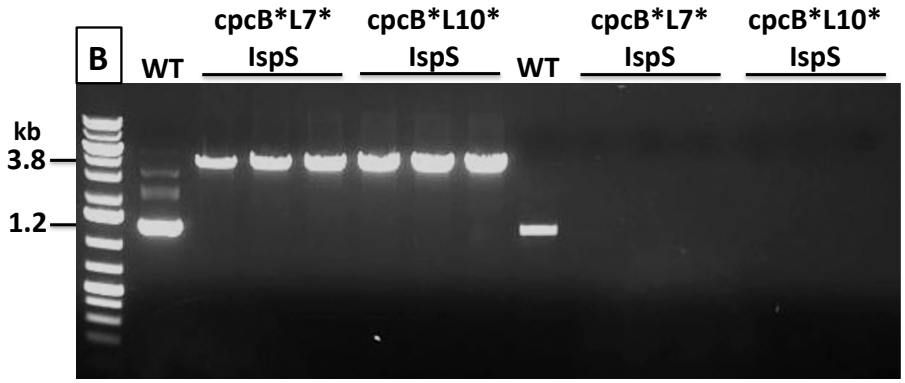
B
WT
cpcB*L7*
IspS
cpcB*L10*
IspS
WT
cpcB*L7*
IspS
cpcB*L10*
IspS
kb
3.8
1.2

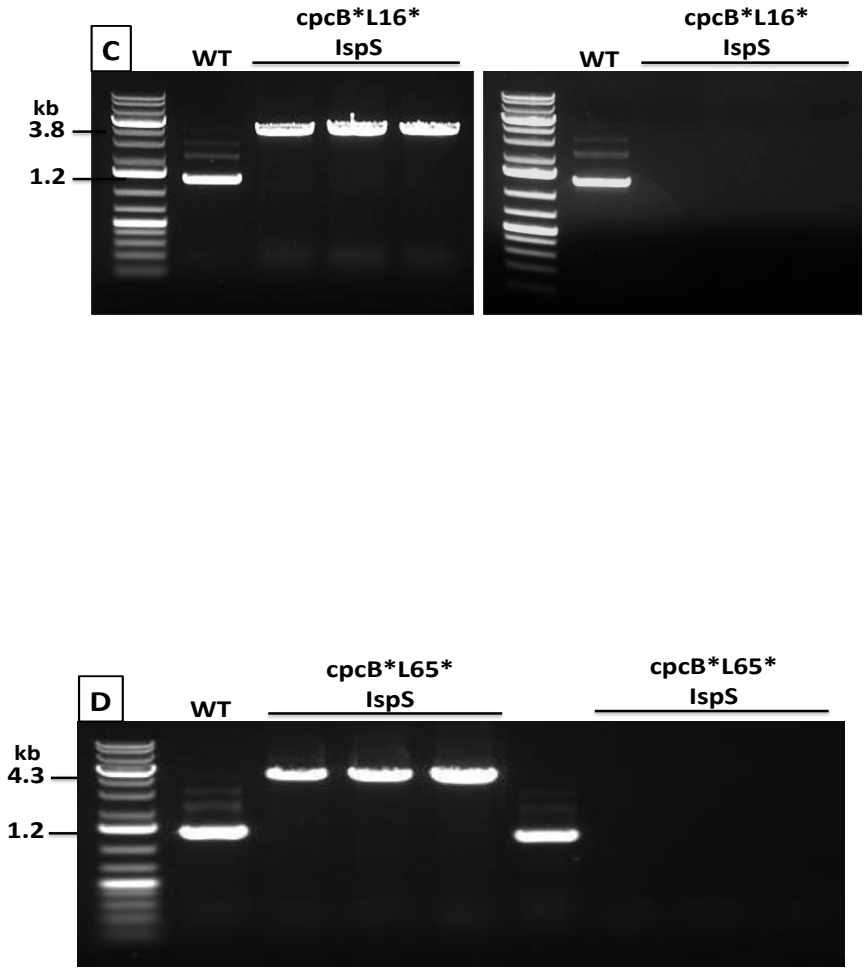

Figure 4.3. Genomic DNA PCR analysis of wild type and *IspS* transformants. The state of homoplasmy of the transformant strains was tested by PCR analysis of the *Synechocystis* genomic DNA using primers (forward, F1 and reverse, R1) flanking the site of the homologous recombination. In the wild type, the F1 and R1 primers amplified a 1.2 kb product (**A-D, left side**). The *cpcB-IspS* and *cpcB*IspS* transformants **(A)**, and *cpcB*L(7, 10, 16)IspS* transformants **(B** and **C)**, amplified a 3.8 kb product. The *cpcB*L65*IspS* transformant generated a 4.3 kb product **(D)**. Exclusion PCR was performed using the same primers (F1 and R1) with a shorter extension time (30 s), sufficient for the wild type to generate a product, but not so for the transgenes. In each case the wild type generated a 1.2 kb product, while the transgenic strains failed to amplify any product **(A-D, right side)**.

Protein expression in wild type and IspS strains. Transgenic protein expression levels were determined by SDS-PAGE analysis, loading ~1 μg Chl per sample. The wild type recipient strain (**Fig. 4.4, WT**) showed a dominant protein band at about 58 kD attributed to the large subunit of Rubisco, and abundant protein bands at about 20 kD from the cpcB phycocyanin β-subunit, as well as at about 15 kD from the cpcA phycocyanin α-subunit. The *cpcB-IspS, cpcB*IspS,* and *cpcB*L(7,10,16,65)*IspS* transformants failed to accumulate the 20 and 15 kD phycocyanin subunits, evidenced by the lack of these proteins from the respective SDS-PAGE lanes (Fig. 4). Instead, the fusion *cpcB*IspS* and *cpcB*L(7,10,16,65)*IspS* transformants showed noticeable accumulation of the corresponding fusion proteins, migrating to about 80-85 kD (**Fig. 4.4,** protein bands marked by asterisk). Of the various transformants, the cpcB*IspS, cpcB*L7*IspS, and cpcB*L65*IspS constructs showed the highest recombinant protein expression. Constructs cpcB*L10*IspS and cpcB*L16*IspS, also showed expression of the recombinant proteins, albeit at somewhat lower levels than the cpcB*IspS and cpcB*L7*IspS fusions. A faint band at ~24 kD in this SDS-PAGE analysis was attributed to expression of the chloramphenicol resistance protein (**Fig. 4.4,** CmR).

The relative expression of the IspS and cpcB*IspS fusion proteins was further investigated by Western blot analysis, measuring the specific cross reactions at 65 kD, attributed to the IspS protein, and ~80-85 kD, attributed to the fusion proteins (**Fig. 4.5**). In this analysis, cellular extracts were loaded differently than in the SDS-PAGE analysis of Fig. 4. The WT and cpcB-IspS lanes were loaded with 1 μg Chl of cell extract, while the cpcB*IspS and cpcB*L(*7,10,16,65*)*IspS sample extracts were loaded with 0.01 μg Chl. This loading adjustment was necessitated because of the asymmetry in the cross-reaction response between the two groups of samples. Results from the intensity of the cross reactions in Fig. 5 were consistent with the differential intensity of the Coomassie stain in Fig. 4 for the fusion proteins. The cpcB*IspS, cpcB*L7*IspS, and cpcB*L65*IspS proteins were more abundant in the transformant cells than the cpcB-IspS, cpcB*L10*IspS and cpcB*L16*IspS fusion proteins. The Bio-Rad ChemiDoc imaging system was used to document the Western blots and the Bio-Rad Image Lab software was employed to quantify the relative IspS protein levels in the different strains. The results were normalized to the cross-reaction intensity of the cpcB-IspS sample (=1 relative unit) and corrected for the uneven loading of the cpcB*IspS and cpcB*L(*7,10,16,65*)*IspS samples. This semi-quantitative Western blot analysis showed the presence of 275, 254, and 234 relative units (Relative Quantity in **Fig. 4.5**) of IspS in the cpcB*IspS, cpcB*L7*IspS and cpcB*L65*IspS, respectively. A lower amount equal to 61 and 67 relative units of IspS was measured in the cpcB*L10*IspS and cpcB*L16*IspS transformants, respectively.

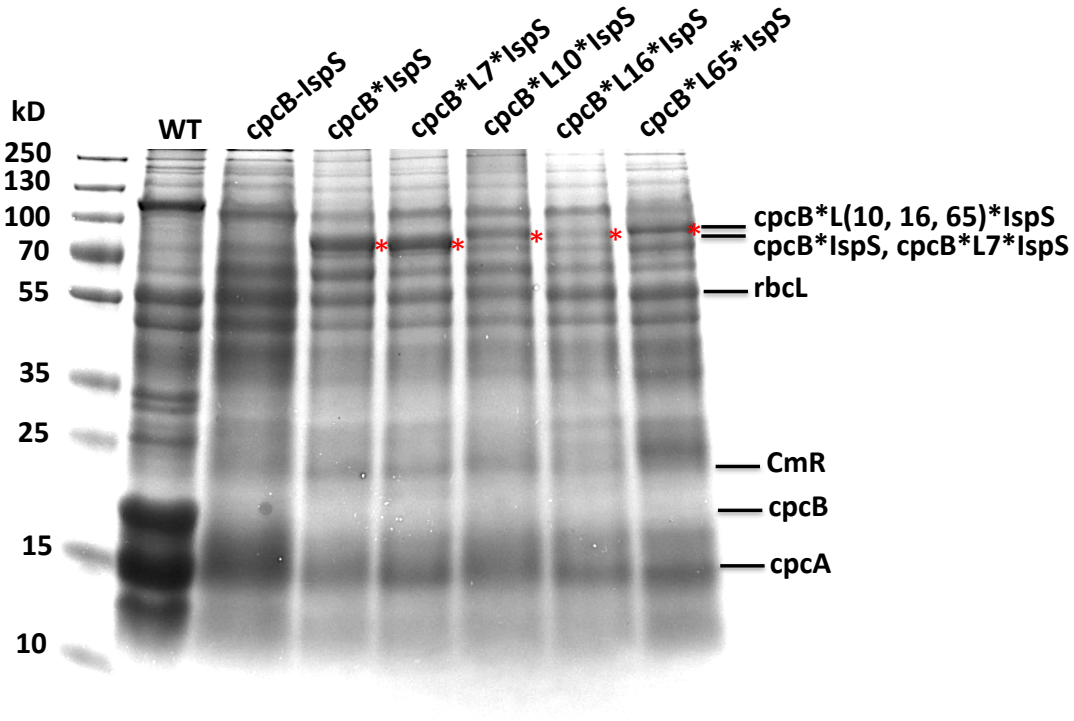

Figure 4.4. SDS-PAGE analysis of total protein extract from *Synechocystis* wild type and *IspS* transformants. Transgenic protein expression levels were determined from the Coomassie stain of the SDS-PAGE resolved proteins. Lane loadings were 1 µg Chl per sample. The wild type strain showed a dominant protein band at about 58 kD attributed to the large subunit of Rubisco, and abundant protein bands at about 20 kD from the cpcB phycocyanin β-subunit, as well as at about 15 kD from the cpcA phycocyanin α-subunit. The *cpcB-IspS, cpcB*IspS,* and *cpcB*L(7,10,16,65)*IspS* transformants all failed to accumulate the 20 and 15 kD phycocyanin subunits. The *cpcB*IspS* and *cpcB*L(7,10,16,65)*IspS* transformants showed substantial accumulation of the fusion proteins, migrating to about 80-85 kD (marked by asterisk). A faint band at ~24 kD in this SDS-PAGE analysis was attributed to expression of the chloramphenicol resistance protein.

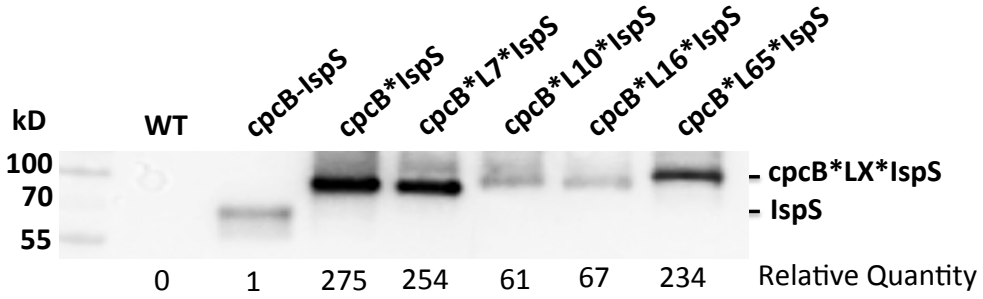

Figure 4.5. Western blot analysis of wild type and *IspS* transformants using specific polyclonal antibodies raised against the IspS protein. Total cell protein extracts were loaded differentially due to great differences in the IspS expression level between the non-fused, and fused versions of the constructs. The *cpcB-IspS* sample was loaded with 1 µg Chl, and the *cpcB*L(7, 10, 16, 65)*IspS* samples were loaded with 0.01 µg Chl. The Bio-Rad ChemiDoc imaging system was used to document the Western blot and the Bio-Rad Image Lab software was employed to quantify the relative IspS protein levels between the different strains based on the band intensity in the PVDF membrane. "Relative Quantity" of the IspS proteins shown here have been corrected for the uneven sample loading.

Pigment analysis. The visual phenotype of the *cpcB-IspS, cpcB*IspS* and *cpcB*L(7,10,16,65)*IspS* transformant strains was noticeably different from the wild type and from a strain with a complete *cpc* operon deletion (*Δcpc*). Absorbance spectra and carotenoid to chlorophyll *a*-ratios were measured to better determine differences in pigment accumulation. The absorbance spectra of wild type cell lysates showed the specific chlorophyll *a* absorbance at 680 and 435 nm, phycocyanin at 625 nm, and carotenoids at 470 nm regions (**Fig. 4.6**, black line). Carotenoid to chlorophyll (Car / Chl) ratio in the wild type was 0.51:1 (**Table 4.1**). The *Δcpc* strain showed the same chlorophyll *a*-peaks at 680 and 435 nm, but significantly lower absorbance at 625 nm, attributed to the deletion of the *cpc* operon and the ensuing absence of phycocyanin, and retention of allophycocyanin as the only remaining phycobilisome pigment (Kirst et al. 2014). Carotenoids were slightly elevated in the *Δcpc* strain (Car/Chl=0.61:1) compared to the wild type, evidenced both in the absorbance spectra (**Fig. 4.6**, green line) and from the biochemical analysis in methanol pigment extracts (**Table 4.1**), consistent with previous measurements conducted on these strains (Kirst et al. 2014). In the *cpcB-IspS, cpcB*IspS* and *cpcB*L(7,10,16,65)*IspS* strains, the absorbance maximum at 625 nm was also suppressed and at about the same amplitude as that of the *Δcpc* strain, attributed to inability of these strains to assemble a functional phycocyanin antenna due to fusion of the *IspS* gene to the C-terminus of the *cpcB* gene in the *cpc* operon. The total carotenoid absorbance was significantly lower in the *cpcB-IspS (*Car/Chl=0.42:1), *cpcB*IspS* and *cpcB*L(7,10,16,65)*IspS* transformant strains (Car/Chl=0.36:1) compared to the wild type and *Δcpc* strains, evidenced both in the absorbance spectra (Fig. 6), and from readings of the carotenoid/chlorophyll *a*-ratio in methanol pigment extracts of these strains (**Table 4.1**).

The differential pigmentation of the strains examined in this work was reflected in the coloration of the liquid cultures. The wild type appeared blue-green (**Fig. 4.7, WT**), whereas the *Δcpc* strain had a more yellowish coloration (**Fig. 4.7, Δcpc**). The CpcB*fusion strains had an intermediate greenish coloration (**Fig. 4.7A, cpcB*IspS and cpcB*L(1,10,16)*IspS**)). These differences in coloration among the strains were also evident under higher density cultivation conditions (**Fig. 4.7B**).

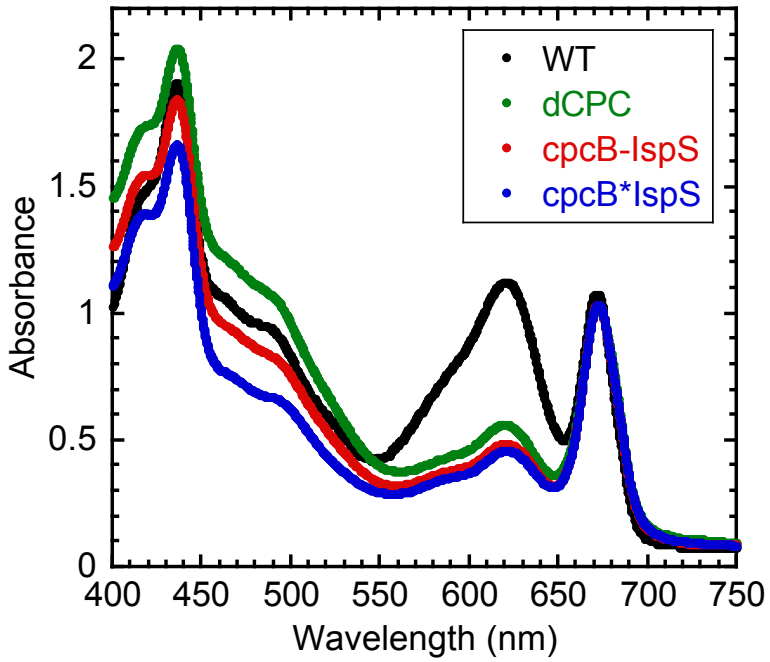

Figure 4.6. Absorbance spectra of cell lysates were analyzed to determine pigment differentiation in the various fusion strains. The absorbance spectra of wild type cell lysates showed the specific chlorophyll *a* absorbance at 680 and 435 nm, phycocyanin at 625 nm, and carotenoids at about 470 nm regions (**black line**). The *Δcpc* strain showed the same chlorophyll *a*-peaks at 680 and 435 nm, but significantly lower absorbance at 625 nm, attributed to the deletion of the *cpc* operon and the ensuing absence of phycocyanin, and retention of allophycocyanin as the only remaining phycobilisome pigment (**green line**). Carotenoids were slightly elevated in the *Δcpc* strain relative to the wild type (470 nm region). In the *cpcB-IspS* (**red line**), *cpcB*IspS* and *cpcB*L(7,10,16,65)*IspS* strains (**Blue line**), the absorbance maximum at 625 nm was also suppressed and at about the same amplitude as that of the *Δcpc* strain, attributed to inability of these strains to assemble a functional phycocyanin antenna due to fusion of the *IspS* gene to the C-terminus of the *cpcB* gene in the *cpc* operon. Carotenoids (absorbance in the 470 nm region) were slightly lower in these strains relative to that in the wild type.

Table 4.1. Pigment analysis was conducted on cells grown for 96 h in gaseous-aqueous two-phase photobioreactors loaded with 500 mL of 100% CO_2 to fill the headspace. Continuous illumination of 100 µmol photons $m^{-2}s^{-1}$ and temperature of 25°C were applied during cultivation. Carotenoid and chlorophyll *a* content was measured spectrophotometrically from the absorbance of methanol extracts of the pigment at 470 nm and 665 nm.

Strain	Car/Chl
Wild Type (WT)	0.51 ± 0.0034
Δcpc	0.61 ± 0.0057
cpcB-IspS	0.42 ± 0.0002
cpcB*IspS	0.36 ± 0.0418

Figure 4.7A. Coloration of cells from liquid cultures of wild type (WT: blue-green), *Δcpc* (yellow-green), and *cpcB-IspS, cpcB*IspS* and *cpcB*L(7,10,16,65)*IspS* strains (greenish).

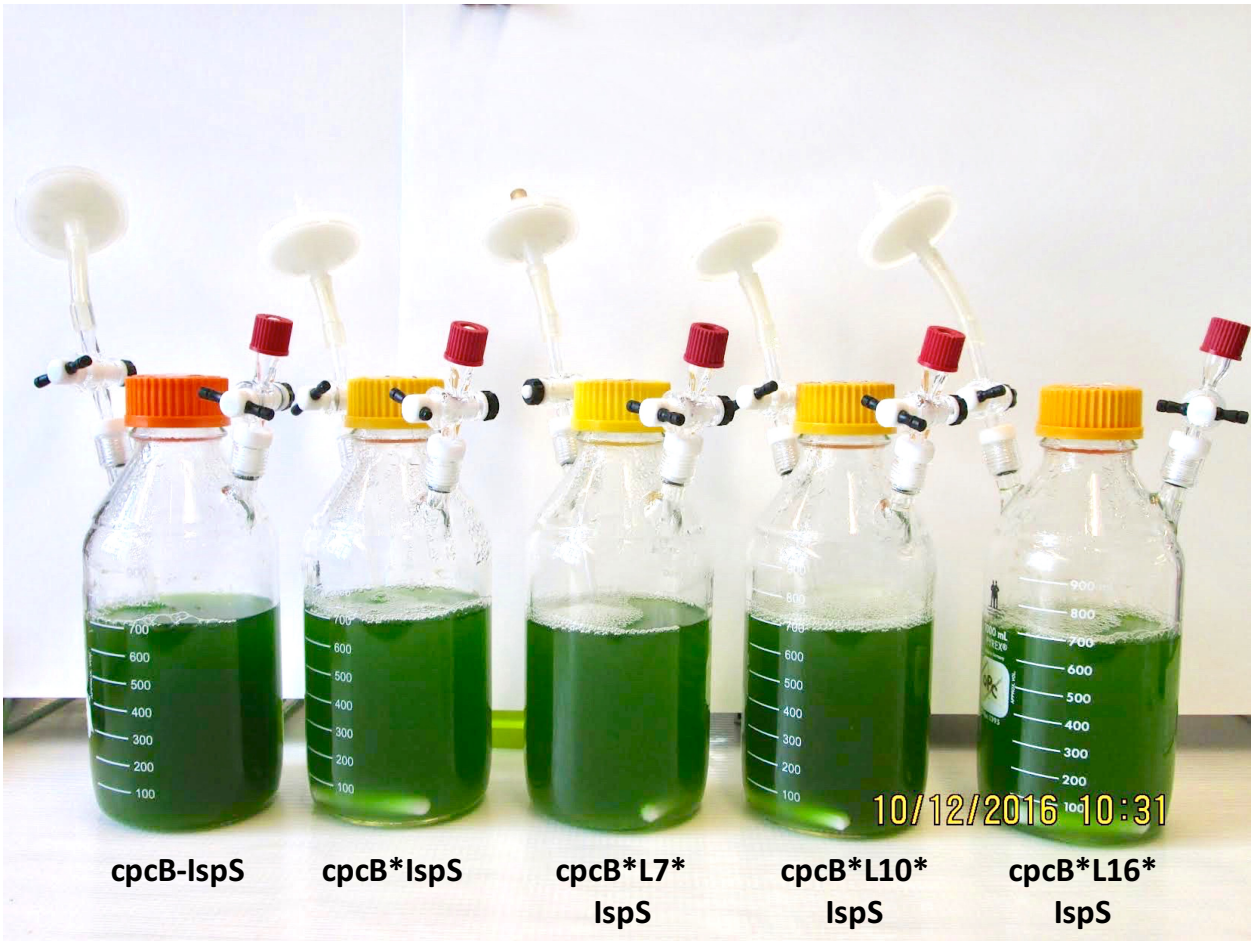

Fig. 4.7B Liquid cultures of control and fusion strains. Cultivated in gaseous aqueous two-phase photobioreactors for 96 hours with 500 mL of 100% CO_2 to fill the headspace, at a constant illumination of 100 µmol photons $m^{-2}s^{-1}$.

Photosynthetic activity. The functionality of the photosynthetic apparatus, as a result of the disruption of the phycocyanin expression and the introduction of transgenes was measured from the light saturation curves of photosynthesis. The rate of oxygen evolution was negative at zero light intensity and was determined to be in the range of 4±1 mmol O_2 consumption mol^{-1} Chl s^{-1} in the *cpcB-IspS, cpcB*IspS* and *cpcB*L(7,10,16)*IspS* strains. Increase in the rate of oxygen evolution as a function of light intensity was steeper for the wild type than for the transformants (**Fig. 4.8**), resulting in dissimilar saturation intensities for the two groups. The light intensity for the saturation of photosynthesis was determined from the intersect of the initial linear increase in the rate of photosynthesis with the asymptotic light-saturated state-state rate (P_{max}). This analysis showed that photosynthesis in the wild type was saturated at about 100 μmol photons m^{-2} s^{-1}, whereas that of the transformants saturated at higher light intensities, ranging from 145 to 200 μmol photons m^{-2} s^{-1} (**Fig. 4.8**). A photosynthesis-saturation intensity in the 145 to 200 μmol photons m^{-2} s^{-1} range was also noted for the *cpcB*L65*IspS* strain (not shown). The higher intensity for the saturation of photosynthesis in the transformants is attributed to their smaller light-harvesting antenna size, as they lack functional phycocyanin, have a truncated phycobilisome light-harvesting antenna (Kirst et al. 2014) and, therefore, a diminished absorption cross section for light-harvesting.

In spite of the different antenna configuration and light-saturation curves of photosynthesis in wild type and *IspS* transformants, all strains examined in this work showed about the same light-saturated rate of photosynthesis (Pmax), equal to about 55±5 mmol O_2 evolved mol^{-1} Chl s^{-1}. These findings show that transformations performed to effect a change in the expression level of the IspS gene have altered the pigment characteristics and phycobilisome antenna size of *Synechocystis* but have not affected the basic cell photosynthetic capacity, metabolism, or fitness.

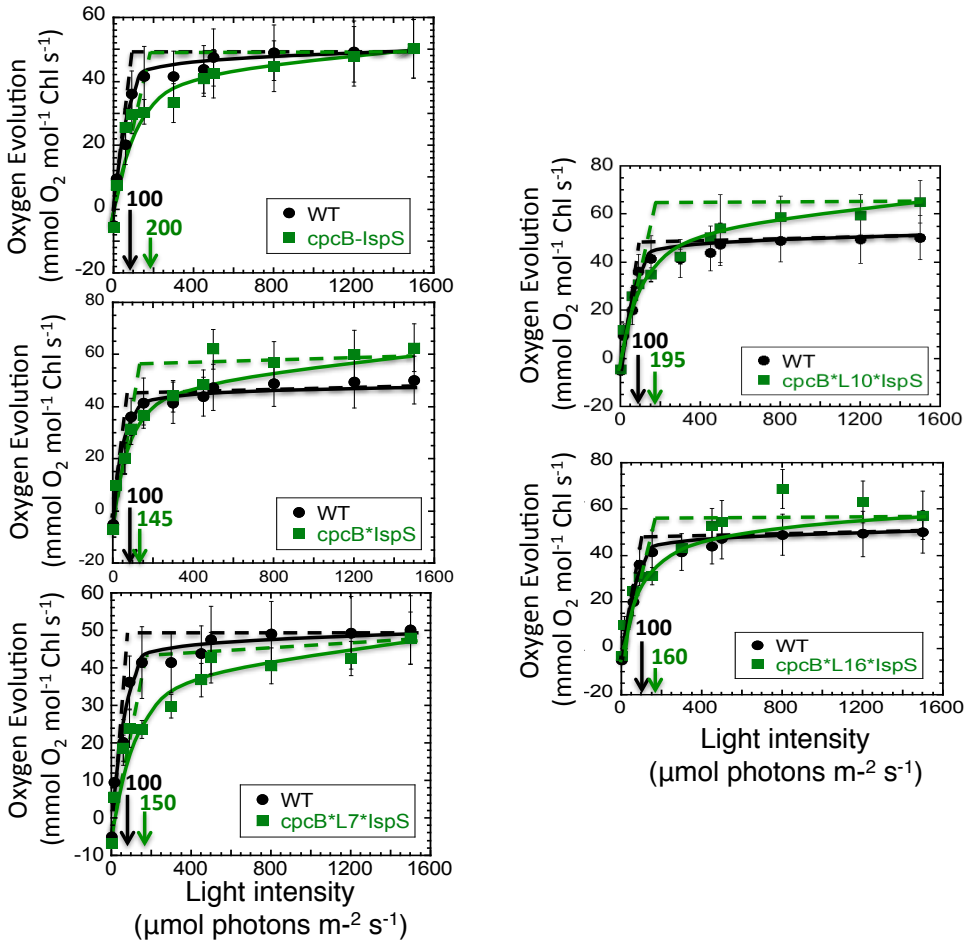

Figure 4.8. Light-saturation curves of photosynthesis. Oxygen evolution measurements of wild type, *cpcB-IspS, cpcB*IspS* and *cpcB*L(7,10,16)*IspS* strains were conducted with a Clark-type O_2 electrode. The rate of oxygen evolution was negative at zero light intensity and was determined to be in the range of 4±1 mmol O_2 consumption mol^{-1} Chl s^{-1} in the *cpcB-IspS, cpcB*IspS* and *cpcB*L(7,10,16)*IspS* strains. Increase in the rate of oxygen evolution as a function of light intensity was steeper for the wild type than for the transformants resulting in dissimilar saturation intensities for the two groups. The light intensity for the saturation of photosynthesis was determined from the intersect of the initial linear increase in the rate of photosynthesis with the asymptotic light-saturated state-state rate (P_{max}). This analysis showed that photosynthesis in the wild type was saturated at about 100 µmol photons m^{-2} s^{-1}, whereas that of the transformants saturated at higher light intensities, ranging from 145 to 200 µmol photons m^{-2} s^{-1}.

Rate of cell growth and isoprene accumulation. Cell growth and isoprene accumulation experiments were conducted using the gaseous-aqueous two-phase photobioreactor system designed by Bentley and Melis (2012). Measurements of cell biomass accumulation were obtained either from the culture optical density at 730 nm ($OD_{730\ nm}$; **Fig. 4.9A**) or from the dry cell weight (DCW; **Fig. 4.9B)** of culture aliquots sampled as a function of growth time. All fusion strains (*cpcB*IspS, cpcB*L(7,10,16,65)*IspS*) grew at a rate similar to that of the control (*cpcB-IspS*) (**Fig. 4.9**). Two of the fusion strains, *cpcB*L7*IspS* and *cpcB*L16*IspS* showed a slight lag in their initial growth (0-48 h) and then continued to grow with a rate comparable to that of the other strains (**Fig. 4.9**). Rates of cell growth and biomass accumulation were estimated from the slope of the linear biomass increase (48-96 h). Under our experimental conditions, the average rate of biomass accumulation among all strains was about 6.9 mg dcw L^{-1} h^{-1} (**Fig. 4.9B**). Rates of biomass accumulation for each of the individual strains examined in this work are reported in **Table 4.2**.

Isoprene accumulated in the reactor headspace concomitant with cell growth. Unlike the rate of biomass, rate of isoprene accumulation differed substantially between the different transformants (**Fig. 4.10A**). All fusion strains produced more isoprene than the *cpcB-IspS* control. The latter generated about 1.7 μg L^{-1} h^{-1}, whereas the fusion strain without a linker (*cpcB*IspS*) produced about 5.8 μg L^{-1} h^{-1}. The strain with the 65 amino acids linker (*cpcB*L65*IspS*) generated isoprene at slightly greater yields (7.6 μg L^{-1} h^{-1}). The *cpcB*L16*IspS* strain produced 10.3 μg L^{-1} h^{-1}, and the *cpcB*L10*IspS* produced 15.3 μg L^{-1} h^{-1}. The highest overall producer was the *cpcB*L7*IspS* strain, generating about 28.9 μg L^{-1} h^{-1} (**Table 4.2**).

Isoprene-to-biomass (w:w) partition ratios provide a more pertinent measurement of the yield of the process. Such ratios are also shown in **Table 4.2.** Strain *cpcB*IspS* showed a 4.5-fold increase in the yield of isoprene, over what was measured with the *cpcB-IspS* non-fusion transformant. By the same token, strain *cpcB*L7*IspS* showed a 27-fold increase in the yield of isoprene, over what was measured with the *cpcB-IspS* non-fusion transformant. Intermediate gains were observed with the other linker constructs. For better visualization of the results, the isoprene-to-biomass (w:w) partition ratio was plotted for the various strains examined in this work (**Fig. 4.10B)**.

A relative measure of the specific activity, i.e., efficacy of the different IspS fusion configurations to generate isoprene was offered from the isoprene-to-biomass ratio normalized for the relative quantity of the enzyme present in the different transformants (Fig. 5). These estimates are shown in **Table 4.2,** column 5. It is seen that the non-fusion configuration of the IspS (cpcB-IspS) has the highest specific activity (200 μg Isp g^{-1} Bms $[IspS]^{-1}$), whereas the fusion without linker (cpcB*IspS) has the lowest specific activity (3.27 μg Isp g^{-1} Bms $[IspS]^{-1}$). L10, L16, and L7 transformants showed intermediate levels of IspS specific activity. These results are evidence that specific activity was compromised in all fusion transformants, possibly because of allosteric effects exerted by the leader cpcB fusion protein, albeit this inhibition was substantially modulated by the nature of the linker amino acids placed between the cpcB and IspS proteins. In terms of isoprene production, the results further showed a tradeoff between specific activity and amount of transgenic enzyme accumulation. For example, the *cpcB*L7*IspS* strain showed only about 10% the isoprene synthase specific-activity of the unfused *cpcB-IspS* control but it accumulated a 254-fold greater amount of IspS enzyme. The

latter more than countered the lower specific activity and contributed to making the *cpcB*L7*IspS* strain the best isoprene producing strain in this work.

The cpcB*IspS and the cpcB*L7*IspS transformants accumulated equivalent amounts of the transgenic fusion protein (Fig. 4), but produced substantially different amounts of isoprene. These results suggested that the cpcB*L7*IspS fusion was substantially more active in catalysis than the cpcB*IspS counterpart. A question was asked as to whether fusion of the cpcB to the IspS in the cpcB*IspS construct impedes substrate access to the catalytic site, and whether the L7 linker changed the stereochemical and spatial relationship between the cpcB and IspS proteins, making the catalytic site of the isoprene synthase enzyme more easily accessible to the DMAPP substrate, thus leading to higher rates of isoprene synthesis? These two hypotheses, enzyme catalytic activity and stereochemistry of the fusion constructs, were investigated in greater detail.

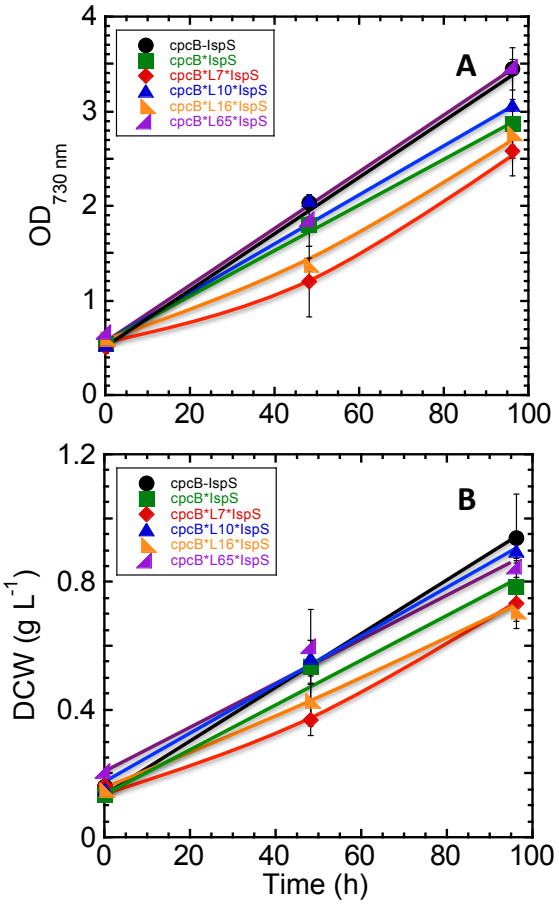

Figure 4.9. Biomass accumulation in *Synechocystis* liquid cultures. Liquid cultures of all strains were grown using the gaseous-aqueous two-phase bioreactor method, supplemented with 500 mL 100% CO_2 to fill the headspace, sealed, and stirred slowly under continuous illumination of 100 µmol photons m^{-2} s^{-1} intensity. Biomass accumulation was measured every 48 h for 96 h total by (**A**) optical density of the liquid culture and (**B**) by dry cell weight. All cpcB*IspS fusion strains (*cpcB*IspS, cpcB*L(7,10,16,65)*IspS*) grew at a rate similar to that of the control (*cpcB-IspS*). Two of the fusion strains, *cpcB*L7*IspS* and *cpcB*L16*IspS* showed a slight lag in their initial growth (0-48 h) and then continued to grow at a rate comparable with that of the other strains.

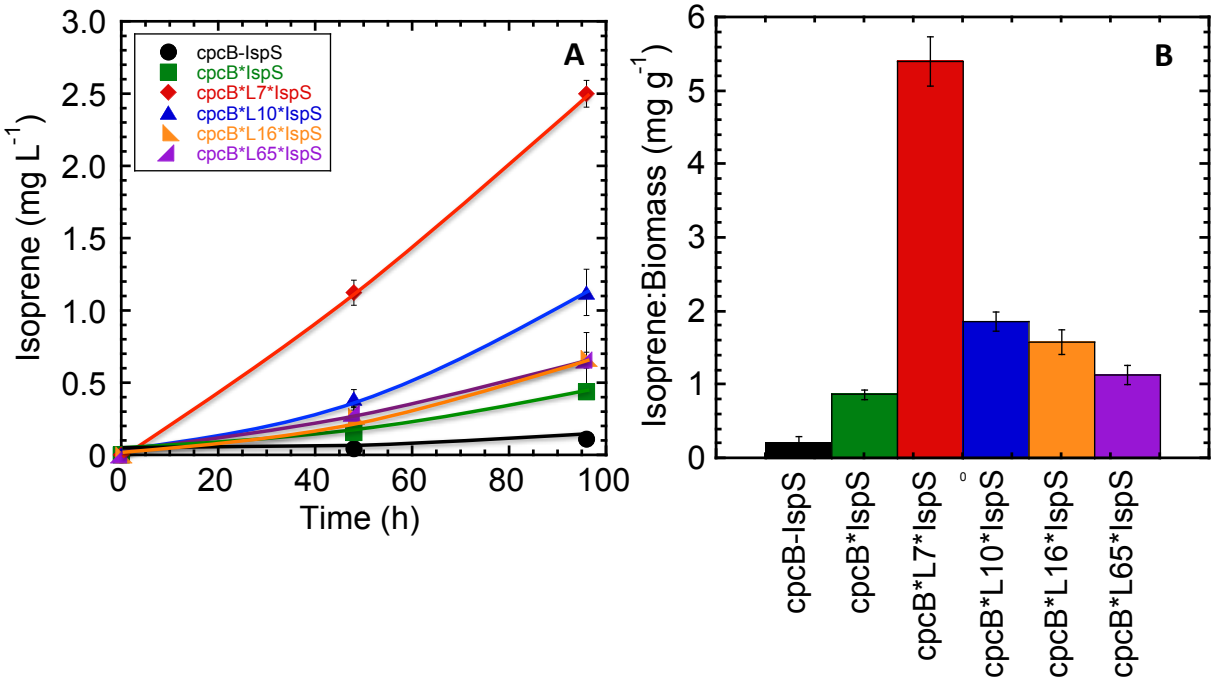

Figure 4.10. Isoprene accumulation in the reactor gaseous phase. Measurements were taken concurrently with those for biomass accumulation, every 48 h for a total of 96 h. Gas chromatography was employed to analyze 1 mL samples taken from the headspace using a gas tight syringe. Isoprene quantification was based on a calibration of isoprene standard (Acros Organics, Fair Lawn, NJ, USA), as described (Chaves et al. 2015). Note the dissimilar rates of isoprene accumulation.

Table 4.2. Synechocystis liquid cultures were cultivated in gaseous-aqueous two-phase photobioreactors for 96 h upon provision of 500 mL of 100% CO_2 to fill the reactor headspace. Continuous illumination of 100 µmol photons $m^{-2}s^{-1}$ and temperature of 25°C were applied during cultivation. Rates of biomass (mg L^{-1} h^{-1}), isoprene (µg L^{-1} h^{-1}), and isoprene to biomass ratio (mg g^{-1}) were calculated for each strain. The IspS specific activity (µg Isp g^{-1} Bms $[IspS]^{-1}$) was estimated from the isoprene to biomass ratio normalized to the relative IspS content in the respective biomass.

Strain	Rate of biomass accumulation (mg L^{-1} h^{-1})	Rate of isoprene accumulation (µg L^{-1} h^{-1})	Isoprene to biomass ratio (mg g^{-1})	IspS specific activity (µg Isp g^{-1} Bms $[IspS]^{-1}$)
cpcB-IspS	8.1 ± 0.32	1.7 ± 0.32	0.2 ± 0.05	200 ± 50.0
cpcB*IspS	6.8 ± 1.20	5.8 ± 0.62	0.9 ± 0.16	3.27 ± 0.60
cpcB*L65*IspS	6.7 ± 0.07	7.6 ± 0.62	1.1 ± 0.22	4.70 ± 0.94
cpcB*L16*IspS	5.8 ± 0.27	10.3 ± 1.28	1.6 ± 0.45	23.9 ± 7.00
cpcB*L10*IspS	8.3 ± 0.74	15.3 ± 2.18	1.8 ± 0.33	29.5 ± 5.41
cpcB*L7*IspS	5.4 ± 0.18	28.9 ± 1.06	5.4 ± 0.49	21.3 ± 1.93

Enzymatic properties of cpcB*IspS, cpcB*L7*IspS, and cpcB*L16*IspS *in vitro*. To determine the effect of the cpcB*IspS fusion, and that of the linker amino acids, on the isoprene synthase specific catalytic activity, in vitro assays were conducted on the enzymatic properties of the lowest (cpcB*IspS), intermediate (cpcB*L16*IspS), and highest (cpcB*L7*IspS) isoprene producers. Highly concentrated *Synechocystis* cell lysates of each of the strains were used as the catalyst for the in-vitro reactions. Aliquots of each soluble cell lysate fraction were run on an SDS-PAGE gel to determine the concentration of the cpcB*IspS, cpcB*L16*IspS, and cpcB*L7*IspS enzymes relative to a bovine serum albumin (BSA) standard (**Fig. 4.11**). BSA samples were loaded at 0.2, 0.4, 0.6, 0.8, and 1.0 µg per lane to establish a calibration curve of the 66.5 kD band density, measured by the Bio-Rad Image Lab software, as a function of protein amount loaded (**Fig. 4.11A,** BSA). Similarly, cell lysates from the cpcB*IspS fusion strain were loaded at five different volumes (2, 4, 6, 8, and 10 µL) in parallel with the BSA standard (**Fig. 4.11A,** cpcB*IspsS). This analysis showed the cpcB*IspS fusion protein band migrating to about 84 kD, while the rbcL and CmR proteins were also visible, migrating to 58 and 24 kD, respectively (**Fig. 4.11A,** cpcB*IspsS). This comparative protein calibration approach helped define the cell lysate volume that contained 12 µg of BSA-equivalent cpcB*IspsS protein. The latter was used in the isoprene synthase enzymatic analysis undertaken in this work (see work below).

A similar comparative protein calibration approach was undertaken for the cell lysates from the cpcB*L16*IspS (**Fig. 4.11B**) and cpcB*L7*IspS (**Fig. 4.11C**) strains, which helped define the cell lysate volume that contained 12 µg of BSA-equivalent cpcB*L16*IspS (**Fig. 4.11B**) and cpcB*L7*IspS (**Fig. 4.11C**) protein.

In vitro isoprene synthesis reactions were conducted in the presence of varying concentrations of DMAPP at 42°C for 15 min (Zurbriggen et al. 2012). Volatile products collected in the headspace of the reaction vessel were subjected to gas chromatography analysis to quantify isoprene yields (Chaves et al. 2015). Reaction mixtures without cell lysate were used as a control. These did not produce any isoprene. Lineweaver-Burk analysis of the enzymatic kinetics of isoprene production are shown in **Fig. 4.12**. It is evident from the results that cellular extracts from the cpcB*IspS transformant had the lowest in vitro activity, consistent with the in-vivo measurements. The Lineweaver-Burk plot of the cpcB*IspS fusion protein (**Fig. 4.12A**) showed a nearly flat line, indicating a slow enzymatic activity with minimal dependence on substrate (DMAPP) concentration, consistent with the slow in-vivo IspS specific activity of this construct. Analysis of the results showed a k_{cat} = 0.0159 s^{-1}, K_m = 0.0145 mM, and V_{max} = 0.0113 µmol (mg protein)$^{-1}$ min^{-1} (**Fig. 4.12A**). Addition of the amino acids linker L16 in the cpcB*L16*IspS fusion protein substantially enhanced the catalytic activity of the enzyme, also consistent with the in-vivo isoprene yields. The cpcB*L16*IspS enzyme displayed a two-fold higher specific activity than the cpcB*IspS with k_{cat}=0.0318 s^{-1}, K_m=1.30 mM, and V_{max}=0.0225 µmol (mg protein)$^{-1}$ min^{-1} (**Fig. 4.12B**). Addition of the L7 linker conferred isoprene synthase enzymatic properties with a k_{cat} = 0.346 s^{-1}, K_m = 1.73 mM, and V_{max} = 0.250 µmol (mg protein)$^{-1}$ min^{-1} (**Fig. 4.12C**). Thus, the cpcB*L7*IspS strain had the highest specific activity, 22-fold greater than the cpcB*IspS. A summary of the enzymatic properties of the cpcB*IspS, cpcB*L16*IspS, and cpcB*L7*IspS fusion enzymes is given in **Table 4.3**.

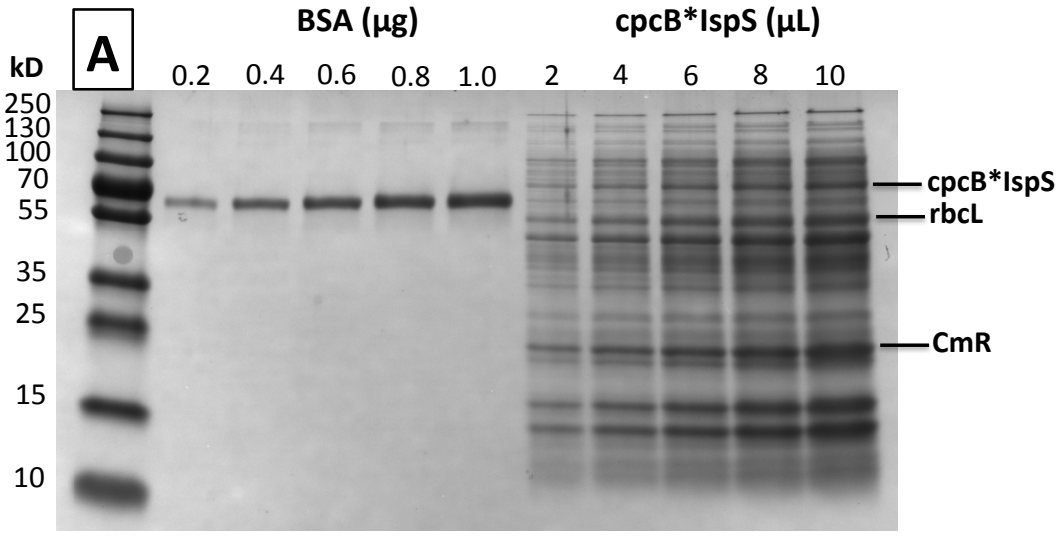
A
BSA (µg)
cpcB*IspS (µL)
kD
0.2
0.4
0.6
0.8
1.0
2
4
6
8
10
250
130
100
70
55
35
25
15
10
cpcB*IspS
rbcL
CmR

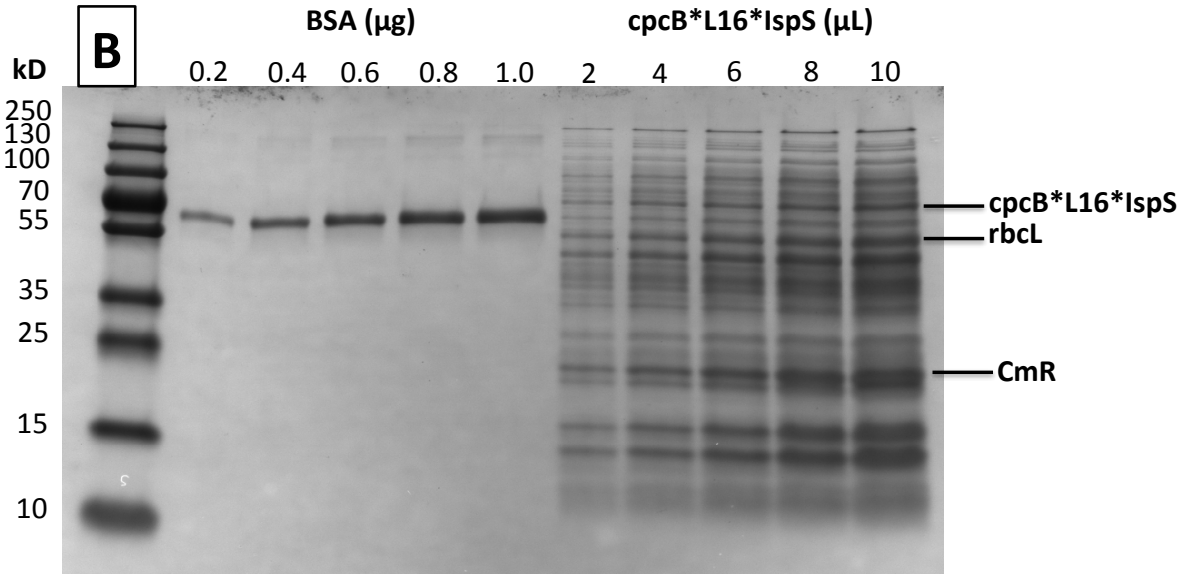
B
BSA (µg)
cpcB*L16*IspS (µL)
kD
0.2
0.4
0.6
0.8
1.0
2
4
6
8
10
250
130
100
70
55
35
25
15
10
cpcB*L16*IspS
rbcL
CmR

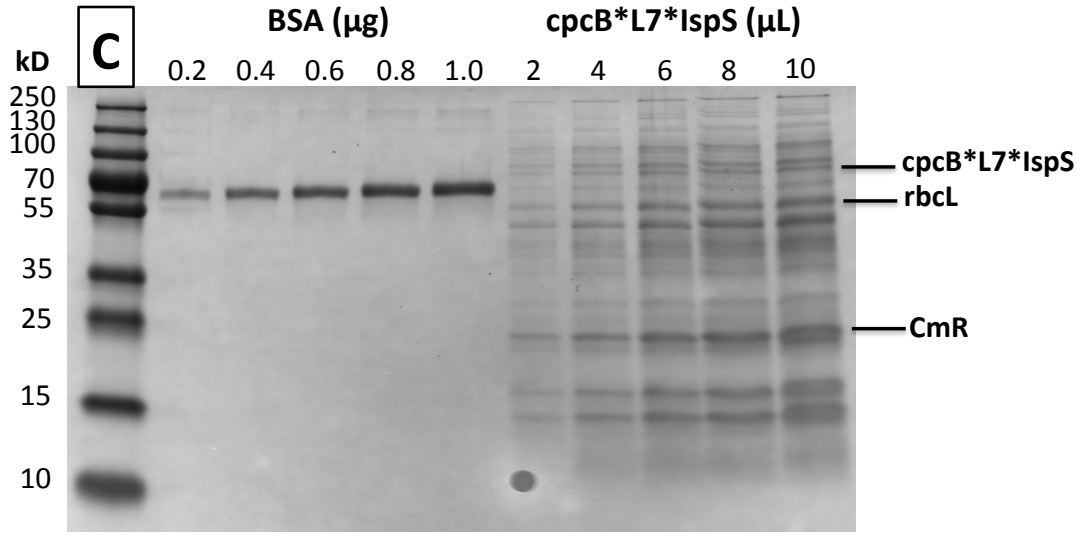

Figure 4.11. Calibration of protein content. Liquid cultures of *Synechocystis* containing the fusion isoprene synthase constructs *cpcB*IspS*, *cpcB*L16*IspS* and *cpcB*L7*IspS* were grown in 5 L cultures, cells were concentrated, and lysed by French press. The soluble fraction of the cell lysate was then filtered and further concentrated using Amicon Ultra 15 50 kD filters (Millipore, USA). Aliquots of the concentrated crude cell extracts were solubilized, proteins resolved in SDS-PAGE, and stained with Coomassie brilliant blue. Protein concentrations were determined based on the intensity of (**A**) the *cpcB*IspS,* (**B**) *cpcB*L16*IspS,* and (**C**) *cpcB*L7*IspS* fusion proteins appearing at 85 kD relative to a BSA standard. The Bio-Rad ChemiDoc imaging system was used to document the Coomassie-stained intensity of the bands and the Bio-Rad Image Lab software was employed to quantify the relative IspS protein levels from the different strains relative to that of BSA.

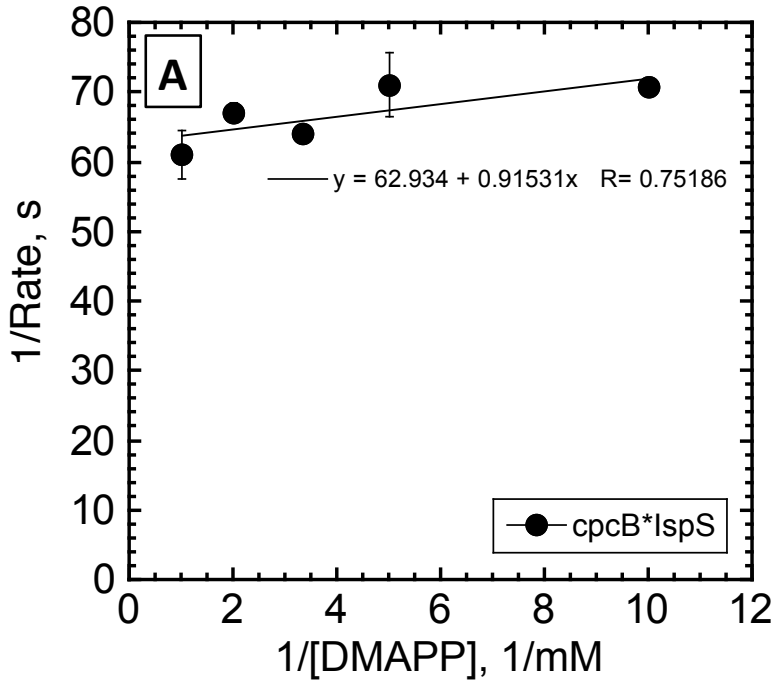
A
y = 62.934 + 0.91531x R= 0.75186
cpcB*IspS
1/Rate, s
1/[DMAPP], 1/mM
0
10
20
30
40
50
60
70
80
0
2
4
6
8
10
12

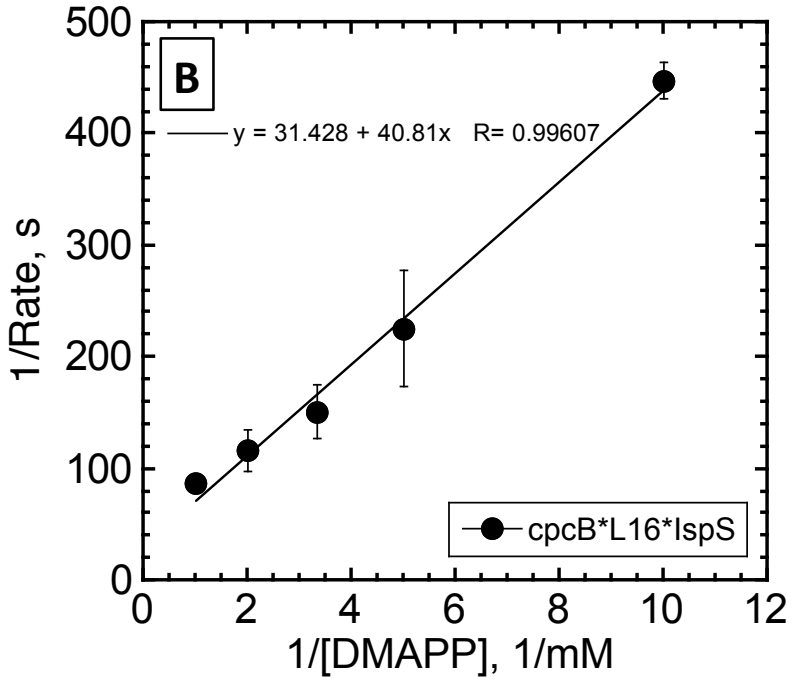
B
y = 31.428 + 40.81x R= 0.99607
cpcB*L16*IspS
1/Rate, s
1/[DMAPP], 1/mM
0
100
200
300
400
500
0
2
4
6
8
10
12

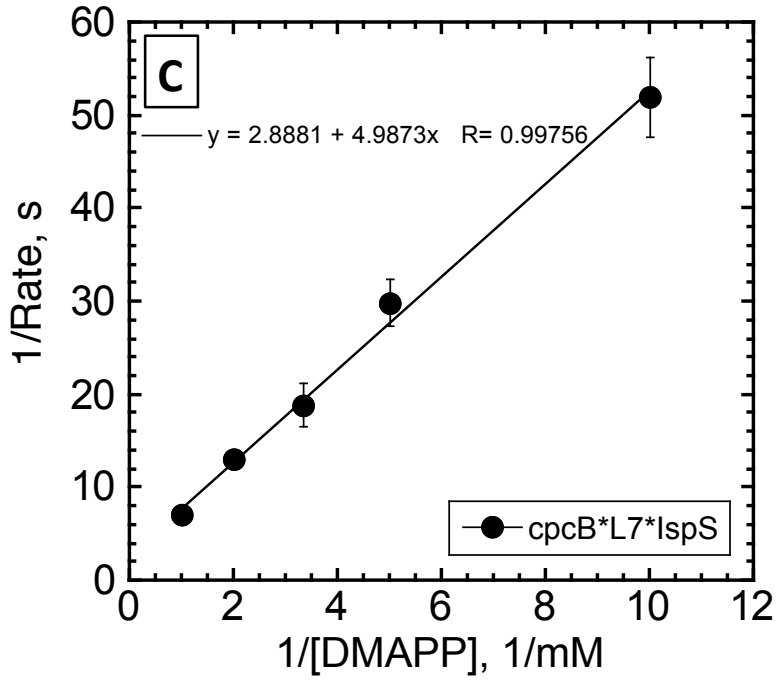

Figure 4.12. Lineweaver-Burk plots of the IspS enzymatic kinetic analyses. In vitro IspS enzymatic reactions of (**A**) the *cpcB*IspS,* (**B**) *cpcB*L16*IspS,* and (**C**) *cpcB*L7*IspS* fusion proteins were conducted in 100 μL mixtures containing 50 mM Bicine, pH 8.0, 30 mM NaCl, 50 mM $MgCl_2$, 50 mM KCl, 5% glycerol, 1 mM DTT, 12 μg cpcB*LX*IspS, and varying concentrations of DMAPP. Reaction mixtures were incubated for 15 min at 42°C, then 1 mL aliquots from the headspace were sampled for isoprene content by gas chromatography.

Table 4.3. In-vitro IspS enzyme kinetics were measured with crude protein extracts from the fusion strains cpcB*IspS, cpcB*L16*IspS, and cpcB*L7*. Reactions were conducted in 100 µL mixtures containing 50 mM Bicine, pH 8.0, 30 mM NaCl, 50 mM $MgCl_2$, 50 mM KCl, 5% glycerol, 1 mM DTT, 12 µg of BSA-equivalent cpcB*LX*IspS protein extract, and varying concentrations of DMAPP. Reactions were incubated for 15 min at 42°C, then 1 mL aliquots of the headspace were sampled for isoprene content by gas chromatography. K_{cat}, K_m, and V_{max} were calculated from Lineweaver Burk plots of the reaction parameters for each fusion enzyme.

Construct	**K_{cat}** (s^{-1})	**K_m** (mM)	**V_{max}** µmol (mg protein)$^{-1}$ min^{-1}
cpcB*IspS	0.016 ± 0.002	0.015 ± 0.002	0.011 ± 0.002
cpcB*L16*IspS	0.032 ± 0.006	1.30 ± 0.420	0.023 ± 0.005
cpcB*L7*IspS	0.350 ± 0.020	1.73 ± 0.225	0.250 ± 0.018

Modeling. To further address the question of whether fusion of the cpcB to the IspS impedes catalytic activity, and whether the linkers change the stereochemical and spatial relationship between the cpcB and IspS proteins, making the catalytic site of the isoprene synthase enzyme more easily accessible to the substrate, thus leading to higher rates of isoprene synthesis, protein folding modeling was undertaken. RaptorX software (Källberg et al. 2012) analysis of the cpcB*IspS fusion showed the cpcB protein with the N-terminus and the subsequent two short α-helices exposed (**Fig. 4.13A**, blue arrow). In this cpcB*IspS fusion model, the IspS folded near and to the east side of the cpcB. The first nine amino acids of the IspS are shown facing the medium immediately after the last amino acid of the cpcB protein (**Fig. 4.14A,** white arrow). This configuration resulted in a slow catalytic activity and uncompetitive inhibition of the IspS (**Tables 4.2 and 4.3**).

In the subsequent RaptorX software analysis, an effort was made to orient the fusion construct structures with respect to the N-terminus coordinates of the cpcB protein, as shown in supporting information Fig. 2S. In the cpcB*L7*IspS folding model (**Fig. 4.13B**), the IspS is shown to have flipped by more than 180 degrees to the west of the cpcB relative to the orientation shown in the folding model cpcB*IspS. Similarly, the cpcB*L10*IspS **(Fig. 4.13C**) and the cpcB*L16*IspS **(Fig. 4.13D)** showed the IspS rotated to the west of the cpcB. The cpcB*L65*IspS was rotated to an even greater degree (about 270 degrees), with the IspS positioned to the south of the cpcB (**Fig. 4.13E**). Each linker increased the distance between the two proteins, and caused a slightly different orientation of the IspS relative to the cpcB, both of which appear to contribute to the differing enzymatic activities. An amino acid alignment of several IspS enzymes from different plant species (Zubriggen et al. 2012) showed conserved regions among the isoprene synthases, especially so at the N-terminal domain comprising tandem arginine residues followed by an absolutely conserved tryptophan residue. This highly conserved $RR(X)_8W$ terpene synthase motif (amino acid residues 17 through 28 from the N-terminus of the mature protein) was suggested to play a role in diphosphate walking and/or terpene cyclization reactions (Cunningham et al. 1994; Williams et al. 1998) and is present in all terpene synthases. It appears that use of different amino acid spacers changed the relative orientation and distance of the cpcB relative to the N-terminal domain of the IspS, and it may thus impact the function of the IspS N-terminal domain RR(X)8W motif comprising the conserved tandem arginine and tryptophan residues, thereby affecting activity.

4.13 A.

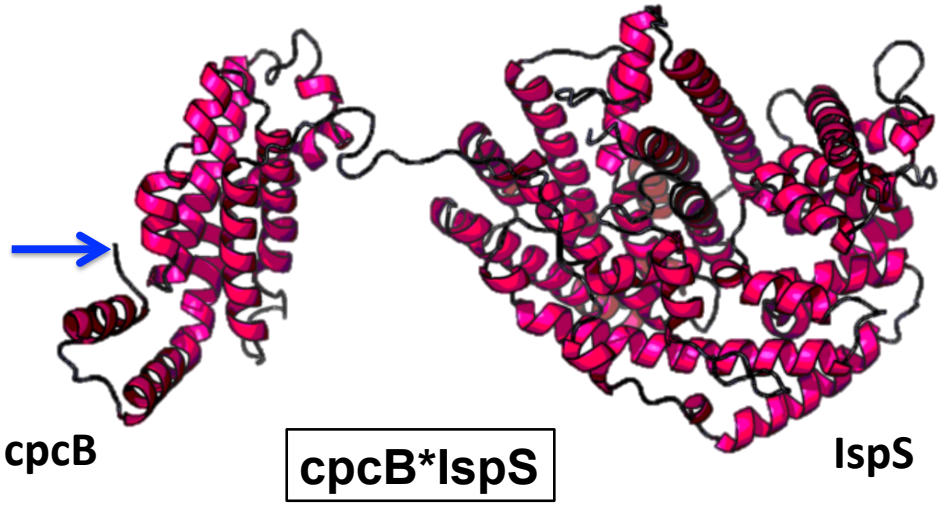

4.13 B.

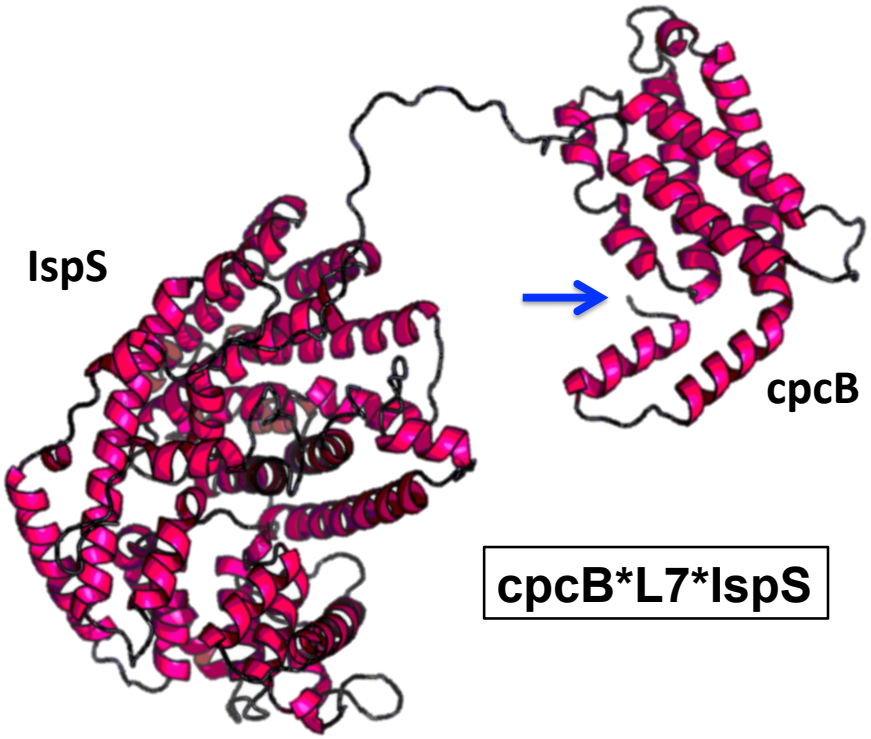

4.13 C.

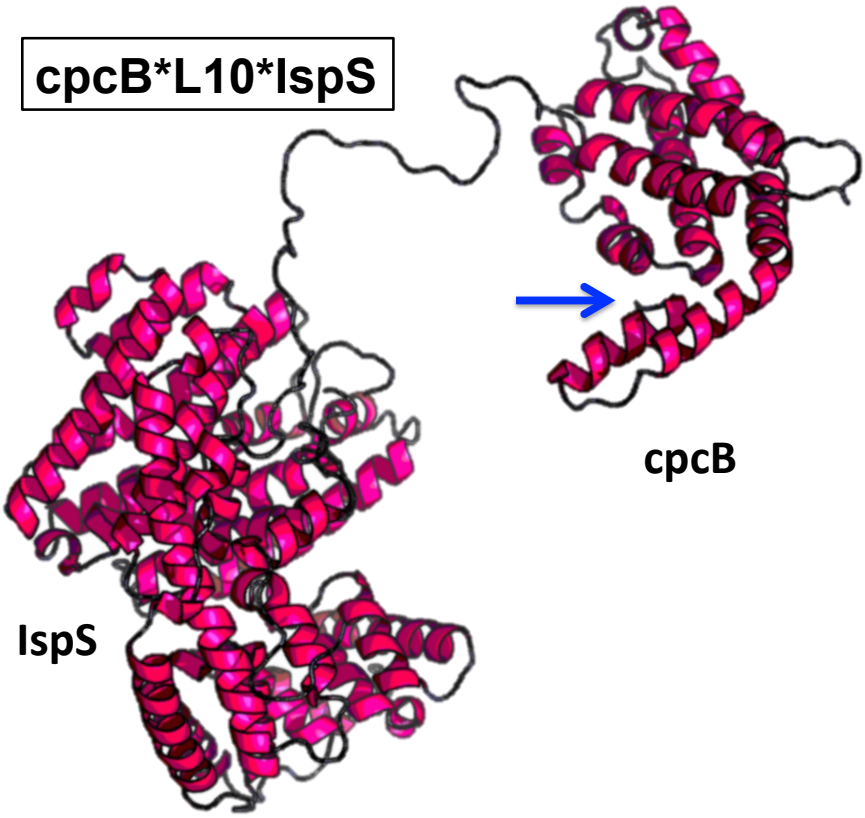

4.13 D.

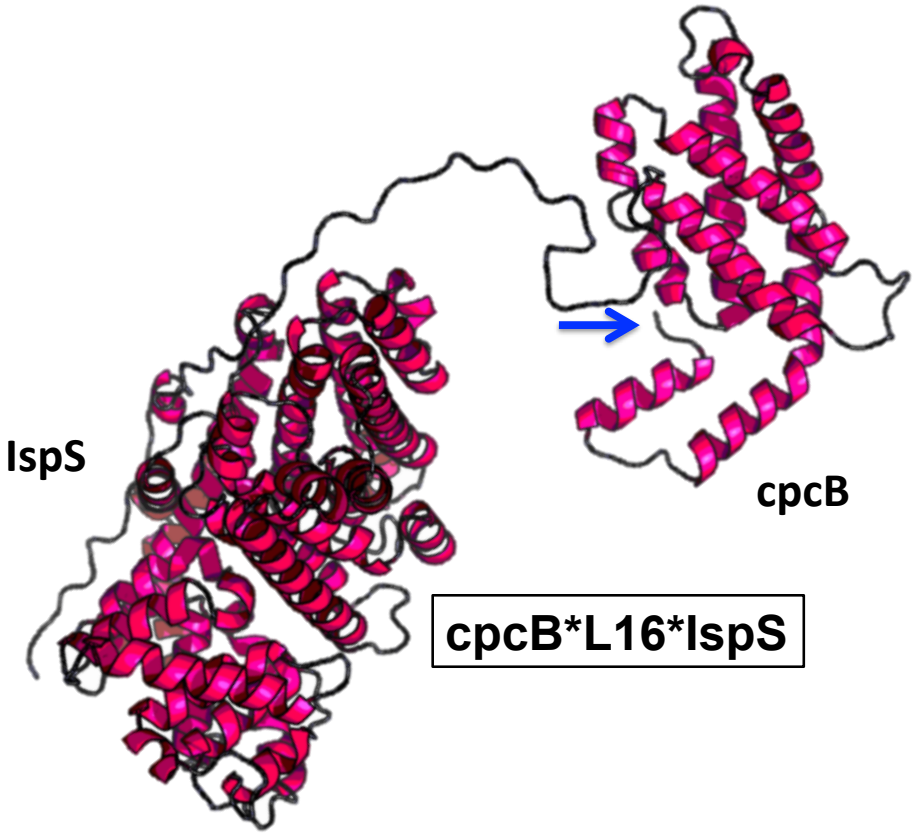

4.13 E.

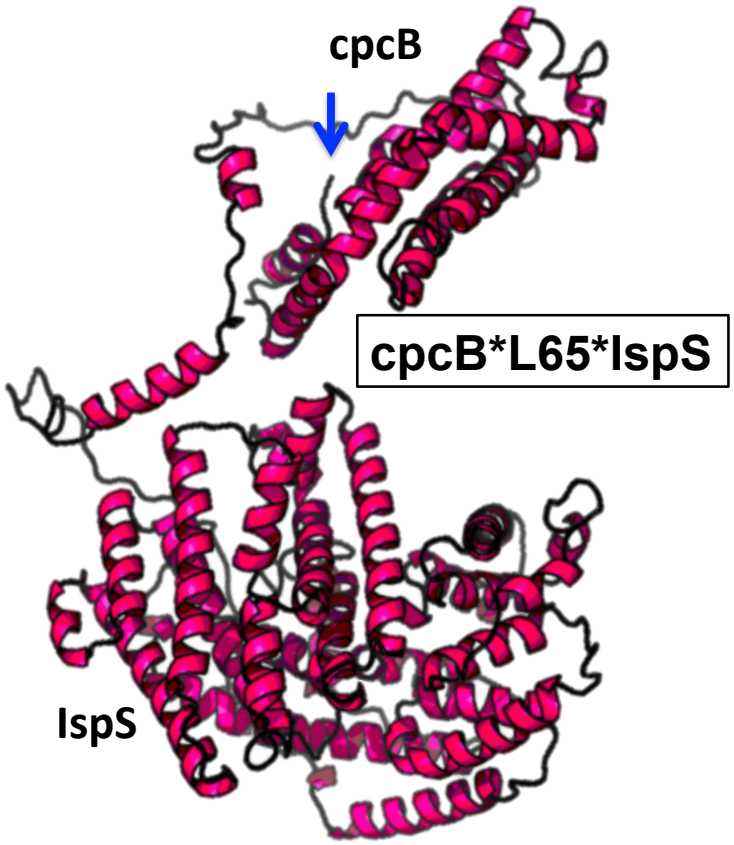

Figure 13. RaptorX software was employed to visualize possible folding patterns of the various cpcB and IspS fusion proteins. **(A)** *cpcB*IspS*, **(B)** *cpcB*L7*IspS*, **(C)** *cpcB*L10*IspS*, **(D)** *cpcB*L16*IspS*, **(E)** *cpcB*L65*IspS*. Protein models have been oriented with respect to the cpcB protein, with the N-terminus of the cpcB marked by a blue arrow. Note the substantially different orientation and distance of the IspS relative to the cpcB in the *cpcB*IspS* versus the *cpcB*L7*IspS*, *cpcB*L10*IspS*, *cpcB*L16*IspS*, and *cpcB*L65*IspS* constructs.

Fig. 4.14A Protein folding model of cpcB*IspS, zoomed in to cpcB and IspS interface. White arrow points to the last amino acid of the cpcB, yellow arrow points to the first amino acid of the IspS (also indicated by white ball figure).

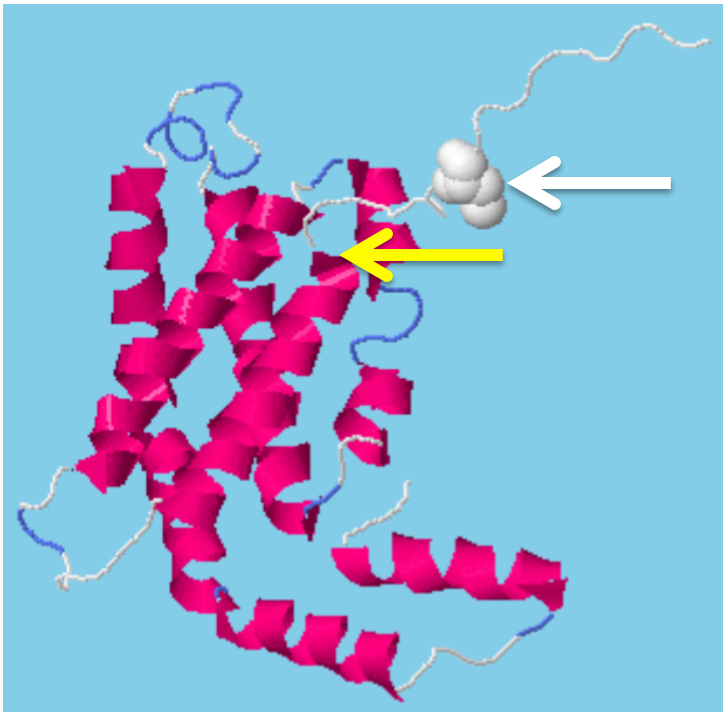

Fig. 4.14B Protein folding model of cpcB*L7*IspS, zoomed in to cpcB and IspS interface. White arrow points to the last amino acid of the cpcB, yellow arrow points to the first amino acid of the IspS (also indicated by white ball figure).

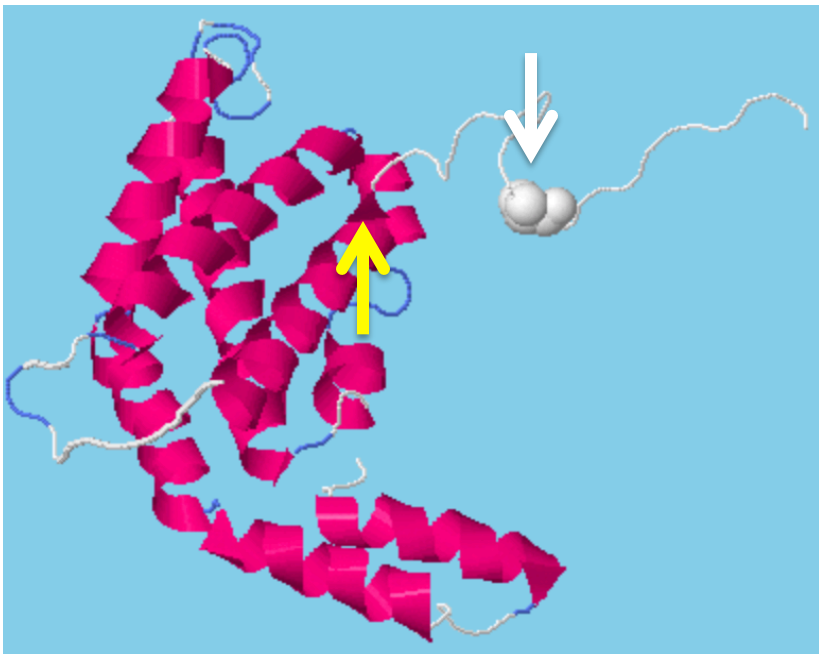

Fig. 4.14C Protein folding model of cpcB*L10*IspS, zoomed in to cpcB and IspS interface. White arrow points to the last amino acid of the cpcB, yellow arrow points to the first amino acid of the IspS (also indicated by white ball figure).

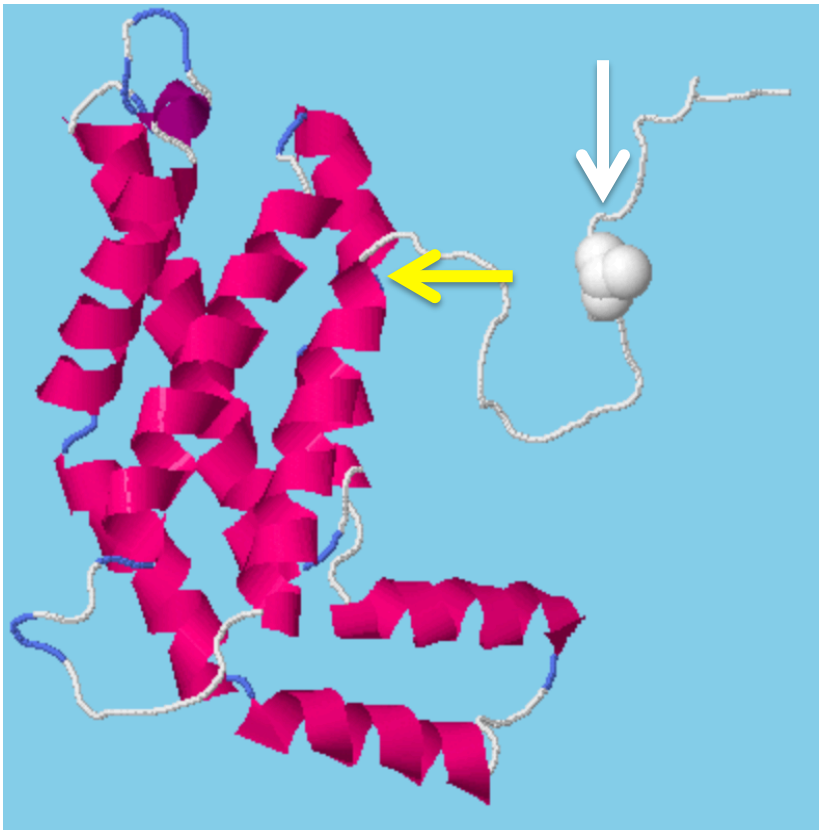

Fig. 4.14D Protein folding model of cpcB*L16*IspS, zoomed in to cpcB and IspS interface. White arrow points to the last amino acid of the cpcB, yellow arrow points to the first amino acid of the IspS (also indicated by white ball figure).

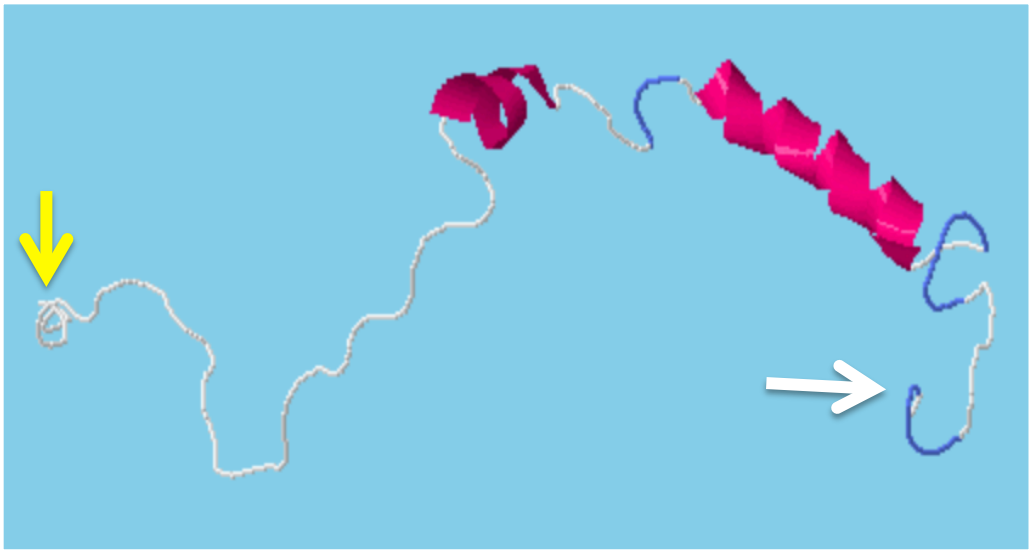

Fig. 4.14E Protein folding model of cpcB*L65*IspS, linker portion only. White arrow points to the last amino acid of the cpcB, yellow arrow points to the first amino acid of the IspS.

4.4 DISCUSSION

Isoprene synthase enzymes have been studied in-vitro to characterize their kinetic properties. This includes the *Populus alba* (poplar) and *Pueraria montana* (kudzu) IspS proteins (Sasaki et al. 2005; Sharkey et al. 2005; Zurbriggen et al. 2012). Further, the IspS gene was codon optimized and applied for expression to *Synechocystis* (Lindberg et al. (2010), showing the feasibility of driving the cyanobacterial photosynthesis and metabolism toward the heterologous production of isoprene. However, terpene synthases have notoriously slow turnover kinetics, and the kudzu isoprene synthase proved to fit in the family with a K_{cat} = 4.4 s^{-1}, and K_m = 2.5 mM (Zubriggen et al. 2012). The present study conducted enzymatic kinetic analyses of the cyanobacterial codon-optimized kudzu IspS, as previously used in this lab, but with the enzyme in different fusion configurations with the cpcB protein (the β-subunit of phycocyanin), as this fusion construct was highly expressed in transformant *Synechocystis*. Although a direct fusion of the *IspS* to the *cpcB* gene (cpcb*IspS) substantially enhanced (275-fold) the concentration of the IspS protein in the cells (Fig. 4 and 5), the catalytic ability of the enzyme was compromised with a specific activity (functional efficiency) equal to only 1.64% of the unfused enzyme.

The use of amino acid spacers mitigated the degree to which the enzymatic activity was inhibited by the cpcB fusion, while retaining the high level of the fusion protein. For example, the best isoprene producer (*cpcB*L7*IspS*) resulted in a 254-fold increase in the concentration of the IspS protein in the cells and had a specific activity 10.65% of the unfused enzyme. Thus, the combined result of specific activity times enzyme concentration translated in superior yields, as evidenced by the productivity of the *cpcB*L7*IspS* strain, when compared to the unfused control (*cpcB-IspS*). Overall, the large increase in enzyme concentration outweighed the decrease in specific activity in terms of isoprene production, resulting in 27-fold gains in production compared to non-fused IspS. This compares favorably to recent independent attempts at improving the catalytic activity of an IspS enzyme through directed evolution, which resulted in modest improvements, i.e., 1.6- to 1.8-fold increase in isoprene production yield (Wang et al. 2017). Together, these results show that concentration of the isoprene synthase enzyme and its specific activity are substantially important determinants of yield in the cyanobacterial isoprene production process.

Alleviating bottlenecks in the MEP isoprenoid biosynthetic pathway toward isoprene production included attempts to alleviate rate-limiting enzymatic steps, such as those defined by the DXS (Liu *et al*. 2013; Lv *et al*. 2013; Ramos *et al*. 2014; Xue and Ahring 2011), DXR (Lv *et al*. 2013; Zhao *et al*. 2011), and the IPP isomerase (Chaves et al., 2016; Gao et al., 2016). As endogenous carbon partitioning to the MEP pathway is limited (Lindberg et al. 2010), co-expression of feeding pathways such as the Embden-Meyerhof pathway (EMP) and Entner-Doudoroff Pathway (EDP) (Liu et al. 2013) have resulted in enhanced isoprenoid production in *E. coli*. Cellular concentrations of the universal isoprenoid precursors (DMAPP and IPP) are also limiting, and use of acetyl-CoA as an additional primary substrate feedstock through an exogenous mevalonic acid pathway improved isoprenoid production in both *Synechocystis* (Bentley et al. 2012) and *E. coli* (Zubriggen et al. 2012; Yang et al. 2012). Thus, the combination of improved global carbon flux to DMAPP with overexpression of the IspS fused to the cpcB is promising in efforts to generate even greater yields of isoprene (Bentley et al. 2014).

A goal of biotechnology today is to develop the ability of utilizing sunlight, CO_2, and water in order to renewably generate fuel and chemicals as efficiently as possible. Cyanobacteria offer a unique opportunity to develop such technologies, with the microorganism acting as a single-cell factory, capturing carbon dioxide and converting it into useful products. This work contributed to the identification of a barrier in the renewable generation of isoprene through photosynthesis in cyanobacteria and further provided evidence of ways by which to alleviate some of the associated level-of-expression problems.

4.5 REFERENCES

Aremu O, Borchert C, Bastian JA, Knutson A, Budzynski C, Cai JY, Chen X, Guo H, Lu P, Venkataramanan SS, Sethi AK (2015) Inactivation of competing pathways and increased gene copies for enhanced isoprene production in *Synechococcus* sp. PCC 7002. Cyanobacteria 2015

Bentley FK, Melis A (2012) Diffusion-based process for carbon dioxide uptake and isoprene emission in gaseous/aqueous two-phase photobioreactors by photosynthetic microorganisms. Biotech Bioeng 109:100-109

Bentley FK, Zurbriggen A, Melis A (2014) Heterologous expression of the mevalonic acid pathway in cyanobacteria enhances endogenous carbon partitioning to isoprene. Mol Plant 7(1):71-86.

Chaves JE, Kirst H, Melis A (2015) Isoprene production in *Synechocystis* under alkaline and saline growth conditions. J Appl Phycol 27:1089–1097

Chaves JE, Romero P, Kirst H, Melis A (2016) Role of isopentenyl-diphosphate isomerase in heterologous cyanobacterial (*Synechocystis*) isoprene production. Photosynth Res 130:517-527

Chen X, Zaro JL, Shen WC (2013) Fusion protein linkers: property, design and functionality. Advanced Drug Delivery Reviews 65(10):1357-1369.

Cunningham FX Jr, Sun Z, Chamovitz D, Hirschberg J, Gantt E (1994) Molecular structure and enzymatic function of lycopene cyclase from the cyanobacterium Synechococcus sp strain PCC7942. Plant Cell 6(8):1107–1121

Formighieri C, Melis A (2014) Regulation of β-phellandrene synthase gene expression, recombinant protein accumulation, and monoterpene hydrocarbons production in *Synechocystis* transformants. Planta 240:309–324

Formighieri C, Melis A (2015) A phycocyanin•phellandrene synthase fusion enhances recombinant protein expression and β-phellandrene (monoterpene) hydrocarbons production in *Synechocystis* (cyanobacteria). Metab Eng 32:116–124

Formighieri C, Melis A (2016) Sustainable heterologous production of terpene hydrocarbons in cyanobacteria. Photosynth Res 130:123-135

Gao X, Gao F, Liu D, Zhang H, Nie X, Yang C (2016) Engineering the methylerythritol phosphate pathway in cyanobacteria for photosynthetic isoprene production from CO_2. Energy & Env Sci 9(4):1400-1411.

Källberg M, Wang H, Wang S, Peng J, Wang Z, Lu H, Xu J (2012) Template-based protein structure modeling using the RaptorX web server. Nature Protocols 7(8):1511-22.

Kim, J-H, Wang CL, Jang H-J et al. (2016) Isoprene production by *Escherichia coli* through the exogenous mevalonate pathway with reduced formation of fermentation byproducts. *Microbial Cell Factories* 15.1: 214.

Kirst H, Formighieri C, Melis A (2014) Maximizing photosynthetic efficiency and culture productivity in cyanobacteria upon minimizing the phycobilisome light-harvesting antenna size. Biochim Biophys Acta - Bioenergetics 1837(10):1653-1664

Lichtenthaler HK (1987) Chlorophylls and carotenoids: pigments of photosynthetic biomembranes. Methods Enzymol 148:350–382

Lindberg P, Park S, Melis A (2010) Engineering a platform for photosynthetic isoprene production in cyanobacteria, using *Synechocystis* as the model organism. Metabol Eng 12:70-79

Liu H, Sun Y, Ramos KR, Nisola GM, Valdehuesa KN, Lee WK, Park SJ, Chung WJ (2013) Combination of Entner-Doudoroff pathway with MEP increases isoprene production in engineered *Escherichia coli.* PloS One 8(12):e83290.

Lv X, Xu H, Yu H (2013) Significantly enhanced production of isoprene by ordered coexpression of genes *dxs*, *dxr*, and *idi* in *Escherichia coli*. Appl Microbiol Biotech 97(6):2357-2365.

McNevin D, von Caemmerer S, Farquhar G (2006) Determining RuBisCO activation kinetics and other rate and equilibrium constants by simultaneous multiple non-linear regression of a kinetic model. J Exp Bot 57:3883–3900

Melis A (2013) Carbon partitioning in photosynthesis. Curr Opin Chem Biol. 17:453–456;

Oliver JW, Machado IM, Yoneda H, Atsumi S (2014) Combinatorial optimization of cyanobacterial 2, 3-butanediol production. Metab Eng. 22:76-82.

Pade N, Erdmann S, Enke H, Dethloff F, Dühring U, Georg J, Wambutt J, Kopka J, Hess WR, Zimmermann R, Kramer D (2016) Insights into isoprene production using the cyanobacterium *Synechocystis* sp. PCC 6803. Biotech Biofuels 18,9(1):89.

Ramos KR, Valdehuesa KN, Liu H, Nisola GM, Lee WK, Chung WJ (2014) Combining De Ley–Doudoroff and methylerythritol phosphate pathways for enhanced isoprene biosynthesis from d-galactose. Bioprocess Biosystems Eng 37(12):2505-2513.

Sasaki K, Ohara K, Yazaki K (2005) Gene expression and characterization of isoprene synthase from *Populus alba*. FEBS Lett 579:2514–2518

Sharkey TD, Yeh S, Wiberley AE, Falbel TG, Gong D, Fernandez DE (2005) Evolution of the isoprene biosynthetic pathway in kudzu. Plant Physiol 137(2):700-712.

Wang F, Lv X, Xie W, Zhou P, Zhu Y, Yao Z, Yang C, Yang X, Ye L, Yu H (2017) Combining Gal4p-mediated expression enhancement and directed evolution of isoprene synthase to improve isoprene production in *Saccharomyces cerevisiae*. Metab Eng 39:257-66.

Williams DC, McGarvey DJ, Katahira EJ, Croteau R (1998) Truncation of limonene synthase preprotein provides a fully active 'pseudomature' form of this monoterpene cyclase and reveals the function of the amino-terminal arginine pair. Biochemistry 37(35):12213–12220

Xue J, Ahring BK (2011) Enhancing isoprene production by genetic modification of the 1-deoxy-d-xylulose-5-phosphate pathway in *Bacillus subtilis*. Appl Env Microbiol 77(7):2399-2405.

Yang J, Xian M, Su S, Zhao G, Nie Q, Jiang X, Zheng Y, Liu W (2012) Enhancing production of bio-isoprene using hybrid MVA pathway and isoprene synthase in *E. coli*. PloS One 7(4):e33509.

Zhao Y, Yang J, Qin B, Li Y, Sun Y, Su S, Xian M (2011) Biosynthesis of isoprene in *Escherichia coli* via methylerythritol phosphate (MEP) pathway. Appl Microbiol Biotech 90(6):1915.

Zhou J, Zhang H, Meng H et al. (2014) Discovery of a super-strong promoter enables efficient production of heterologous proteins in cyanobacteria. *Scientific reports* 4: 4500.

Zurbriggen A, Kirst H, Melis A (2012) Isoprene production via the mevalonic acid pathway in *Escherichia coli* (bacteria). BioEnergy Res. 5(4):814-828.

4.6 Supplementary Materials

Oligonucleotides:

F1- CCATTAGCAAGGCAAATCAAAGAC
R1- GGTGGAAACGGCTTCAGTTAAAG

DNA constructs:

Isoprene synthase fusion proteins

Lower case= *cpcB*
HIGHLIGHTED= Linker
UPPERCASE= *IspS*

cpcB*IpsS

atgttcgacgtattcactcgggttgtttcccaagctgatgctcgcggcgagtacctctctggttctcagttagatgctttgagcgctaccgttgct
gaaggcaacaaacggattgattctgttaaccgcatcaccggtaatgcttccgctatcgtttccaacgctgctcgtgctttgttcgccgaacagc
cccaattaatccaacccggtggaaacgcctacaccagccgtcgtatggctgcttgtttgcgtgacatggaaatcatcctccgctatgttaccta
cgcaaccttcaccggcgacgcttccgttctagaagatcgttgcttgaacggtctccgtgaaacctacgttgccctgggtgttcccggtgcttcc
gtagctgctggcgttcaaaaaatgaaagaagctgccctggacatcgttaacgatcccaatggcatcacccgtggtgattgcagtgctatcgtt
gctgaaatcgctggttacttcgaccgcgccgctgctgccgtagccTGTGCAACTTCTTCCCAATTTACTCAAATT
ACCGAGCACAATTCCCGGCGTAGTGCCAACTATCAACCCAATCTGTGGAACTTTGAG
TTCTTACAGAGCCTGGAAAATGATTTAAAGGTCGAGAAATTGGAGGAGAAGGCCAC
TAAATTGGAAGAGGAAGTGCGGTGTATGATTAATCGTGTAGACACCCAACCATTGA
GTCTGTTAGAATTGATCGATGATGTGCAACGTCTCGGCCTGACATACAAATTCGAAA
AAGATATCATTAAGGCCCTAGAAAACATTGTCTTATTGGATGAAAACAAGAAAAAT
AAGTCTGACTTGCATGCCACCGCTTTAAGTTTCCGCTTGTTGCGGCAGCACGGCTTTG
AAGTGTCCCAAGATGTTTTTGAACGGTTCAAAGACAAGGAGGGCGGCTTTTCCGGCG
AACTCAAAGGGGATGTTCAGGGCCTATTGTCTTTGTATGAAGCTAGTTACTTGGGAT
TTGAAGGCGAGAATCTGTTAGAAGAAGCTCGCACTTTTTCCATTACACATTTAAAGA
ACAACCTAAAGGAAGGGATTAACACAAAAGTGGCTGAGCAGGTGTCTCATGCTCTG
GAGTTGCCGTATCATCAACGCTTACACCGGCTCGAAGCCCGCTGGTTTTTGGATAAA
TATGAACCGAAAGAACCGCATCATCAATTACTGCTCGAACTGGCGAAGCTGGACTTT
AATATGGTCCAAACACTACATCAGAAAGAACTCCAGGACCTAAGTCGGTGGTGGAC
TGAAATGGGTCTGGCATCCAAGCTAGATTTTGTGCGCGACCGTTTGATGGAGGTGTA
CTTCTGGGCACTAGGCATGGCTCCCGACCCGCAGTTTGGTGAGTGTCGTAAGGCAGT
GACCAAGATGTTTGGTTTAGTAACGATCATCGACGACGTTTACGATGTCTATGGCAC
CCTAGACGAATTACAACTCTTTACAGATGCCGTCGAACGTTGGGATGTTAATGCCAT
CAATACCTTACCTGATTACATGAAATTGTGCTTCCTCGCCTTGTATAATACCGTTAAT
GACACCAGCTATTCTATTCTGAAGGAAAAAGGCCACAATAACTTAAGCTACCTAACC
AAAAGTTGGCGGGAATTGTGTAAGGCTTTCTTACAGGAAGCCAAATGGTCCAACAA
CAAAATTATCCCCGCATTTTCTAAATACCTGGAAAATGCCTCCGTGTCCTCTTCCGGG

GTGGCTTTGCTAGCACCCAGCTACTTTTCTGTTTGTCAGCAACAGGAGGACATCAGT
GACCATGCCTTGCGGTCCTTAACGGACTTTCATGGCTTAGTGCGGAGTAGCTGCGTC
ATTTTTCGTTTATGTAACGATTTGGCTACAAGTGCTGCGGAATTGGAACGTGGGGAA
ACAACCAACAGCATTATCAGTTATATGCACGAAAACGATGGCACCAGTGAAGAGCA
GGCACGGGAAGAACTGCGCAAATTAATCGACGCTGAATGGAAGAAGATGAATCGCG
AACGTGTGTCTGATAGTACCTTATTACCTAAAGCCTTCATGGAAATTGCGGTGAATA
TGGCCCGCGTCAGTCATTGCACTTACCAATACGGCGATGGATTAGGTCGGCCCGATT
ACGCAACGGAAAATCGGATCAAATTGCTATTGATTGATCCGTTCCCAATTAATCAAT
TAATGTACGTGTAA

cpcB*L7*IspS

atgttcgacgtattcactcgggttgtttcccaagctgatgctcgcggcgagtacctctctggttctcagttagatgctttgagcgctaccgttgct
gaaggcaacaaacggattgattctgttaaccgcatcaccggtaatgcttccgctatcgtttccaacgctgctcgtgctttgttcgccgaacagc
cccaattaatccaacccggtggaaacgcctacaccagccgtcgtatggctgcttgtttgcgtgacatggaaatcatcctccgctatgttaccta
cgcaaccttcaccggcgacgcttccgttctagaagatcgttgcttgaacggtctccgtgaaacctacgttgccctgggtgttcccggtgcttcc
gtagctgctggcgttcaaaaaatgaaagaagctgccctggacatcgttaacgatcccaatggcatcacccgtggtgattgcagtgctatcgtt
gctgaaatcgctggttacttcgaccgcgccgctgctgccgtagccCCTATGCCCTGGCGTGTAATCTGTGCAAC
TTCTTCCCAATTTACTCAAATTACCGAGCACAATTCCCGGCGTAGTGCCAACTATCA
ACCCAATCTGTGGAACTTTGAGTTCTTACAGAGCCTGGAAAATGATTTAAAGGTCGA
GAAATTGGAGGAGAAGGCCACTAAATTGGAAGAGGAAGTGCGGTGTATGATTAATC
GTGTAGACACCCAACCATTGAGTCTGTTAGAATTGATCGATGATGTGCAACGTCTCG
GCCTGACATACAAATTCGAAAAAGATATCATTAAGGCCCTAGAAAACATTGTCTTAT
TGGATGAAAACAAGAAAAATAAGTCTGACTTGCATGCCACCGCTTTAAGTTTCCGCT
TGTTGCGGCAGCACGGCTTTGAAGTGTCCCAAGATGTTTTTGAACGGTTCAAAGACA
AGGAGGGCGGCTTTTCCGGCGAACTCAAAGGGGATGTTCAGGGCCTATTGTCTTTGT
ATGAAGCTAGTTACTTGGGATTTGAAGGCGAGAATCTGTTAGAAGAAGCTCGCACTT
TTTCCATTACACATTTAAAGAACAACCTAAAGGAAGGGATTAACACAAAAGTGGCT
GAGCAGGTGTCTCATGCTCTGGAGTTGCCGTATCATCAACGCTTACACCGGCTCGAA
GCCCGCTGGTTTTTGGATAAATATGAACCGAAAGAACCGCATCATCAATTACTGCTC
GAACTGGCGAAGCTGGACTTTAATATGGTCCAAACACTACATCAGAAAGAACTCCA
GGACCTAAGTCGGTGGTGGACTGAAATGGGTCTGGCATCCAAGCTAGATTTTGTGCG
CGACCGTTTGATGGAGGTGTACTTCTGGGCACTAGGCATGGCTCCCGACCCGCAGTT
TGGTGAGTGTCGTAAGGCAGTGACCAAGATGTTTGGTTTAGTAACGATCATCGACGA
CGTTTACGATGTCTATGGCACCCTAGACGAATTACAACTCTTTACAGATGCCGTCGA
ACGTTGGGATGTTAATGCCATCAATACCTTACCTGATTACATGAAATTGTGCTTCCTC
GCCTTGTATAATACCGTTAATGACACCAGCTATTCTATTCTGAAGGAAAAAGGCCAC
AATAACTTAAGCTACCTAACCAAAAGTTGGCGGGAATTGTGTAAGGCTTTCTTACAG
GAAGCCAAATGGTCCAACAACAAAATTATCCCCGCATTTTCTAAATACCTGGAAAAT
GCCTCCGTGTCCTCTTCCGGGGTGGCTTTGCTAGCACCCAGCTACTTTTCTGTTTGTC
AGCAACAGGAGGACATCAGTGACCATGCCTTGCGGTCCTTAACGGACTTTCATGGCT
TAGTGCGGAGTAGCTGCGTCATTTTTCGTTTATGTAACGATTTGGCTACAAGTGCTGC
GGAATTGGAACGTGGGGAAACAACCAACAGCATTATCAGTTATATGCACGAAAACG
ATGGCACCAGTGAAGAGCAGGCACGGGAAGAACTGCGCAAATTAATCGACGCTGAA
TGGAAGAAGATGAATCGCGAACGTGTGTCTGATAGTACCTTATTACCTAAAGCCTTC

ATGGAAATTGCGGTGAATATGGCCCGCGTCAGTCATTGCACTTACCAATACGGCGAT
GGATTAGGTCGGCCCGATTACGCAACGGAAAATCGGATCAAATTGCTATTGATTGAT
CCGTTCCCAATTAATCAATTAATGTACGTGTAA

cpcB*L10*IspS

atgttcgacgtattcactcgggttgtttcccaagctgatgctcgcggcgagtacctctctggttctcagttagatgctttgagcgctaccgttgct
gaaggcaacaaacggattgattctgttaaccgcatcaccggtaatgcttccgctatcgtttccaacgctgctcgtgctttgttcgccgaacagc
cccaattaatccaaccccggtggaaacgcctacaccagccgtcgtatggctgcttgtttgcgtgacatggaaatcatcctccgctatgttaccta
cgcaaccttcaccggcgacgcttccgttctagaagatcgttgcttgaacggtctccgtgaaacctacgttgccctgggtgttcccggtgcttcc
gtagctgctggcgttcaaaaaatgaaagaagctgccctggacatcgttaacgatcccaatggcatcacccgtggtgattgcagtgctatcgtt
gctgaaatcgctggttacttcgaccgcgccgctgctgccgtagccCCTGCTCCCGCACCTGCCCCAGCTCCTGC
CTGTGCAACTTCTTCCCAATTTACTCAAATTACCGAGCACAATTCCCGGCGTAGTGC
CAACTATCAACCCAATCTGTGGAACTTTGAGTTCTTACAGAGCCTGGAAAATGATTT
AAAGGTCGAGAAATTGGAGGAGAAGGCCACTAAATTGGAAGAGGAAGTGCGGTGT
ATGATTAATCGTGTAGACACCCAACCATTGAGTCTGTTAGAATTGATCGATGATGTG
CAACGTCTCGGCCTGACATACAAATTCGAAAAAGATATCATTAAGGCCCTAGAAAA
CATTGTCTTATTGGATGAAAACAAGAAAAATAAGTCTGACTTGCATGCCACCGCTTT
AAGTTTCCGCTTGTTGCGGCAGCACGGCTTTGAAGTGTCCCAAGATGTTTTTGAACG
GTTCAAAGACAAGGAGGGCGGCTTTTCCGGCGAACTCAAAGGGGATGTTCAGGGCC
TATTGTCTTTGTATGAAGCTAGTTACTTGGGATTTGAAGGCGAGAATCTGTTAGAAG
AAGCTCGCACTTTTTCCATTACACATTTAAAGAACAACCTAAAGGAAGGGATTAACA
CAAAAGTGGCTGAGCAGGTGTCTCATGCTCTGGAGTTGCCGTATCATCAACGCTTAC
ACCGGCTCGAAGCCCGCTGGTTTTTGGATAAATATGAACCGAAAGAACCGCATCATC
AATTACTGCTCGAACTGGCGAAGCTGGACTTTAATATGGTCCAAACACTACATCAGA
AAGAACTCCAGGACCTAAGTCGGTGGTGGACTGAAATGGGTCTGGCATCCAAGCTA
GATTTTGTGCGCGACCGTTTGATGGAGGTGTACTTCTGGGCACTAGGCATGGCTCCC
GACCCGCAGTTTGGTGAGTGTCGTAAGGCAGTGACCAAGATGTTTGGTTTAGTAACG
ATCATCGACGACGTTTACGATGTCTATGGCACCCTAGACGAATTACAACTCTTTACA
GATGCCGTCGAACGTTGGGATGTTAATGCCATCAATACCTTACCTGATTACATGAAA
TTGTGCTTCCTCGCCTTGTATAATACCGTTAATGACACCAGCTATTCTATTCTGAAGG
AAAAAGGCCACAATAACTTAAGCTACCTAACCAAAAGTTGGCGGGAATTGTGTAAG
GCTTTCTTACAGGAAGCCAAATGGTCCAACAACAAAATTATCCCCGCATTTTCTAAA
TACCTGGAAAATGCCTCCGTGTCCTCTTCCGGGGTGGCTTTGCTAGCACCCAGCTAC
TTTTCTGTTTGTCAGCAACAGGAGGACATCAGTGACCATGCCTTGCGGTCCTTAACG
GACTTTCATGGCTTAGTGCGGAGTAGCTGCGTCATTTTTCGTTTATGTAACGATTTGG
CTACAAGTGCTGCGGAATTGGAACGTGGGGAAACAACCAACAGCATTATCAGTTAT
ATGCACGAAAACGATGGCACCAGTGAAGAGCAGGCACGGGAAGAACTGCGCAAAT
TAATCGACGCTGAATGGAAGAAGATGAATCGCGAACGTGTGTCTGATAGTACCTTAT
TACCTAAAGCCTTCATGGAAATTGCGGTGAATATGGCCCGCGTCAGTCATTGCACTT
ACCAATACGGCGATGGATTAGGTCGGCCCGATTACGCAACGGAAAATCGGATCAAA
TTGCTATTGATTGATCCGTTCCCAATTAATCAATTAATGTACGTGTAA

cpcB*L16*IspS

atgttcgacgtattcactcgggttgtttcccaagctgatgctcgcggcgagtacctctctggttctcagttagatgctttgagcgctaccgttgct
gaaggcaacaaacggattgattctgttaaccgcatcaccggtaatgcttccgctatcgtttccaacgctgctcgtgctttgttcgccgaacagc
cccaattaatccaacccggtggaaacgcctacaccagccgtcgtatggctgcttgtttgcgtgacatggaaatcatcctccgctatgttaccta
cgcaaccttcaccggcgacgcttccgttctagaagatcgttgcttgaacggtctccgtgaaacctacgttgccctgggtgttcccggtgcttcc
gtagctgctggcgttcaaaaaatgaaagaagctgccctggacatcgttaacgatcccaatggcatcacccgtggtgattgcagtgctatcgtt
gctgaaatcgctggttacttcgaccgcgccgctgctgccgtagccGAAGCTGCCGCAAAAGAAGCTGCGGCCA
AAGAGGCTGCCGCTAAAGCATGTGCAACTTCTTCCCAATTTACTCAAATTACCGAGC
ACAATTCCCGGCGTAGTGCCAACTATCAACCCAATCTGTGGAACTTTGAGTTCTTAC
AGAGCCTGGAAAATGATTTAAAGGTCGAGAAATTGGAGGAGAAGGCCACTAAATTG
GAAGAGGAAGTGCGGTGTATGATTAATCGTGTAGACACCCAACCATTGAGTCTGTTA
GAATTGATCGATGATGTGCAACGTCTCGGCCTGACATACAAATTCGAAAAAGATATC
ATTAAGGCCCTAGAAAACATTGTCTTATTGGATGAAAACAAGAAAAATAAGTCTGA
CTTGCATGCCACCGCTTTAAGTTTCCGCTTGTTGCGGCAGCACGGCTTTGAAGTGTCC
CAAGATGTTTTTGAACGGTTCAAAGACAAGGAGGGCGGCTTTTCCGGCGAACTCAA
AGGGGATGTTCAGGGCCTATTGTCTTTGTATGAAGCTAGTTACTTGGGATTTGAAGG
CGAGAATCTGTTAGAAGAAGCTCGCACTTTTTCCATTACACATTTAAAGAACAACCT
AAAGGAAGGGATTAACACAAAAGTGGCTGAGCAGGTGTCTCATGCTCTGGAGTTGC
CGTATCATCAACGCTTACACCGGCTCGAAGCCCGCTGGTTTTTGGATAAATATGAAC
CGAAAGAACCGCATCATCAATTACTGCTCGAACTGGCGAAGCTGGACTTTAATATGG
TCCAAACACTACATCAGAAAGAACTCCAGGACCTAAGTCGGTGGTGGACTGAAATG
GGTCTGGCATCCAAGCTAGATTTTGTGCGCGACCGTTTGATGGAGGTGTACTTCTGG
GCACTAGGCATGGCTCCCGACCCGCAGTTTGGTGAGTGTCGTAAGGCAGTGACCAA
GATGTTTGGTTTAGTAACGATCATCGACGACGTTTACGATGTCTATGGCACCCTAGA
CGAATTACAACTCTTTACAGATGCCGTCGAACGTTGGGATGTTAATGCCATCAATAC
CTTACCTGATTACATGAAATTGTGCTTCCTCGCCTTGTATAATACCGTTAATGACACC
AGCTATTCTATTCTGAAGGAAAAAGGCCACAATAACTTAAGCTACCTAACCAAAAG
TTGGCGGGAATTGTGTAAGGCTTTCTTACAGGAAGCCAAATGGTCCAACAACAAAA
TTATCCCCGCATTTTCTAAATACCTGGAAAATGCCTCCGTGTCCTCTTCCGGGGTGGC
TTTGCTAGCACCCAGCTACTTTTCTGTTTGTCAGCAACAGGAGGACATCAGTGACCA
TGCCTTGCGGTCCTTAACGGACTTTCATGGCTTAGTGCGGAGTAGCTGCGTCATTTTT
CGTTTATGTAACGATTTGGCTACAAGTGCTGCGGAATTGGAACGTGGGGAAACAAC
CAACAGCATTATCAGTTATATGCACGAAAACGATGGCACCAGTGAAGAGCAGGCAC
GGGAAGAACTGCGCAAATTAATCGACGCTGAATGGAAGAAGATGAATCGCGAACGT
GTGTCTGATAGTACCTTATTACCTAAAGCCTTCATGGAAATTGCGGTGAATATGGCC
CGCGTCAGTCATTGCACTTACCAATACGGCGATGGATTAGGTCGGCCCGATTACGCA
ACGGAAAATCGGATCAAATTGCTATTGATTGATCCGTTCCCAATTAATCAATTAATG
TACGTGTAA

cpcB*L65*IspS

atgttcgacgtattcactcgggttgtttcccaagctgatgctcgcggcgagtacctctctggttctcagttagatgctttgagcgctaccgttgct
gaaggcaacaaacggattgattctgttaaccgcatcaccggtaatgcttccgctatcgtttccaacgctgctcgtgctttgttcgccgaacagc
cccaattaatccaacccggtggaaacgcctacaccagccgtcgtatggctgcttgtttgcgtgacatggaaatcatcctccgctatgttaccta
cgcaaccttcaccggcgacgcttccgttctagaagatcgttgcttgaacggtctccgtgaaacctacgttgccctgggtgttcccggtgcttcc
gtagctgctggcgttcaaaaaatgaaagaagctgccctggacatcgttaacgatcccaatggcatcacccgtggtgattgcagtgctatcgtt
gctgaaatcgctggttacttcgaccgcgccgctgctgccgtagccCCTTGGCGGGTGATTTGTGCTACCAGTAG
TCAGTTCACTCAAATCACCGAGCACAACAGTCGGCGGAGTGCCAATTATCAACCCA
ACCTGTGGAACTTCGAATTCCTGCAATCCCTGGAAAACGACTTGAAAGTGGAAAAG
CTGGAAGAAAAAGCCACCAAGCTGGAGGAGGAAGTGCGCCCCTGGCGTGTAATCTG
TGCAACTTCTTCCCAATTTACTCAAATTACCGAGCACAATTCCCGGCGTAGTGCCAA
CTATCAACCCAATCTGTGGAACTTTGAGTTCTTACAGAGCCTGGAAAATGATTTAAA
GGTCGAGAAATTGGAGGAGAAGGCCACTAAATTGGAAGAGGAAGTGCGGTGTATG
ATTAATCGTGTAGACACCCAACCATTGAGTCTGTTAGAATTGATCGATGATGTGCAA
CGTCTCGGCCTGACATACAAATTCGAAAAAGATATCATTAAGGCCCTAGAAAACATT
GTCTTATTGGATGAAAACAAGAAAAATAAGTCTGACTTGCATGCCACCGCTTTAAGT
TTCCGCTTGTTGCGGCAGCACGGCTTTGAAGTGTCCCAAGATGTTTTTGAACGGTTC
AAAGACAAGGAGGGCGGCTTTTCCGGCGAACTCAAAGGGGATGTTCAGGGCCTATT
GTCTTTGTATGAAGCTAGTTACTTGGGATTTGAAGGCGAGAATCTGTTAGAAGAAGC
TCGCACTTTTTCCATTACACATTTAAAGAACAACCTAAAGGAAGGGATTAACACAAA
AGTGGCTGAGCAGGTGTCTCATGCTCTGGAGTTGCCGTATCATCAACGCTTACACCG
GCTCGAAGCCCGCTGGTTTTTGGATAAATATGAACCGAAAGAACCGCATCATCAATT
ACTGCTCGAACTGGCGAAGCTGGACTTTAATATGGTCCAAACACTACATCAGAAAG
AACTCCAGGACCTAAGTCGGTGGTGGACTGAAATGGGTCTGGCATCCAAGCTAGAT
TTTGTGCGCGACCGTTTGATGGAGGTGTACTTCTGGGCACTAGGCATGGCTCCCGAC
CCGCAGTTTGGTGAGTGTCGTAAGGCAGTGACCAAGATGTTTGGTTTAGTAACGATC
ATCGACGACGTTTACGATGTCTATGGCACCCTAGACGAATTACAACTCTTTACAGAT
GCCGTCGAACGTTGGGATGTTAATGCCATCAATACCTTACCTGATTACATGAAATTG
TGCTTCCTCGCCTTGTATAATACCGTTAATGACACCAGCTATTCTATTCTGAAGGAAA
AAGGCCACAATAACTTAAGCTACCTAACCAAAAGTTGGCGGGAATTGTGTAAGGCT
TTCTTACAGGAAGCCAAATGGTCCAACAACAAAATTATCCCCGCATTTTCTAAATAC
CTGGAAAATGCCTCCGTGTCCTCTTCCGGGGTGGCTTTGCTAGCACCCAGCTACTTTT
CTGTTTGTCAGCAACAGGAGGACATCAGTGACCATGCCTTGCGGTCCTTAACGGACT
TTCATGGCTTAGTGCGGAGTAGCTGCGTCATTTTTCGTTTATGTAACGATTTGGCTAC
AAGTGCTGCGGAATTGGAACGTGGGGAAACAACCAACAGCATTATCAGTTATATGC
ACGAAAACGATGGCACCAGTGAAGAGCAGGCACGGGAAGAACTGCGCAAATTAAT
CGACGCTGAATGGAAGAAGATGAATCGCGAACGTGTGTCTGATAGTACCTTATTACC
TAAAGCCTTCATGGAAATTGCGGTGAATATGGCCCGCGTCAGTCATTGCACTTACCA
ATACGGCGATGGATTAGGTCGGCCCGATTACGCAACGGAAAATCGGATCAAATTGC
TATTGATTGATCCGTTCCCAATTAATCAATTAATGTACGTGTAA

Chapter 5: *Remodeling terpenoid metabolism in cyanobacteria for isoprene production*

This work was performed with the following persons:

JEC designed and performed the experiments. Dr. Cinzia Formighieri designed the FNI construct. JEC and AM wrote the manuscript.

5.1 Introduction

A major limiting factor towards cyanobacterial production of isoprene is the poor expression and low specific activity of the terminal enzyme, the isoprene synthase (IspS). Recently, our group successfully addressed this issue through a fusion of the IspS to the *cpcB*-encoded β-subunit of phycocyanin (Chaves et al. 2017). This fusion-protein approach resulted in up to 270-fold increase in transgenic IspS accumulation, and up to a 27-fold increase in the yield of isoprene production. However, the specific activity and affinity of the fusion enzyme for the dimethylallyl diphosphate (DMAPP) substrate was low in these transformants, necessitating further metabolic engineering to enhance the concentration of DMAPP in these photosynthetic microorganisms.

In all biological systems, isopentenyl diphosphate (IPP) and dimethylallyl diphosphate (DMAPP) are the universal precursors of all terpenoids. The precursor enzyme 4-hydroxy-3-methyl-but-2-enyl pyrophosphate (HMBPP) reductase generates both IPP and DMAPP from a single substrate. However, the HMBPP reductase preferentially catalyzes the synthesis of IPP and thus generates an IPP:DMAPP ratio of up to ~6:1 (Tritsch et al. 2010). In photosynthetic systems, this ratio is then adjusted through the isomerization of IPP to DMAPP by the isopentenyl diphosphate isomerase (IDI), leading to a steady-state IPP:DMAPP ratio of 3:1 (Barkley et al. 2004). This ratio is optimal to satisfy the cellular demand for longer chain terpenoids that require an IPP:DMAPP ratio of 3:1, such as the phytol tail of chlorophyll, carotenoids, and quinone prenyl tails, among other neeeds (McGarvey and Croteau 1995, Lichtenthaler 2007). As DMAPP is the sole reactant for the synthesis of isoprene (no IPP is involved), the low steady-state levels of DMAPP limit the rate and yield of isoprene production. In this respect, the isopentenyl diphosphate isomerase (IDI) has recently been shown to be an important limiting factor for cyanobacterial isoprene production (Chaves et al. 2016; Gao et al. 2016), as it helps to maintain a low DMAPP-to-IPP ratio in the cyanobacterial cells. It was also shown that heterologous expression of the *FNI* gene, an alternative IPP isomerase from the non-photosynthetic bacterium *Streptococcus pneumoniae*, shifted the DMAPP-IPP isomerization toward DMAPP, thereby enhancing rate and yield of isoprene production [Chaves et al. 2016].

The present work sought to test the effect of combining the two improvements, i.e., simultaneously alleviating two different major bottlenecks in cyanobacterial isoprene production. The effort entailed enhancement in the expression levels of the isoprene synthase enzyme and also enhancement in the MEP carbon flux to DMAPP and isoprene. The challenge was addressed through the overexpression of two enzymes, the isoprene synthase fused to the highly-expressed cpcB protein (the β-subunit of phycocyanin) and the isopentenyl diphosphate isomerase FNI. The combination of these modifications resulted in a significant isoprene production enhancement, and constitutes a major step forward in the development of this cyanobacterial engineering platform.

5.2 Materials and Methods

Strains and culturing conditions. *Synechocystis* sp. PCC 6803 was employed as the experimental strain and is referred to as the wild type (WT). Transgenic isoprene-producing recipient strains contain a codon optimized *IspS* gene from *Pueraria montana* (kudzu) (Sharkey

et al. 2005; Lindberg et al. 2010) fused to the *cpcB* gene with a spacer nucleotide sequence encoding either a 7 amino acid linker **PMPWRVI** (*cpcB*L7*IspS*) or a 16 amino acid linker **EAAAKEAAAKEAAAKA** (*cpcB*L16*IspS*), followed by a chloramphenicol resistance cassette. Fusion constructs were inserted between the *cpcB* upstream region and the *cpcA* gene in the phycocyanin-encoding *cpc* operon of *Synechocystis*.

All strains employed in this work were maintained on 1% agar-BG11 media supplemented with 10 mM TES-NaOH pH 8.2, and 0.3% Na-thiosulfate. Agar plates were supplemented with Chloramphenicol (30 µg/mL) and/or streptomycin (50 µg/mL) to maintain transformants. Liquid cultures were grown in BG11 media buffered with 25 mM NaH_2PO_4 (pH 7.5) at 28°C, under continuous aeration and gradually increasing illumination. Cultures inoculated from a plate started in the lowest illumination at 30 µmol photons m^{-2} s^{-2} until an $OD_{730\ nm}$=0.3 was reached. Illumination was then increased to 50 µmol photons m^{-2} s^{-2} until an $OD_{730\ nm}$=0.65-0.75 was reached. Illumination was then increased to 100 µmol photons m^{-2} s^{-2} until the culture reached a density sufficient to support dilution in a total volume of 700 mL growth medium so as to attain an $OD_{730\ nm}$=0.65.

FNI-containing constructs. Transformations were performed as previously established (Kirst et al. 2014). DNA constructs were designed to insert the isopentenyl diphosphate isomerase (*FNI*) gene from *Streptococcus pneumoniae* (Zubbrigen et al. 2012) into the glgA1 locus of the *cpcB*L7*IspS* and *cpcB*L16*IspS* recipient strains. The *FNI* gene was expressed under control of the Ptrc promoter, and followed by a streptomycin resistance cassette. Nucleotide sequences are given in the Supplementary Materials.

Protein analysis. Liquid cultures were grown in 300 mL volumes to an OD_{730} of 2.5 and re-suspended in 5-10 mL of 50 mM Tris-HCl (pH 8) after pelleting by centrifugation. Cells were then treated with Protease inhibitor (1 mM PMSF), and lysed by French press (2x1500 psi). Cell lysates were centrifuged at 2,250 g for 3 min to pellet glycogen grains and unbroken cells. A small sample from the supernatant was used for chlorophyll *a* concentration determination, as described previously (Chaves et al. 2016). The lysate was supplemented with an equal volume of solubilization solution, comprising 250 mM Tris-HCl, pH 6.8, 7% w/v SDS, 20% w/v glycerol, 2 M urea, and a few grains of bromophenol blue. Samples were then incubated for 2 h at room temperature, followed by supplementation with β-mercaptoethanol to make a 5% final concentration. The solubilized total cellular proteins were resolved by SDS-PAGE and Western blot analysis. Proteins separated by SDS-PAGE were either stained with Coomassie brilliant blue or transferred to a nitrocellulose membrane for immunodetection using rabbit immune serum containing specific polyclonal antibodies against the ISPS protein (Lindberg et al. 2010) or the FNI protein (Zubriggen et al. 2012).

Isoprene and biomass accumulation. Biomass accumulation and isoprene production were measured in sealed liquid cultures grown photoautotrophically in the absence of antibiotics. Gaseous-aqueous photobioreactors were designed in this lab specifically for quantitative biomass and isoprene production measurements, (Bentley and Melis 2012). The 1 L bioreactors were filled with ~700 mL liquid BG11 growth medium containing 25 mM NaH_2PO_4 (pH 7.5), and then seeded with *Synechocystis* starter cultures to an $OD_{730\ nm}$ = 0.65. The bioreactors were then slowly bubbled with 500 mL of 100% CO_2 gas through the bottom of the liquid culture to fill the

reactor headspace. Bioreactors were then sealed for up to 48 h and stirred slowly and continuously at 28°C under constant illumination at 100 µmol photons m^{-2} s^{-2}.

Isoprene production was quantified by measuring a 1 mL sample from the reactor headspace with gas chromatography (Shimadzu 8A GC-FID). Isoprene quantification was determined based on a calibration of isoprene standard (Acros Organics, Fair Lawn, NJ, USA), as described (Chaves et al. 2015). Biomass accumulation in the liquid phase of the reactor was determined upon collection of 50 mL aliquots, followed by centrifugation, rinsing with deionized water, and cell re-suspension in 2 mL of deionized water. Re-suspended samples were directly transferred and dried on aluminum trays for 6 h at 90°C, and weighed to determine the dry cell weight (dcw). Cell growth was also determined spectrophotometrically by measuring the optical density of live cell cultures at 730 nm with a Shimadzu UV-1800 UV-visible spectrophotometer.

5.3 Results

Transformations. Recipient *Synechocystis* strains encoding the isoprene synthase fusion proteins cpcB*L7*IspS and cpcB*L16*IspS were generated by introducing the *cpcB*L7*IspS* and *cpcB*L16*IspS* fusion constructs with the attendant chloramphenicol resistance cassette (*CmR*) into the ***cpc*** operon locus. The latter encodes for components of the phycocyanin peripheral rods in the phycobilisome light-harvesting antenna of cyanobacteria (**Fig. 5.1A**). Each of the two constructs replaced the native *cpcB* gene, while maintaining the rest of the native *cpc* operon (*cpcA, cpcC1, cpcC2, cpcD* genes) in place (**Fig. 5.1B**). The above fusion constructs contained a defined oligopeptide linker / spacer between the cpcB and IspS proteins. Detailed descriptions of the linker L7 and L16 amino acid sequences are given in **Fig. 5.1C and 5.1D**, respectively.

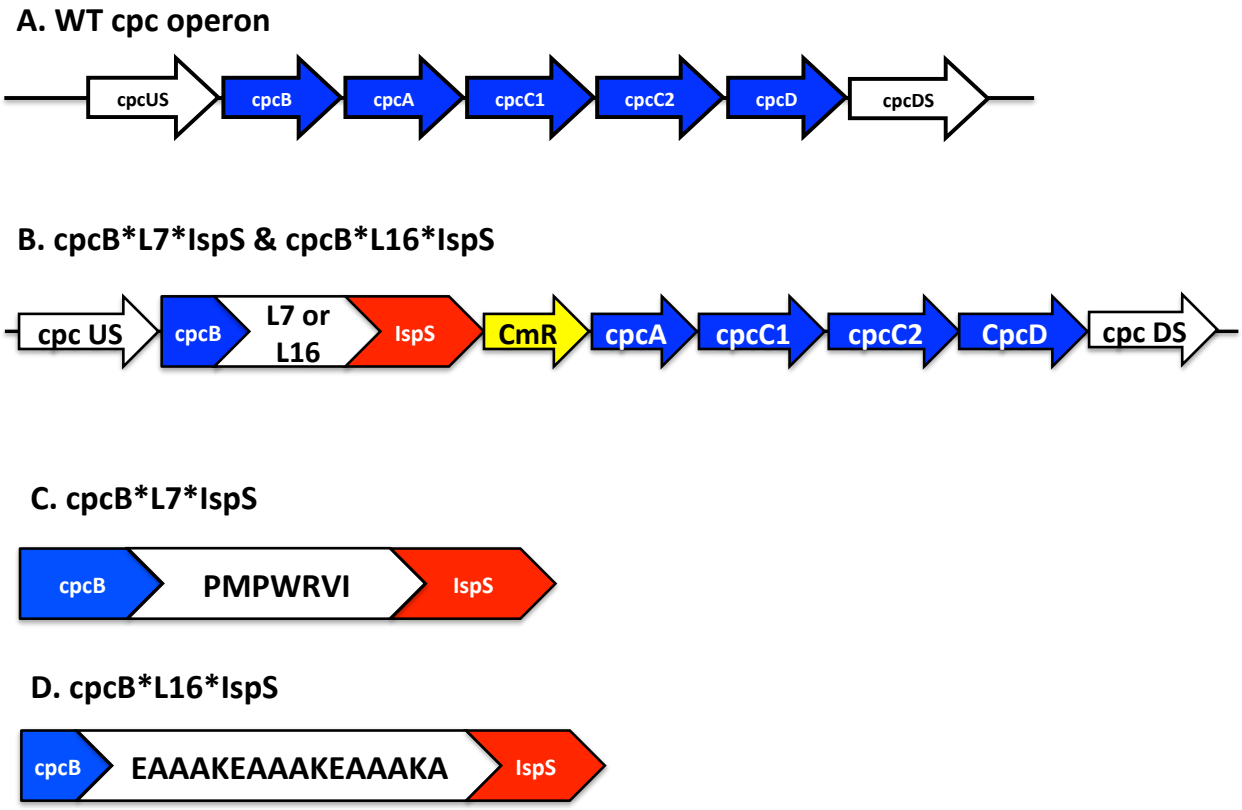

Fig. 5.1 Configurations of the ***cpc*** operon, as used in this work. (**A**) Gene sequence in the native (WT) *Synechocystis* ***cpc*** operon. **(B)** *cpcB*L7*IspS* and *cpcB*L16*IspS* fusion constructs and the attendant chloramphenicol resistance cassette designed to replace the *cpcB* gene upon a double homologous recombination. The amino acid sequences of the linker / spacers introduced between the cpcB and IspS is given for the fusion proteins ate given in **(C)** for the cpcB*L7*IspS and **(D)** for the cpcB*L16*IspS construct.

The FNI construct with the attendant streptomycin resistance cassette (SmR) was inserted into the *glgA1* locus (sll0945, encoding the glycogen synthase 1, which is a protein of the glycogen biosynthetic pathway, **Fig. 5.2A**). In this case, the cpcB*L7*IspS and cpcB*L16*IspS transformants acted as the recipient strains. The FNI transformation replaced the native *glgA1* gene (**Fig. 5.2B**). Genomic DNA PCR analysis was utilized to test for the state of homoplasmy achieved in each set of these transformants. We first confirmed that the recipient strains cpcB*L7*IspS and cpcB*L16*IspS (discussed in our recent work, Chaves et al. 2017) had reached a state of homoplasmy (not shown).

State of homoplasmy for the subsequent FNI transformants was then tested. Primers F1 and R1, with the former sitting in the *glgA1* upstream region of the insertion site and the latter inside the coding sequence of the *glgA1* gene, were designed for specific amplification of wild type copies of the *Synechocystis* DNA, as these are denoted by the presence of the *glgA1* gene (**Fig. 5.2A**). Primers F1 and R2, with the latter sitting in the *glgA1* downstream region of the insertion site, were designed to flank the site of homologous recombination for the *FNI* gene, hence they could amplify different size products from the wild type and FNI transformants (**Fig. 5.2A and 5.2B**). Primer sequences are given in the Supplementary Materials.

Primers F1 and R2 amplified a 1.2 kb product in the wild type *Synechocystis*, and a 2.4 kb product in the cpcB*L7*IspS + FNI transformant (**Fig. 5.3A, left panel**). Primers F1 and R1 amplified a 1.0 kb product in the wild type *Synechocystis* only, and failed to amplify any product in the cpcB*L7*IspS + FNI transformant (**Fig. 5.3A, right panel**). Similar results were obtained with the cpcB*L16*IspS + FNI transformant strain (**Fig. 5.3B**). These results showed that primers F1 and R2 successfully amplified the expected size product in the FNI transformants only, providing evidence for the presence of the FNI construct in the *glgA1* locus. At the same time, primers F1 and R1 failed to amplify a wild type product in the these transformants, providing evidence that a state of DNA homoplasmy has been reached in which wild type copies of the DNA have been eliminated with the attendant segregation of the transgenic DNA in the transformants.

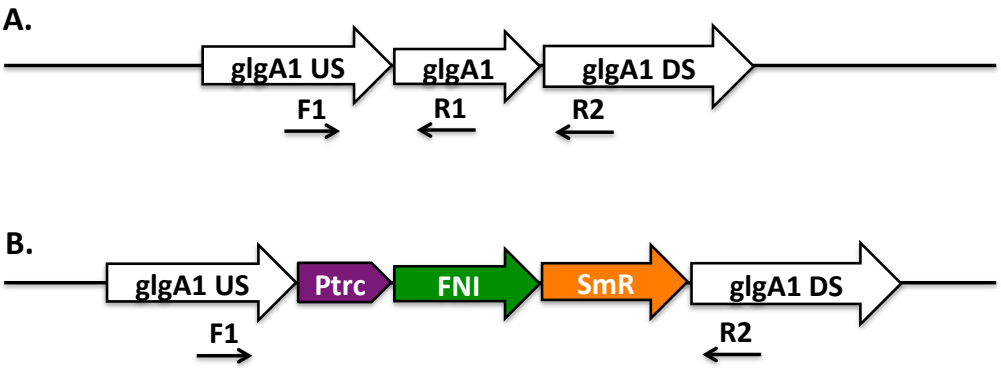

Fig. 5.2 Configurations of the *glgA1* locus, as used in this work. **(A)** Wild type schematic of the *glgA1* gene and location of the F1, R1 and R2 primers for genomic DNA PCR reactions. **(B)** Schematic of the *glgA1* locus in which the glgA1 gene was replaced by a construct comprising the Ptrc promoter, the *FNI* transgene, and the streptomycin resistance cassette. Location of the F1 and R2 primers for genomic DNA PCR reactions is also shown.

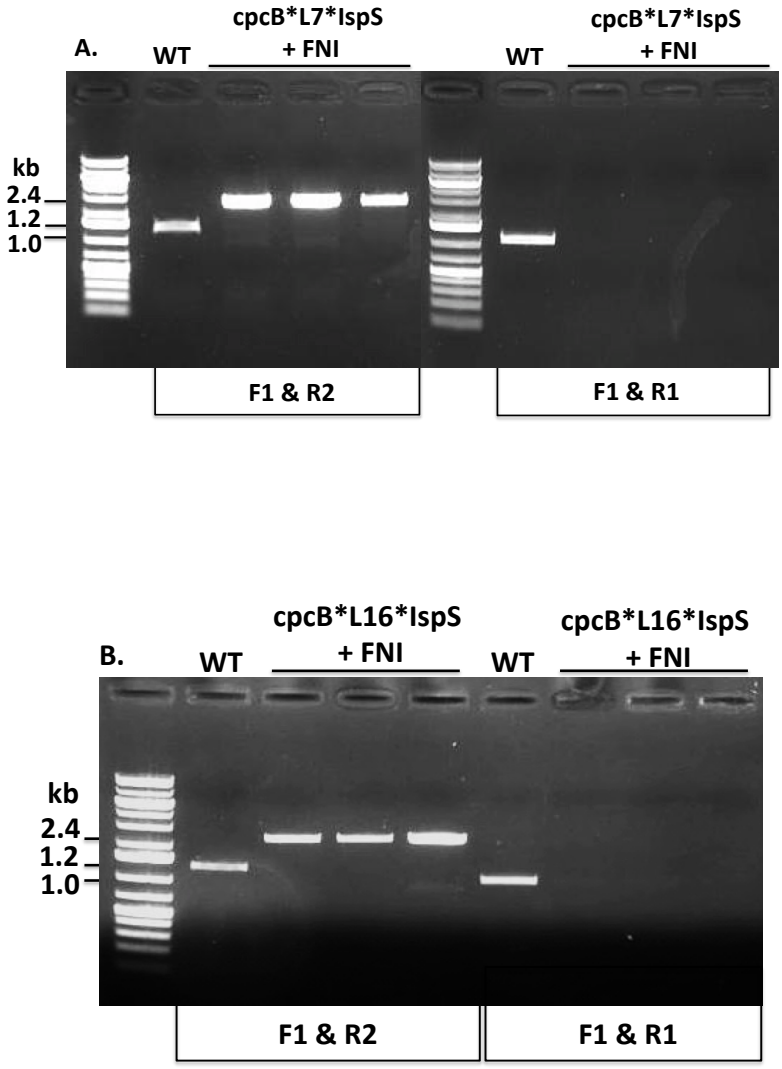

Fig. 5.3 State of homoplasmy of **(A)** the cpcB*L7*IspS + FNI and **(B)** the cpcB*L16*IspS + FNI transformant strains, as determined by genomic DNA PCR analysis. Primers F1 and R1 flank the upstream *glgA1* site and coding region of the *glgA1* gene, respectively, probing for the presence of wild type copies of the *glgA1* gene in *Synechocystis* (anticipated product size=1 kb). Primers F1 and R2 flank outside the coding region of the *glgA1* gene and the regions of the transgene homologous recombination, amplifying a 1.2 kb product in the recipient strains, and a 2.4 kb product in the FNI transgenic lines.

Protein Analysis. Protein profiles of each strain were examined by SDS-PAGE and Western blot analysis. In the SDS-PAGE Coomassie-stain analysis, the wild type showed dominant bands at 55, 20, and 15 kD attributed to the large subunit of rubisco (rbcL), the *cpcB*-encoded β-subunit of phycocyanin, and the *cpcA*-encoded α-subunit of phycocyanin, respectively (**Fig. 5.4A, WT**). The recipient strains showed dominant bands at 84 and 55 kD, attributed to the cpcB*L7*IspS and cpcB*L16*IspS fusion proteins, and the rbcL, respectively (**Fig. 5.4A, Lanes 1 and 5**). In the recipient strains, the wild type cpcB and cpcA proteins were absent resulting in a Δcpc (phycocyanin-less) phenotype, which was previously characterized (Kirst et al. 2014). Three independent lines of the cpcB*L7*IspS + FNI double transformant (**Fig. 5.4A, lanes 2-4**) and three independent lines of the cpcB*L16*IspS + FNI double transformant (**Fig. 5.4A, lanes 6-8**) showed presence of the same dominant ~84 kD protein bands as the recipient strains, and further addition of the FNI recombinant protein at ~37 kD. Antibiotic resistance proteins showed faint bands at 23 kD (CmR) and 27 kD (SmR).

Western blot analysis (**Fig. 5.4B**) showed strong cross-reactions of the IspS polyclonal antibodies with a protein band at 84 kD in all transformant strains. Likewise, a strong cross reaction of the FNI polyclonal antibodies was observed with a protein band at 37 kD in the cpcB*L7*IspS + FNI (**Fig. 5.4B, lanes 2-4**) and cpcB*L16*IspS + FNI (**Fig. 5.4B, lanes 6-8**) transformants. These observations confirmed that transformations performed in this work truly result in overexpression of the heterologous IspS fusion and FNI recombinant proteins in *Synechocystis*.

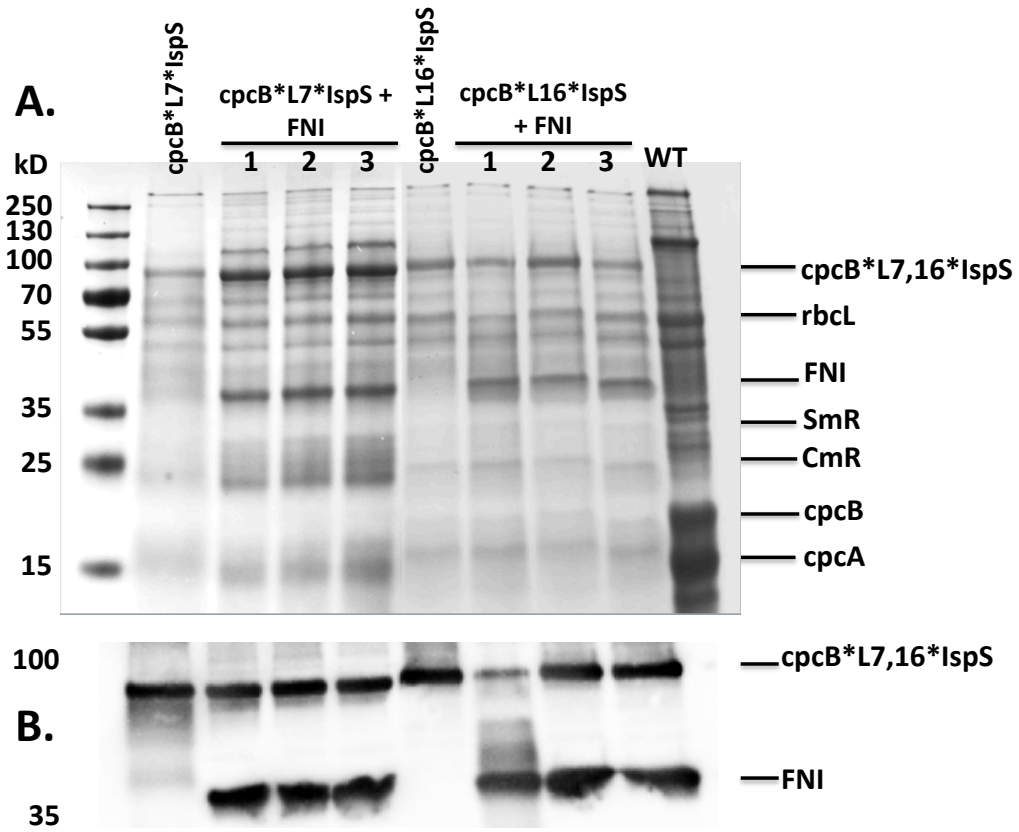

Fig. 5.4 SDS-PAGE and Western blot analysis of *Synechocystis* wild type (WT) and transgenic cell proteins. (**A**) Total protein extracts were resolved by SDS-PAGE and Coomassie stain, loading about 1 μg Chl per lane. The wild type showed a dominant protein band at about 58 kD attributed to the large subunit of Rubisco, and abundant protein bands at about 20 kD from the cpcB phycocyanin β-subunit, as well as at about 15 kD from the cpcA phycocyanin α-subunit. The cpcB*L7*IspS, cpcB*L7*IspS + FNI, cpcB*L16*IspS, and the cpcB*L16*IspS + FNI transformants failed to accumulate the 20 and 15 kD phycocyanin subunits. The transformants showed substantial accumulation of the fusion proteins cpcB*L7*IspS, cpcB*L16*IspS, and FNI proteins, migrating to about 80-85 kD and 37 kD, respectively. A faint band at ~24 kD in the SDS-PAGE analysis was attributed to expression of the chloramphenicol resistance protein. (**B**) Western blot analysis was conducted using polyclonal antibodies specific to the IspS and FNI. Strong cross reactions at the 84 kD region were identified as the cpcB*(L7 or L16)*IspS fusions, and at the 37 kD region as the FNI.

Isoprene and biomass accumulation. Liquid cultures of all strains were grown for isoprene and biomass accumulation using the gaseous-aqueous two-phase bioreactors developed by Bentley and Melis (2012). Biomass accumulation was determined spectrophotometrically by OD at 730 nm (**Fig. 5.5A**), and dry cell weight (**Fig. 5.5B**). The rates of biomass accumulation were determined from the slope of the average accumulation in nine separate cultures from the 48-96 h growth period. Strains cpcB*L7*IspS and cpcB*L7*IspS + FNI grew at a slightly slower rate (about 4 mg L^{-1} h^{-1} and 5 mg L^{-1} h^{-1}, respectively) than the cpcB*L16*IspS and the cpcB*L16*IspS + FNI (6 mg L^{-1} h^{-1} and 8 mg L^{-1} h^{-1}, respectively). These small variations in the rate may be attributed to greater isoprene production in the former strains (see below), thus leading to slower carbon partitioning for biomass accumulation in the cpcB*L7*IspS and cpcB*L7*IspS + FNI transformants.

Isoprene production was measured concurrently with cell growth, and was found to vary greatly between the four different strains. The slowest isoprene producer was the cpcB*L16*IspS transformant, accumulating 6.3 μg L^{-1} h^{-1}. Addition of the FNI transgene to this recipient strain, converting it to cpcB*L16*IspS + FNI, boosted isoprene production nearly 4-fold to 27 μg L^{-1} h^{-1} (**Fig. 5.6A** and **Table 1**). The cpcB*L7*IspS strain by itself produced isoprene at 27 μg L^{-1} h^{-1}, and the addition of the FNI transgene, converting it to cpcB*L7*IspS + FNI, boosted isoprene production up to 46 μg L^{-1} h^{-1} (**Fig. 5.6A** and **Table 1**). These results translated into different Isoprene-to-Biomass carbon partitioning ratios for the transformants examined in this work. The lowest yield of 1.5 mg isoprene per g biomass was measured with the cpcB*L16*IspS construct, and the highest yield of 12.3 mg isoprene per gram biomass was observed with the cpcB*L7*IspS + FNI double transformant (**Fig. 5.6B**). The latter is the highest verifiable constitutive photosynthetic isoprene production measured with homoplasmic lines, in which the heterologous isoprene biosynthesis pathway genes are encoded by the *Synechocystis* genomic DNA.

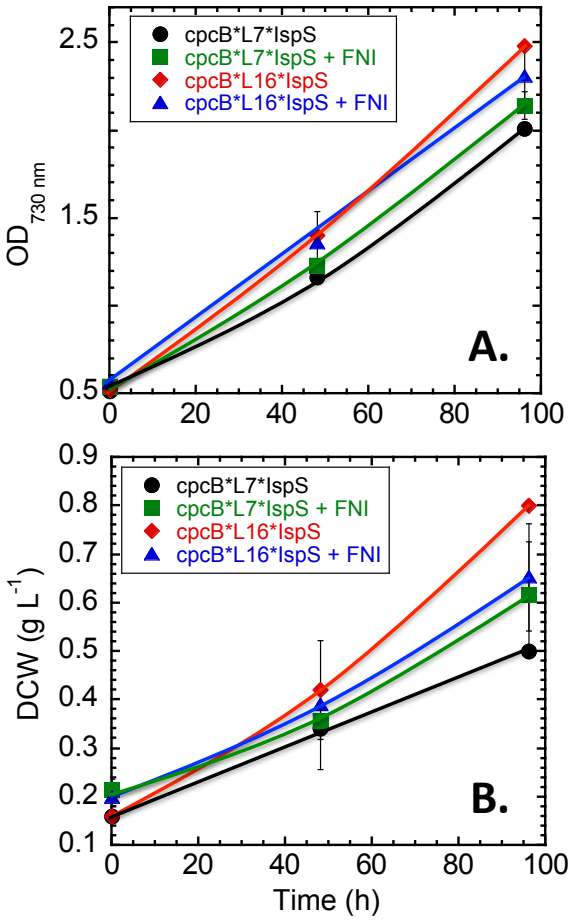

Fig. 5.5 Liquid cultures of all strains used in this work were grown using the gaseous-aqueous two-phase bioreactor developed in this lab (Bentley and Melis 2012), bubbled with 500 mL 100% CO_2 through the culture to fill the reactor headspace, sealed and stirred slowly by magnetic stir bar, under constant illumination of 100 µmol photons m^{-2} s^{-1}. Biomass accumulation was measured every 48 h, for a total of 96 h, by optical density and dry cell weight.

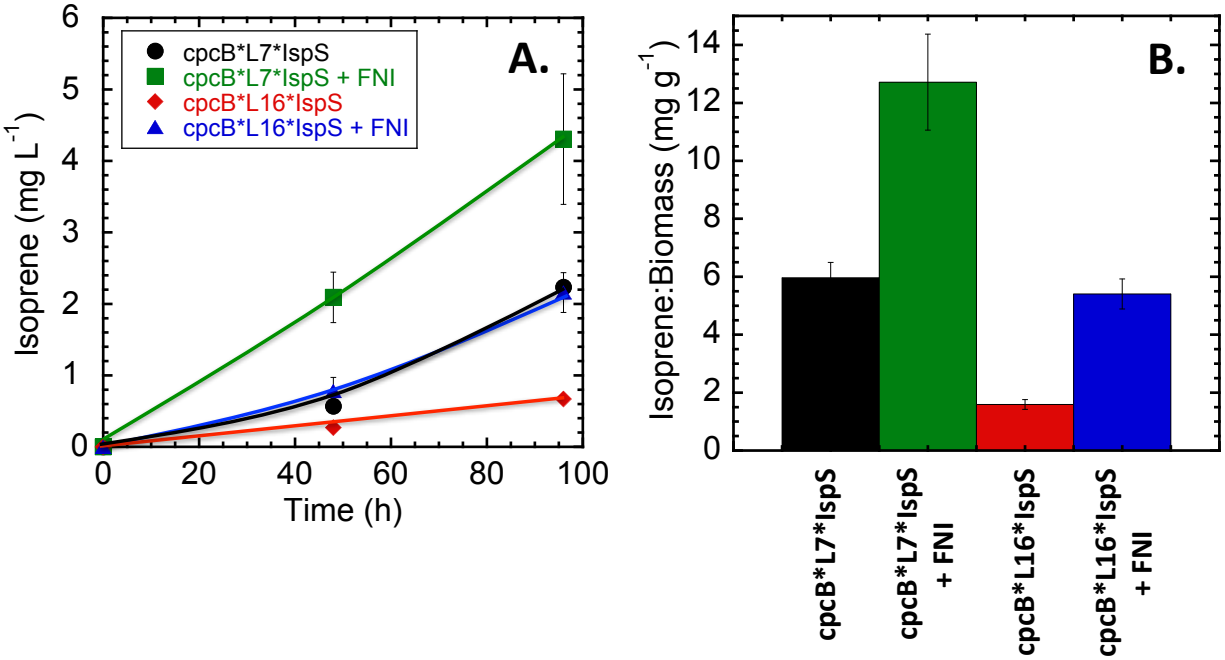

Fig. 5.6 **(A)** Isoprene accumulation measurements were conducted concurrently with biomass measurements, every 48 h for a total of 96 h. Gas chromatography was used to analyze 1 mL samples taken from the headspace of the reactor using a gas tight syringe. Isoprene quantification was determined based on a calibration curve of isoprene standard (Acros Organics, Fair Lawn, NJ, USA), as described (Chaves et al. 2015). **(B)** Isoprene production was calculated relative to biomass accumulation in mg isoprene produced per g of dry cell weight.

Table 5.1. Liquid cultures were grown in gaseous-aqueous two-phase photobioreactors for 96 h with provision of 500 mL of 100% CO_2 slowly bubbled through the culture to fill the reactor headspace. A constant illumination of 100 µmol photons m^{-2} s^{-1} was also provided. Rates of biomass accumulation (mg dcw L^{-1} h^{-1}), isoprene (µg L^{-1} h^{-1}), and isoprene-to-biomass (w:w) ratio (mg g^{-1}) were calculated for each strain.

Strain	**Rate of biomass accumulation (mg L^{-1} h^{-1})**	**Rate of isoprene accumulation (µg L^{-1} h^{-1})**	**Isoprene to biomass ratio (mg g^{-1})**
IspS*	8.0	1.7	0.2
cpcB*L16*IspS	6.0	6.3	1.5
cpcB*L16*IspS +FNI	8.0	27	5.5
cpcB*L7*IspS	4.0	27	6.0
cpcB*L7*IspS + FNI	5.0	46	12.3

* Results from Chaves et al. (2017).

5.4 Discussion

Rerouting carbon flux to isoprene has been established in this work upon alleviation of two key bottlenecks, i.e., inadequate IspS enzyme concentration in the cell and limited MEP pathway flux to DMAPP, which is the sole isoprene precursor. We showed that expression of the combination of the cpcB*L7*IspS and the FNI transgenes can improve isoprene production up to 62-fold (12.3 mg g^{-1}), relative to previous results from the heterologous expression of a single isoprene synthase gene, which yielded a mere 0.2 mg isoprene per g biomass generated (**Table 5.1**, Chaves et al. 2017, 2016, 2015; Bentley and Melis 2012). This yield improvement was due to the synergy of the effects from the overexpression of the cpcB*L7*IspS fusion protein, aiding in the catalysis of DMAPP conversion to isoprene, and also due to the overexpression of FNI, shifting the DMAPP-to-IPP steady state ratio in the cells more toward DMAPP.

A summary of the resulting state of the art in *Synechocystis* isoprene production is presented by the modified MEP pathway flux schematic shown in **Fig. 5.7**. In wild type cyanobacteria, substrate flux through the MEP pathway leads to the synthesis of HMBPP, which then partitions unevenly with a preference toward accumulation of IPP and, secondarily DMAPP. The 6:1 IPP:DMAPP distribution is consistent with the high IPP:DMAPP ratios needed for the synthesis of cellular terpenoids. However, this high IPP:DMAPP steady-state does not promote isoprene production. Heterologous expression of the FNI shifted this steady-state toward the DMAPP, enhancing the pool size of this isoprene precursor metabolite. Overexpression of the isoprene synthase as a fusion with the highly expressed cpcB protein (the β-subunit of phycocyanin) effectively converted DMAPP to isoprene, thereby enhancing the isoprene-to-biomass partitioning ratio, as shown in this work.

Future work on the terpenoid pathway for isoprene production will involve optimization of the pertinent protein concentration and engineering the pathway's properties of enzyme catalysis. Previous studies of the terpenoid biosynthetic pathway enzyme sequences have shown that the terpene synthases evolved upon gene duplications, and then diverged to form the enormous variety of enzymes leading to different terpenoid structures (Tholl 2006). Evolution of these enzymes is facilitated from the promiscuous nature of their activity (Christianson 2008), thus leading to poor catalytic activity and unwanted product formation from the point of view of metabolic engineering objectives (Nobeli et al. 2009). In this respect, isoprene synthase enzymes have been shown to also bind geranyl diphosphate (GPP), which then inhibits the binding of DMAPP (Koksal et al. 2010), thereby slowing down isoprene production. Combining the strategies of enhanced enzyme concentration and improved rates of catalysis (Kcat) has the potential to further increase terpenoid product generation (Leonard et al. 2010) over what is achieved today. Our approach in this work has provided a key piece of the complex puzzle towards the renewable photosynthetic production of isoprene.

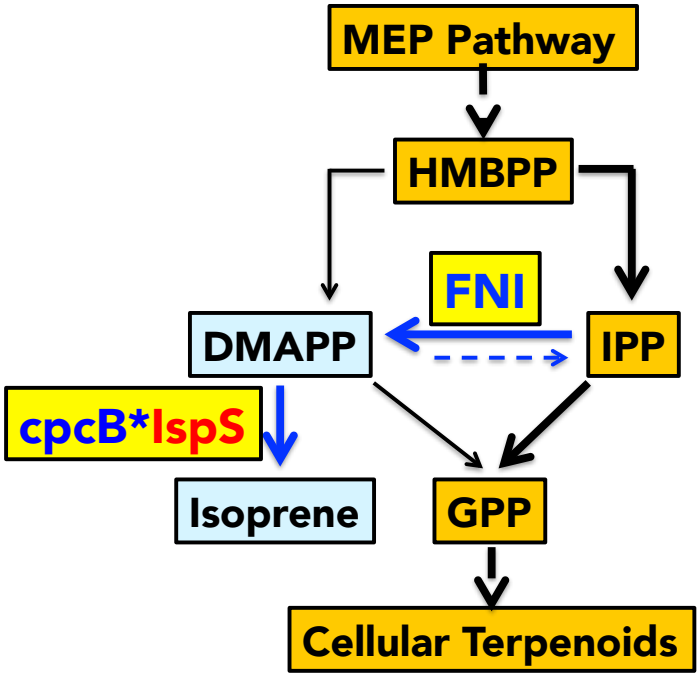

Fig. 5.7 Schematic of carbon flow through the MEP biosynthetic pathway leading to isoprene production. The IspH enzyme utilizes a single substrate, (E)-4-Hydroxy-3-methyl-but-2-enyl pyrophosphate (HMBPP) to generate the two precursor molecules for the synthesis of all terpenoids, isopentenyl diphosphate (IPP) and dimethylallyl diphosphate (DMAPP). Native terpenoid production requires substrate flux primarily through the IPP precursor and a steady state DMAPP:IPP ratio of 1:3 in the cell. Isoprene synthesis requires only the DMAPP reactant. The overexpression of the heterologous isopentenyl diphosphate isomerase (FNI) in *Synechocystis* shifted the IPP to DMAPP steady state ratio toward DMAPP, thereby enhancing the catalytic activity of the cpcb*IspS fusion enzyme and leading to greater yields of isoprene production.

5.5 References:

Bentley FK, Melis A (2012) Diffusion-based process for carbon dioxide uptake and isoprene emission in gaseous/aqueous two-phase photobioreactors by photosynthetic microorganisms. Biotech Bioeng 109(1):100-109.

Barkley SJ, Desai SB, Poulter CD (2004) Type II isopentenyl diphosphate isomerase from *Synechocystis* sp. strain PCC 6803. J Bacteriol 186(23):8156-8158.

Chaves JE, Kirst H, Melis A (2015) Isoprene production in *Synechocystis* under alkaline and saline growth conditions. J Appl Phycol 27:1089–1097

Chaves JE, Romero P, Kirst H, Melis A (2016) Role of isopentenyl-diphosphate isomerase in heterologous cyanobacterial (*Synechocystis*) isoprene production. Photosyn Res 130:517-527

Chaves JE, Rueda-Romero P, Kirst H, Melis A (2017) Engineering isoprene synthase expression and activity in cyanobacteria. Submitted

Christianson DW (2008) Unearthing the roots of the terpenome. Current Opinion Chem Biol 12(2):141-150.

Gao X, Gao F, Liu D, Zhang H, Nie X, Yang C (2016) Engineering the methylerythritol phosphate pathway in cyanobacteria for photosynthetic isoprene production from CO_2. Energy & Environmental Science 9(4):1400-1411

Kirst H, Formighieri C, Melis A (2014) Maximizing photosynthetic efficiency and culture productivity in cyanobacteria upon minimizing the phycobilisome light-harvesting antenna size. Biochim Biophys Acta - Bioenergetics 1837(10):1653-1664

Köksal M, Zimmer I, Schnitzler JP, Christianson DW (2010) Structure of isoprene synthase illuminates the chemical mechanism of teragram atmospheric carbon emission. J Mol Biol 402(2):363-373.

Leonard E, Ajikumar PK, Thayer K, Xiao WH, Mo JD, Tidor B, Stephanopoulos G, Prather KL (2010) Combining metabolic and protein engineering of a terpenoid biosynthetic pathway for overproduction and selectivity control. Proc Natl Acad Sci USA 107(31):13654-13659.

Lichtenthaler HK (2007) Biosynthesis, accumulation and emission of carotenoids, α-tocopherol, plastoquinone, and isoprene in leaves under high photosynthetic irradiance. Photosynth Res 92(2):163-179.

Lindberg P, Park S, Melis A (2010) Engineering a platform for photosynthetic isoprene production in cyanobacteria, using *Synechocystis* as the model organism. Metabol Engin 12:70-79

McGarvey DJ, Croteau R (1995) Terpenoid metabolism. Plant Cell 7(7):1015-1026.

Nobeli I, Favia AD, Thornton JM (2009) Protein promiscuity and its implications for biotechnology. Nature Biotech 27(2):157-167

Sharkey TD, Yeh S, Wiberley AE, Falbel TG, Gong D, Fernandez DE (2005) Evolution of the isoprene biosynthetic pathway in kudzu. Plant Physiol. 137:700–712

Tholl D (2006) Terpene synthases and the regulation, diversity and biological roles of terpene metabolism. Current Opinion Plant Biol 9(3):297-304.

Tritsch D, Hemmerlin A, Bach TJ, Rohmer M (2010) Plant isoprenoid biosynthesis via the MEP pathway: In vivo IPP/DMAPP ratio produced by (E)-4-hydroxy-3-methylbut-2-enyl diphosphate reductase in tobacco BY-2 cell cultures. FEBS Lett 584(1):129-134.

Zurbriggen A, Kirst H, Melis A (2010) Isoprene production via the mevalonic acid pathway in *Escherichia coli* (bacteria). BioEnergy Res 5(4):814-828

5.6 Supplementary Materials

Oligonucleotides:

F1- GATAGTCCACGGACAAAGCAC
R1- GACATGAAGCGGTCAAGGATC
R2- GGGATACAGCCATAACGCATG

DNA constructs:

Codon optimized *Streptococcus pneumoniae* FNI and streptomycin resistance gene

Ptrc promoter-lowercase bold
FNI- UPPERCASE
ribosome binding site- lowercase underlined
SPECTINOMYCIN RESISTANCE- UPPERCASE BOLD

attctgaaatgagctgttgacaattaatcatccggctcgtataatgtgtggaaattgtgagcggataacaattaggaggttaattaac
aATGACTACCAATCGCAAGGATGAGCACATCTTGTATGCACTAGAGCAAAAATCCAG
TTACAACAGCTTTGACGAAGTGGAATTGATCCACTCCTCCTTACCCCTATACAATTTA
GATGAAATTGACTTGTCTACCGAGTTTGCCGGACGCAAATGGGACTTTCCCTTTTAC
ATTAATGCCATGACTGGGGGCAGCAACAAAGGACGGGAGATCAATCAAAAATTAGC
TCAGGTTGCCGAAACTTGTGGCATCCTATTTGTTACCGGCAGTTATAGTGCAGCCCT
GAAAAATCCGACGGATGATTCCTTTAGTGTGAAAAGTTCCCATCCGAATCTCCTCTT
AGGTACAAACATTGGCCTAGATAAACCCGTTGAACTGGGCTTGCAAACAGTGGAAG
AAATGAACCCCGTATTGTTGCAAGTGCATGTTAACGTAATGCAGGAGCTGTTGATGC
CCGAAGGAGAACGGAAATTTCGTTCCTGGCAGTCTCATTTAGCCGACTATTCCAAAC
AAATTCCCGTGCCGATTGTATTGAAAGAAGTTGGGTTTGGCATGGACGCCAAGACA
ATCGAACGCGCTTATGAATTTGGCGTTCGCACCGTTGATTTGTCTGGCCGTGGCGGA
ACTAGCTTTGCTTATATTGAAAATCGGCGGAGTGGCCAACGTGACTATTTGAATCAA
TGGGGCCAATCCACTATGCAGGCCTTGCTGAATGCCCAAGAATGGAAAGACAAAGT
GGAATTACTAGTGAGTGGCGGGGTGCGTAATCCCTTAGATATGATTAAATGCTTAGT
ATTTGGTGCCAAGGCGGTTGGTCTGAGTCGTACCGTGTTGGAACTGGTAGAAACCTA
TACTGTTGAAGAAGTAATTGGGATCGTCCAGGGGTGGAAGGCCGACCTGCGCCTCA
TCATGTGCTCCTTGAACTGTGCCACCATTGCCGATCTGCAAAAAGTTGATTATCTGCT
GTACGGTAAATTGAAAGAAGCGAACGATCAAATGAAAAAAGCGTAGggcgcgcctctagag
gatccaggaggtaatatatgagggaagcggtgatcgctgaggatcaccaaggtagtcggcaaataaggatcctcaggatccaggaggtaa
tat**ATGAGGGAAGCGGTGATCGCCGAAGTATCGACTCAACTATCAGAGGTAGTTG**
GCGTCATCGAGCGCCATCTCGAACCGACGTTGCTGGCCGTACATTTGTACGGC
TCCGCAGTGGATGGCGGCCTGAAGCCACACAGTGATATTGATTTGCTGGTTAC
GGTGACCGTAAGGCTTGATGAAACAACGCGGCGAGCTTTGATCAACGACCTTT
TGGAAACTTCGGCTTCCCCTGGAGAGAGCGAGATTCTCCGCGCTGTAGAAGTC
ACCATTGTTGTGCACGACGACATCATTCCGTGGCGTTATCCAGCTAAGCGCGA
ACTGCAATTTGGAGAATGGCAGCGCAATGACATTCTTGCAGGTATCTTCGAGC
CAGCCACGATCGACATTGATCTGGCTATCTTGCTGACAAAAGCAAGAGAACAT

AGCGTTGCCTTGGTAGGTCCAGCGGCGGAGGAACTCTTTGATCCGGTTCCTGA
ACAGGATCTATTTGAGGCGCTAAATGAAACCTTAACGCTATGGAACTCGCCGC
CCGACTGGGCTGGCGATGAGCGAAATGTAGTGCTTACGTTGTCCCGCATTTGG
TACAGCGCAGTAACCGGCAAAATCGCGCCGAAGGATGTCGCTGCCGACTGGGC
AATGGAGCGCCTGCCGGCCCAGTATCAGCCCGTCATACTTGAAGCTAGACAGG
CTTATCTTGGACAAGAAGAAGATCGCTTGGCCTCGCGCGCAGATCAGTTGGAA
GAATTTGTCCACTACGTGAAAGGCGAGATCACCAAGGTAGTCGGCAAATAA